Construction of the attainable region candidates for ball milling operations under downstream size constraints

By

MLANDVO BRIAN THEMBINKOSI DLAMINI

submitted in accordance with the requirements
for the degree of

MAGISTER TECHNOLOGIAE

in the subject

ENGINEERING: CHEMICAL

at the

UNIVERSITY OF SOUTH AFRICA

SUPERVISOR: Prof FRANCOIS MULENGA

September 2019

DECLARATION

I hereby declare that this dissertation submitted for the degree purposes at the University of South Africa (UNISA) is my own original work. It has not been submitted before for any degree or examination in any institution of higher education. The work, ideas and observations presented in this study are my own. I further declare that all sources cited are acknowledged and indicated through a list of reference.

Mlandvo Brian Thembinkosi Dlamini **September 2019**

DEDICATION

I dedicate this research work to my amazing, beautiful wife. This journey would not have been such a success without your continuous support and patience. Thank you for your encouragement where I needed strength; forever indebted to you. I Love You so much.

To my father and mother; I thank you for instilling the belief in me that whatever the mind conceives, it can achieve. I can never ask for greater parents. May the God we worship bless you in abundance.

To our children, if daddy can do it, so can you.

ACKNOWLEDGEMENTS

First and foremost, I would like to give thanks to my father in Heaven, God Almighty; the Omni Present Lord. I would not have done it without Him.

Secondly, my sincere appreciation goes to my supervisor, Prof. Francois Mulenga, for agreeing to mentor me during the course of this research, for his guidance, constructive criticism and patience. His support has resulted to the completion of this work.

Lastly, I am indebted to the University of South Africa for offering me the opportunity to do this work.

ABSTRACT

This study investigated the influence of the attainable region technique to ball milling as applied in reactor technology. Flow rate, ball filling, mill speed, ball size and mill density were varied. When each was varied, the rest of the parameters were kept constant in-order to determine the influence of each parameter on the process of milling. Selection function and breakage function parameters were selected for the mill model. These were kept constant for all four circuit configurations: open milling circuit, normal closed circuit, reverse closed circuit, and combined closed circuit. Flow rate was varied from 10 tph to 150 tph. It was observed that in all circuit configurations the optimum results were obtained from 90 tph upwards. When ball filling was varied, the optimum results were obtained between 30 % and 40 % of ball filling. At this range the mill is neither experiencing under-filling nor over-filling. When the mill speed was varied, at 60 – 80 % of critical speed the product specification was achieved and for grinding balls, sizes of between 60 mm and 90 mm yielded the optimum results. Varying the mill density resulted in insignificant changes. From the results, the combined closed circuit produced more of the product specification.

Keywords: Attainable Region; Population Balance Model; Ball Milling; MODSIM®.

TABLE OF CONTENTS

LIST OF FIGURES

LIST OF TABLES

LIST OF SYMBOLS

Symbol	Description, [units]
a_B	Selection function parameter calculated for the Bond design mill, [min^{-1}]
a_L	Selection function parameter calculated for the laboratory design mill, [min^{-1}]
a_T	Selection function parameter corresponding to the reference ball diameter d_T, [mm]
$B_{i,j}$	Cumulative breakage distribution function for particles of size j reporting to size i after breakage, [-]
C	circulation ratio, [-]
d_k	Diameter of grinding balls corresponding to ball size class k and used in preparing the ball charge mix, [mm]
d_B	Diameter of grinding balls used in the Bond design mill, [mm]
d_L	Diameter of grinding balls used in the laboratory design milling, [mm]
d_T	Reference ball diameter used as the baseline in allowing for the effects of ball size distribution in a ball charge mix, [mm]
D_B	Diameter of the Bond design mill, [m]
D_L	Diameter of the laboratory design mill, [m]
f_i	Mass fraction of the initial feed in size class i, [-]
m	Number of grinding ball size classes, [-]
m_i	Mass fraction of balls of diameter d_i in a ball charge mix, [-]
n	Number of particle size classes, [-]
N_0	Parameter in Equation (9) adjusting for the effects of ball size on milling, [-]
N_1	Parameter in Equation (9) adjusting for the effects of mill diameter on milling, [-]

N_2	Parameter in Equation (10) adjusting for the effects of mill diameter on milling, [-]
N_3	Parameter in Equation (10) adjusting for the effects of ball size on milling, [-]
p_i	Mass fraction of the final mill product present in size class *i*, [-]
$p_i(t)$	Mass fraction of the final mill product present in size class *i* and produced after grinding time *t*, [-]
S_i	Selection function of particles of size x_i, [min^{-1}]
$S_{i,j}$	Selection function of particles of size x_i due to grinding balls of diameter d_j present in a ball charge mix, [min^{-1}]
t	Grinding time used in each batch mill, [min]
W	total mass of the feed, [kg]
w_i	Weight fraction of material of size *i*, [-]
w_j	Weight fraction of material of size *j*, [-]
x_i	Upper limit of particle size interval *i*, [mm]
α	Selection function parameter, [-]
β	Breakage function parameter, [-]
γ	Breakage function parameter, [-]
Λ	Selection function parameter, [-]
μ_B	Selection function parameter dependent on milling conditions and calculated for the Bond design mill, [mm]
μ_L	Selection function parameter dependent on milling conditions and calculated for the laboratory design mill, [mm]
μ_T	Selection function parameter corresponding to the reference ball diameter d_T, [mm]
Φ	Breakage function parameter, [-]

CHAPTER 1 INTRODUCTION

1.1 Background

In mineral processing, comminution is the primary step towards the recovery of minerals from the run-of-mine ore. Valuable material is liberated from within the run-of-mine (ROM) ore in preparation for downstream processing for recovery of that material. Comminution is the breaking of particles down to a smaller size. It can be done by crushing, grinding, and vibration amongst others. In ball milling, the breakage is achieved by impact and collision of particles against freely-moving grinding media in a rotary cylindrical device.

Milling can be described as the heart of comminution. It is the last comminution process before the processes of recovery begin. During the process of comminution, different parameters play a role in the production of the final product. These parameters such as feed flow-rate may vary with time. It is therefore important to note and identify the amounts at which these parameters yield optimum results of the required product. This work will identify such values.

Firstly, previous studies done on this work are reviewed. The literature on ball milling and attainable region theory is detailed. Then simulations on MODSIM® are presented. The results are presented and discussed. Lastly, conclusions are drawn based on the results observed.

1.2 Classical ball milling circuits

This work was important to identify the optimum milling flowsheet for the desired product. Different configurations of ball milling circuits exist and are motivated by the product required for downstream processes as well as end-user needs. The choice of circuit configuration is generally a matter of preference and experience while the final adoption of a particular one is done by trial-and-error. The main

reason behind the trial-and-error method is that it is not easy to estimate grinding performance, with the grinding rate being affected by a number of operational parameters (Akira *et al.*, 2004). What is currently known as an 'industry norm' regarding a certain type of circuit configuration for any mineral process was determined over time driven by the required product specification. In spite of the numerous operations around the work, milling circuits can be grouped into four classical configurations (Austin *et al*., 1984): open circuit, normal closed circuit, reverse closed circuit, and combined circuit. Figure 1.1 shows the combined circuit.

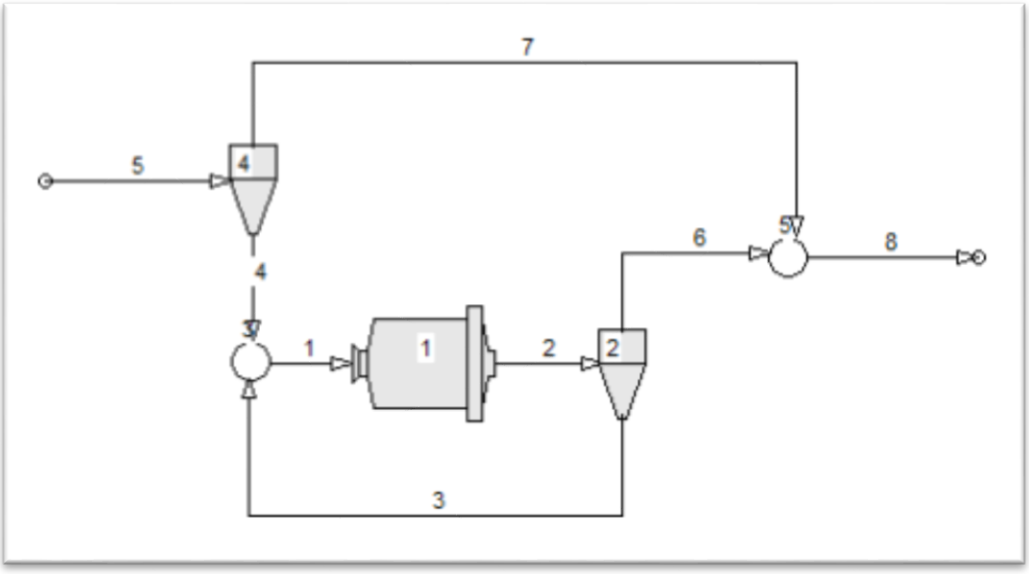

Figure 1.1 General single-stage mill circuit with pre- and post-classifiers known as the combined closed circuit

The other circuits are derived from this circuit. To result to an open circuit, the pre-classifier is set so that all the material fed to it reports as underflow of the classifier (stream 4 on Figure 1.1) to constitute the mill feed and the post-classifier is set such that all the mill product fed to it reports as oversize (stream 6) to be the circuit product stream. If only the pre-classifier is set so that all the material fed to it reports as underflow of the classifier to constitute the mill feed, the normal closed circuit results. If both the pre-classifier and post-classifier are the same

classifier, the reverse closed circuit results. Table 1.1 shows the derivation of the other circuits from the combined closed circuit.

Table 1.1: Derivation of other circuits from combined closed circuit

	Selectivity Values	
Different Configurations	**Pre-classifier**	**Post-classifier**
Open Circuit	All equal to 1	All equal to 0
Normal Closed Circuit	All equal to 1	All defined appropriately
Reverse Closed Circuit	All equal to post-classifier values	All defined appropriately
Combined Closed Circuit	All defined appropriately	All defined appropriately

The open circuit is the simplest type of configuration. What comes in comes out after being processed. The advantage is that it is the most economical of all the circuits. However, it is less efficient compared to the other circuits for complex feed material.

The normal closed circuit is most suited to a feed stream that is normally distributed, ideally comprising of the average of all particle sizes in the feed stream. It ensures that all particles are fed to the mill first. This is the post-classification circuit whereby the mill product not meeting the product specification is recycled back to the mill feed stream after milling. This increases milling efficiency while ensuring that the required product specification is achieved.

The reverse closed circuit is the best comminution circuit for a mono-sized feed stream, a stream of uniform distribution, aiding in the reduction of energy consumption if a sizable amount of the particles already meet the product specification. Through a process of classification, most commonly cyclone classification, the particles meeting the product specification are separated and bypassed from being fed into the mill, whilst the mill discharge is mixed with the cyclone feed stream for size classification. The cyclone is sized to have the

overflow stream as the product, meeting the required specification. The circuit reduces the load on the mill and therefore reduces energy consumption which contributes to reduced operating costs. The reverse closed circuit is also referred to a pre-classification circuit since classification takes place prior to milling.

The general milling circuit (combined circuit) consists of both the pre- and post-classifiers as shown in Figure 1.1. In the first classifier, classification takes place before milling to separate out the material already meeting the required product specification. In the second, classification happens after milling to recycle back the material not yet meeting the product specification. In a sense, this configuration is designed to ensure maximum production of the required product size for most of the feed material. This, however, may also result in an expensive undertaking in terms of energy consumption and capital costs to name but a few.

1.3 Statement of the research problem

A large amount of energy is needed to break the run-of-mine rock from a larger size to smaller sizes. This process needs to be monitored since over-grinding results in unnecessary energy wastage and may compromise the product size distribution thus affecting downstream processes (Samarak *et al.*, 2010). It is also necessary to find ways to reduce the time required for milling to achieve the required product specification (Jankovic and Sinclair, 2006).

Norgate and Jahanshahi (2010) noted that comminution processes consume as much as 70 % of the total energy cost in mineral processing plants. Energy costs in mineral processing have a significant influence on the total costs of operations in plants (Curry *et al.*, 2014). Also due to the strict requirements by downstream size constraints, the optimization of the comminution process is of paramount concern. The problem is in identifying the optimum values of each of the operational parameters involved in ball milling. This work tried to investigate these values. The use of the attainable region and the simulation of the process in

different configurations gave the optimum results of all possible outcomes. This method uses a set of values of all the output variables that can be achieved by any possible steady state process using a given feed.

1.4 Research questions

Comminution remains the most cost-intensive and energy-hungry process in mineral processing plants (Humphries *et al.*, 2010). It is the objective of process plants in mineral processing to increase productivity whilst keeping operating costs minimum. Morrell (2008) noted that different configuration circuits generally have different energy efficiencies. In the reverse closed milling circuit for example, the mill duty is reduced through feed classification. Milling is therefore done only on the fraction of feed that does not meet the product specification. This leads to reduced energy consumption and probably an efficient circuit. Irrespective of the circuit configuration, the ranges of operating parameters that enable the achievement of the product size specification at the highest production throughput while utilizing the lowest energy should be determined. It is equally important to select the best circuit configuration for a particular duty. It is in line with the above that this research work explored the use of the attainable region technique in ball milling operations. The following two questions that this study tried to address are:

- The identification of the optimum values for the operating parameters involved in ball milling; and
- The selection of the best performing circuit configuration.

1.5 Structure of the dissertation

This Chapter introduces the background of the work of this study, the statement of the research problem and the research questions. Chapter 2 presents the

literature around this work, what previous researchers have discovered and presented. It presents the population balance model, the milling process circuits and the attainable region. Chapter 3 discusses how the data was collected and presents in detail the operation of the simulation programme, MODSIM®. Chapter 4 presents the results from the simulations executed. Chapter 5 discusses these results. The last Chapter, Chapter 6, concludes on these results and presents the recommendations from this research work.

CHAPTER 2 LITERATURE REVIEW

The purpose of ball milling operations is to break down particles to smaller sizes for the liberation and subsequent recovery of the desired mineral (Coetzee *et al*., 2009). The breakage is achieved predominantly by abrasion, compression and impact in tumbling mills (Kwon *et al*., 2016; Metzger *et al.*, 2012; Wills and Napier-Munn, 2006; Austin *et al.*, 1984). In order to model ball milling, a detailed understanding of the underlying phenomena taking place inside the mill is required. Gupta and Yan (2006) reasoned that milling involves the selection of particles for breakage, the breakage of these particles and finally their transport through the mill. The processes happening at an infinitesimal level are more clearly described and understood through the population balance model, which is also referred to as size-mass balance model (Austin *et al.*, 1984).

In this chapter, the population balance model applied to milling is reviewed. Classical configurations of ball milling circuits are presented. And finally, the attainable region technique is discussed as a tool for the optimisation of milling circuits.

2.1 Population balance model

The development of a mathematical description of the grinding process was seen in the 20th century (Epstein, 1947). With particulate processes, a balance is required to describe the changes in the particle population during comminution (Verkoeijen *et al.*, 2002). This means that although breakage occurs during comminution, the balance of what goes in and out should be maintained by virtue of the principle of mass conservation.

The population balance model is a mathematical framework which applies to all processes involving particulate systems such as crystallization, agglomeration,

leaching, flotation, sedimentation and breakage. It is used to describe the process of particle evolution within the population of particles in milling. It models the kinetics of particles in all size ranges due to particle breakage, destruction and new particle formation (Bilgili and Scarlett, 2005) as in agglomeration. The population balance model provides a framework for the description of ball milling. The framework is basically a mass balance around the comminution equipment (Otwinowski, 2006). Simply put, the model enables one to calculate the product size distribution expected from a ball mill. The calculation is done for a predefined feed size distribution and under selected milling conditions.

The feed material is generally characterised according to mass fractions falling within predefined size intervals. Indeed, particles are not all of the same size, and thus for sizing purposes, an inventory of particles is made per size classes following the standard sieve sizes. The size classes are size intervals resulting from a sequence of $2^{1/2}$ of sieves. The top size interval is size class 1, the second is size class 2, and the third is size class 3, until the last interval which is the n^{th} size class. The last size class is comprised of the finest of the particles in the material while size class 1 is a selection of the coarsest particles in the feed.

During comminution, new smaller particles are formed as others are broken down. The rates at which particles are broken down and new ones are formed are noted as a function of time (Metzger, 2011). The inventory accounts for three types of particles: those topped up to the mill feed, those created as a result of size reduction inside the mill, and those discharged through the mill product stream.

There are four basic categories of the population balance model: (1) discrete size, time continuous; (2) discrete size, discrete time; (3) size continuous, time continuous; and (4) size continuous, discrete time (Teng *et al*., 2010). The first category is the most common since particle size is defined in terms of size intervals. The second is a simplified version of the first category the same way the fourth is of the third.

The size continuous, time continuous category is the most generic version of the population balance model. It is basically a set of linear differential-integral equations descriptive of processes involving particulate systems amongst others. Henryk (2006) noted that applying discretization methods to the population balance model has made solving the linear differential-integral equations easy with numerical tools. Hence, numerical methods have been developed in the last years (Kumar and Ramkrishna, 1997; Prasher, 1987; Ramkrishna, 2000; Vanni, 2000). The models based on the population balance framework predicting the particle size distribution of the comminution equipments are called stochastic or statistic models. They are regarded as the creators of the stochastic model of comminution (Eipstein, 1947; Sedlatschek and Bass, 1953; Broadbent and Callcott, 1956; Gardner and Austin, 1962). The population balance model of the material particles and required comminution product class takes the simplified form (Teng *et al*., 2010)

$$p_i = f_i + \tau\left(\sum_{\substack{j=1 \\ 1>1}}^{i-1} b_{ij} S_j w_j\right) - S_i w_i \tau \quad n \geq i \geq j \geq 1 \tag{2.1}$$

where

p_i mass fraction of the final mill product present in size class *i*

f_i mass fraction of the initial feed in size class *i*

S_i is the selection function of particles of the ith size interval

B_{ij} is the cumulative breakage distribution function for particles of size *j* reporting to size i after breakage

w_i is the weight fraction of material of size i

w_j is the weight fraction of material of size *j*

2.2 Ball milling

Breakage within a mill occurs in three different ways depending on the stress applied on the particular particle: abrasion, impact and compression (Prasher, 1987). This basically means that a particle will break in relation to how it is impacted for breakage. The selection function defines the rate of breakage whilst the force applied during breakage determines the type of breakage taking place.

2.2.1 Breakage Mechanisms

2.2.1.1 Abrasion breakage

Abrasion in milling is the act of wearing away the parent particle by rubbing or scraping against it during milling, resulting in the birth of one or more particles which are finer in size.

The abrasion breakage mechanism increases with particle size until such a point where the stress exerted results in the particle developing crack, from which time impact breakage mechanism is observed.

2.2.1.2 Impact breakage

Impact breakage occurs when the energy applied onto the particle exceeds its fracture energy (Wills and Napier-Munn, 2006; King, 2001). Different particles within a mill experience different levels of energies applied to them, resulting to the different forms of breakage (Kwon *et al*, 2016). Particles within the mill are subjected to impact breakage when they collide with other particles, with grinding media and/or with the mill shell. The constant application of excessive stress exerted on a particle results to impact breakage (King, 2001).

2.2.1.3 Breakage by compression

Breakage may occur under the compression mechanism. The compressive strength of a particle is its ability to resist breakage before failure occurs. Compression is the act of applying intensely excessive stresses against particles (Monov *et al*., 2012).

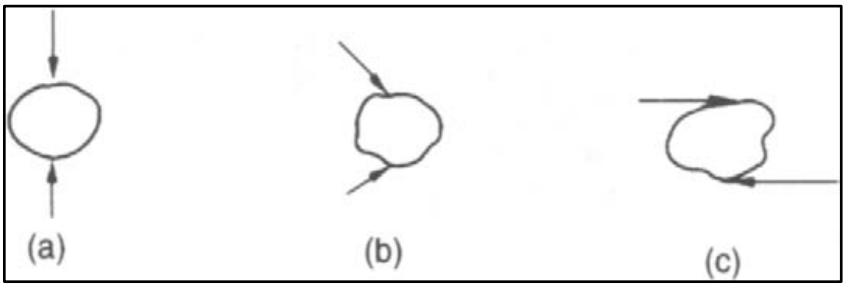

Figure 2.1: Mechanisms of breakage (Wills and Napier-Munn, 2006): (a) impact or compression, (b) chipping, (c) abrasion

2.2.2 Milling parameters

2.2.2.1 Ball and Powder Filling

For efficient milling, the ball and powder loading have to be within a certain range. Ball loading refers to the volume occupied by the balls (grinding media) within a stationery mill relative to the total volume of that mill (Austin et al, 1984). Powder loading refers to the volume of powder (feed) loaded into the mill relative to the volume of ball interstices available for filling within the balls. It is undesirable that at a certain ball loading the mill be under-filled or over-filled with powder. Under-filling is when the powder level within the mill is low such that much of the energy during mill rotation is wasted in ball-to-ball contact (Austin *et al.*, 1984). During under-filling, much energy is lost due to ball-to-ball contact and this occasionally leads to the generation of more fines because the fine material is ground faster resulting in over-grinding (Austin *et al.*, 1984). Overfilling occurs when the ball interstices are completely filled, and the powder is in excess resulting in reduced contact breakage. During overfilling, the powder cushions the breakage action slowing down the rate of breakage. As fine particles accumulate in the mill this

gives rise to non-first-order breakage. An expression was developed by Shoji *et al.* (1979) to model the effects of ball and powder loadings and later simplified by Shoji *et al.* (1982) to be used over the normal breakage region and also incorporating the variation of ball loading. This gave

$$S(f_c,J)\alpha\ a\ \alpha\frac{1}{1+6.6J^{2.3}}exp[-cU], 0.5 \leq U \leq 1.5, 0.2 \leq J \leq 0.6 \quad (2.2)$$

where c is 1.2 for dry grinding and 1.32 for wet grinding.

2.2.2.2 Mill Speed

The specific rates of breakage vary with the rotational speed of the mill. The maximum breakage is a function of mill diameter, ratio of ball to mill diameter, and ball filling and powder filling conditions. Usually the maximum is found anywhere between 70 % and 85 % of the critical speed. The critical speed is the theoretical mill speed at which a ball starts to stick to the mill wall during mill rotation, centrifuging (Austin *et al*, 1984 and Mulenga and Bwalya, 2015). The critical speed is given by the following equation:

$$N_c = \frac{1}{2}.\sqrt{\frac{2g}{D-d}} = \frac{0.705}{\sqrt{D_B-d_B}} \quad (2.3)$$

where

D_B is the mill internal diameter

d_B is the grinding ball under consideration's diameter

g is the gravitational acceleration

The empirical fit to data by Austin *et al.* (1984) gives the following expression to correct S values from one rotational speed to another.

$$S_i\alpha(\emptyset_c - 0.1)\left(\frac{1}{1+exp[15.7(\emptyset_c-0.94)]}\right), 0.4 < \emptyset_c < 0.9 \quad (2.4)$$

2.2.2.3 Ball Diameter

The larger the feed material, the bigger the ball should be, and the opposite is true for smaller balls. Sizes of spherical grinding balls commercially available range between 10 mm and 150 mm. That is the effective operating range for ball sizes in grinding mills and that is the range MODSIM® was based on in its model development. To determine the appropriate initial ball size to be used when for effective breakage in this study Coghill and Devey's equation (Gupta and Yan, 2006) was used:

$$\mathrm{d_B} = 0.4\mathrm{K}\sqrt{\mathrm{W}} \qquad (2.5)$$

where

$\mathrm{d_B}$ is the ball diameter in cm,

W is the feed size in cm

K is a proportionality constant described as the grindability factor.

This equation states that the ball diameter is related to the maximum size of the feed material. The value of K is 37.4 for hard ores and 29.8 for soft ores. This value incorporates the work index, the largest particle size and size distribution and the S.G of the solids.

To determine the largest ball size to be used Rowland and Kjos (1980) considered the same variables and concluded that the size can be estimated by:

$$\mathrm{d_B} = 25.4\left[\left(\frac{\mathrm{W_{80}}}{\mathrm{k}}\right)^{0.5}\left(\frac{\rho_s \mathrm{W_i}}{100\emptyset_c(3.281\mathrm{D}_B)^{0.5}}\right)^{0.33}\right] \text{ in mm} \qquad (2.6)$$

where

$\mathrm{d_B}$ is the ball diameter

D_B is the inside diameter of the mill in m

W_{80} is the 80 % passing size of the feed material

W_i is the Bond work index

ρ_s is particle density

k is the mill factor constant (37.4 for hard ores and 29.8 for soft ores)

2.2.3 Optimisation of Milling Operations

The process of milling is considered as a process of repetitive steps of breakage combined. Eipstein (1948) noted that each step can be described by the selection rate function, the breakage rate function and the distribution function. The population balance model utilises the selection function and breakage function parameters. The estimation of these functions is often determined by impact tests (Rozenblat, 2012). The number of particles that break is determined and by sieving, the size distribution of the classes is determined.

2.2.3.1 Selection Function

The selection function is a breakage rate considering the probability of particles to be reduced. Researchers such as Austin *et al* (1984) concluded that in a breakage size interval process, the disappearance rate of the top size can be described as following a first order trajectory, as described in Section 2.3. A plot on the logarithmic line of the top size interval population balance model gives a straight line if the breakage rate does not vary with time (Wang *et al*, 2011). However, if there is variation of the breakage rate with time, a non-first order breakage is observed.

2.2.3.2 Breakage Function

The breakage function is a function of comminution that describes the size distribution of the sizes and the number of sizes if the breakage mechanisms force

the particle to break (Rozenblat, 2012). The parameters of the breakage function are dependent on the environment in which milling is taking place (Olejnik, 2012).

2.2.3.3 Residence Time Distribution

The residence time distribution (RTD) is an important function to understand the process of milling. Experiments support the assumption that the material entering the mill flows and mixes independently without being influenced by the particle characteristics such as size, shape and density (Austin et al, 1984). Plug flow behaviour and fully mixed behaviour are the two extremes of residence time distribution. Plug flow is associated with batch milling whilst the fully mixed behaviour is associated with continuous milling and expressed as Equation 2.1. This research work is based continuous milling.

2.3 Classical ball milling circuits

There are different ball milling circuit configurations and the choice of the preferred one depends on the required product specification (Steyn *et al*., 2010). To avoid over-grinding, ball milling is usually done in closed circuits (Toneva and Peukert, 2007).

The four classical configurations are shown below: Figure 2.2 depicts the simplest circuit configuration. The feed material is directly fed into the mill to be broken down and the product sent to downstream processes as required. This circuit has no classifier. This circuit is suitable for simple feeds, feeds which can easily and/or immediately be broken down to the required product size specification. However, its reliability and efficiency lowers the more complex the feed is and the more narrow the product specification range is (Austin *et al*., 1984).

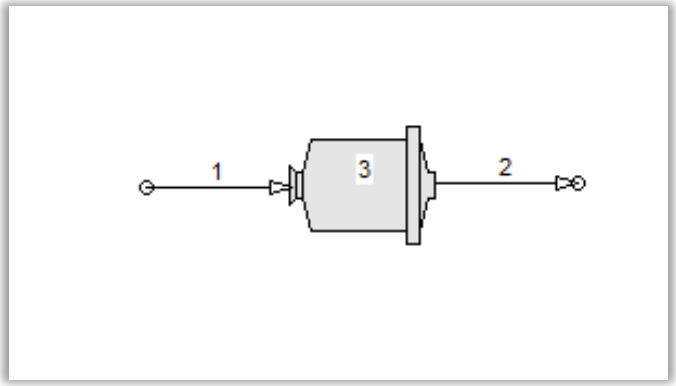

Figure 2.2 Ball milling in open circuit. Stream 1 is the feed stream and stream 2 is the product stream. Unit 3 represents the ball mill

Figure 2.3 shows the normal closed circuit. This circuit has a post-classifier, returning the underflow back into the mill feed for further grinding. The product material not meeting the specification is recycled back to the feed as cyclone underflow to ensure that the final product meets the required specification. If W (stream 2 in Figure 2.3) is the total mass flow rate of the mill feed and G (stream 1) is the total mass flow rate of the fresh feed to be combined with the recycle, then the mill feed is related to the fresh feed according to the following equation (Austin *et al*., 1984):

$$W(1+C) = sP(1+C) + G \tag{2.7}$$

where C is the circulation ratio, given by the flowrates of the recycle stream R (stream 5) to the circuit product stream Q (stream 4)

$$C = \frac{R}{Q} \tag{2.8}$$

The circulating load, being the ration of the total mill feed flow rate to the final circuit product is given by

$$\frac{F}{Q} = 1 + C \tag{2.9}$$

The circulating load is the total flow rate that is recycled back into the mill as cyclone underflow, coarse material, due to failure of meeting the required product specification (Silva *et al.*, 2013).

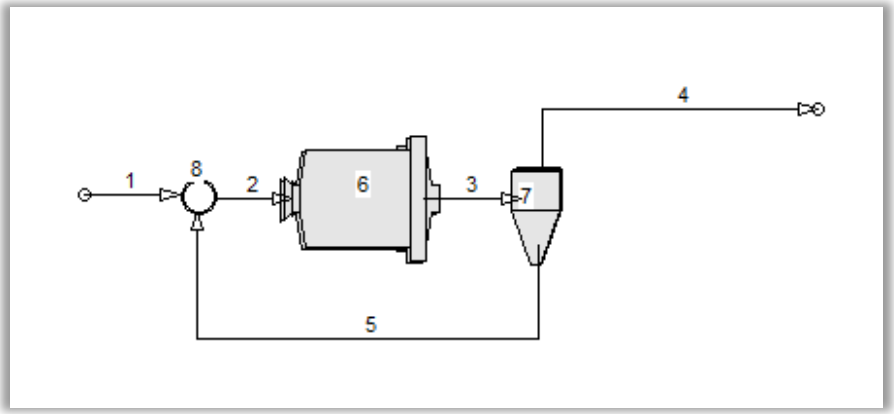

Figure 2.3 Ball milling normal closed circuit. Stream 1 is fresh feed, stream 2 is the total mass flow-rate of the mill feed, stream 3 is the mill product, stream 4 is the circuit product and stream 5 is the recycle stream. Unit 6 is the mill, unit 7 is the hydrocyclone classifier and unit 8 is a mixer

The main purposes of a cyclone, specifically the hydrocyclone, are size classification, desliming and dewatering. In size classification, the objective is to separate the required size of the product specification from the coarse material (Coetzee *et al.*, 2010). In desliming, the objective is to remove the very fine particles from the required coarse material as final product. In dewatering the objective is to remove the excess water as overflow with the purpose of increasing the density of the underflow. The water is usually recovered for re-use in other processes. Mclvor (2006) found that the circuit efficiency can be improved by increasing the circulating load within that circuit. A low circulating load resulted in the production of more fines. Increasing the circulating load gradually increased the circuit production rate, with a slightly greater amount of coarser material within the required product specification.

The third group of milling circuit depicted in Figure 2.4 is the reverse-closed circuit. It separates out those fine particles meeting the product specification before

feeding into the mill. This saves the energy usage. This circuit also acts as a post-classifier with the hydrocyclone classifying the mill product and returning the underflow for further grinding.

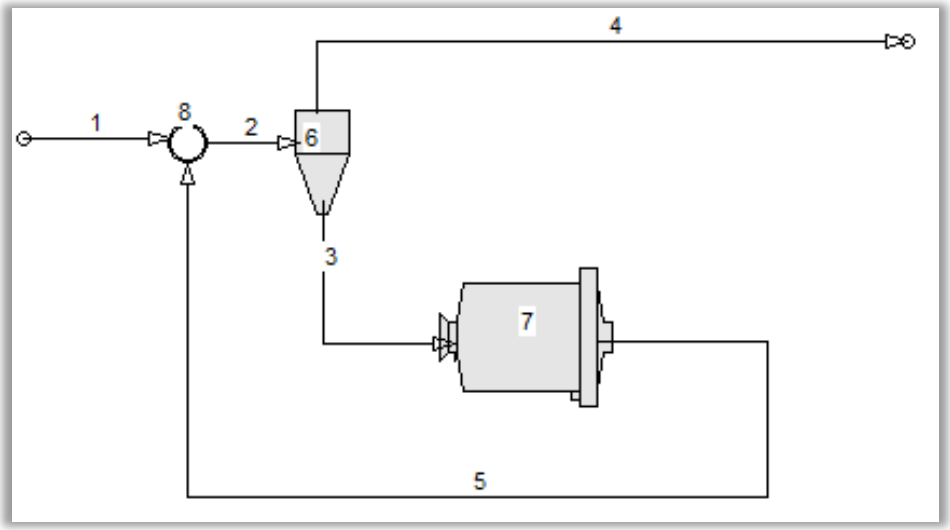

Figure 2.4 Ball milling reverse closed circuit. Stream 1 is fresh feed, stream 2 is the total mass flow-rate of the hydrocyclone classifier, stream 3 is the mill feed, stream 4 is the circuit product and stream 5 is the recycle stream. Unit 6 is the hydrocyclone classifier, unit 7 is the mill and unit 8 is a mixer

The combined milling circuit consists of both the pre-classifier and post-classifier. Both classifier overflows are mixed together as the final product (Austin *et al.*, 1984). This is regarded as the most efficient configuration compared to the previous three since the material meeting the product specification in the feed stream is separated before feeding the mill to be mixed with the product and also the mill product not meeting the product specification is recycled back to the mill. This all ensures that the product specification is met or at the least the product is as close as possible to the required quality as dictated by downstream processes such as flotation and leaching. Figure 2.5 depicts this arrangement.

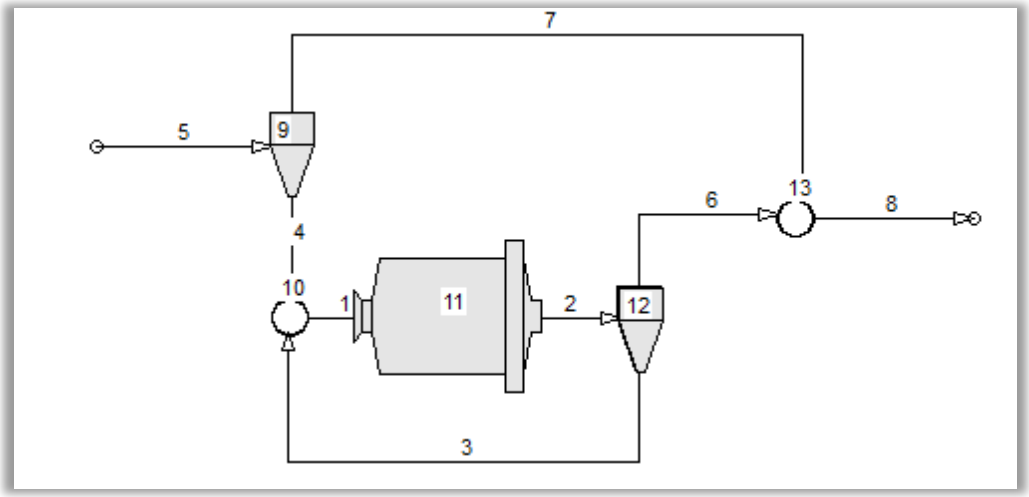

Figure 2.5 Ball milling general combined circuit. Stream 1 is the mill feed, stream 2 is the mill product, stream 3 is the recycle stream, stream 4 is the circuit product and stream 5 is the fresh feed, stream 6 is post-classifier product, stream 7 is the pre-classifier overflow and stream 8 is the combined circuit final product. Unit 9 is the hydrocyclone pre-classifier, unit 10 is the mill feed mixer, unit 11 is the mill, unit 12 is the hydrocyclone post-classifier and unit 13 is the circuit product mixer

It is therefore understood that if a milling parameter such as ball filling is changed, a different product size distribution will be obtained. In addition to this, the efficiency of the milling operation will be altered since the environment within the mill is being altered (Wei and Craig, 2008). For example, it is neither undesirable to over-fill nor under-fill the mill with slurry for a given ball filling. Altering the slurry filling by decreasing it results to a cushioning effect where the particles do not experience enough ball action for breakage. Increasing the amount of ball filling more than necessary results in increased ball-to-ball impact; thus, wasting more energy.

If material is fed into a mill to be ground to smaller sizes for a time interval, analysed and returned back into the mill for further grinding, it has been assumed without fundamental reasons that the rate of disappearance of the parent size (original feed size) fits a first-order criterion as below (Austin *et al*., 1984):

$$-\frac{d[w_1(t)W]}{dt} \ \alpha \ w_1(t)W$$

where W is the total mass. Therefore:

$$\frac{dw_1(t)}{dt} = -S_i w_i(t) \qquad (2.10)$$

where S_i is the proportionality constant, called the specific rate of breakage with units of time^{-1}

The rate of breakage (selection function) in tumbling mills, the ball mill in this study, is determined by (Austin *et al.*, 1984)

$$\mathrm{S_i} = \mathrm{a}\left(\frac{\mathrm{x_i}}{1000\mu\mathrm{m}}\right)^{\alpha} \mathrm{Q_i} \qquad (2.11)$$

where

$\mathrm{x_i}$ is the particle size.

a varies with mill conditions. Its units vary with the values of α.

α is a material dependent characteristic and varies between 0.5 and 1.5.

$\mathrm{Q_i}$ is a correction factor to allow for the smaller mean rate of breakage of the bigger particles in a mill. Large sizes often become too strong to break in a mill, resisting fracturing.

$\mathrm{Q_i} = 1$ for smaller sizes and gets smaller for larger sizes. It is determined by

$$\mathrm{Q_i} = \frac{1}{1+(\mathrm{x_i}/\mu)^{\Lambda}}, \Lambda \geq 0 \qquad (2.12)$$

where

μ is the particle size at which the correction factor is ½. μ varies with mill conditions.

Λ is a characteristic of the material which is a positive number. It is an index of how often the rates of breakage fall as size increases.

The value of α normally ranges between 0.5 and 1.5 whilst the value of a varies with mill conditions. The values at which S is a maximum at the maximum size values of x_m vary from material to material, being larger for weaker particles which break more easily. The relationship between S and μ where μ is the particle size at a certain correction factor is

$$\mu = \left(\frac{\Lambda - \alpha}{\alpha} \right) x_m \tag{2.13}$$

Λ is always greater than α.

2.4 Hydrocyclones

Hydrocyclones are unit operations used to separate or classify particles suspended in a fluid based on their size. They are used either for classification, desliming or dewatering purposes. They separate a feed stream containing water and solid particles into a coarse fraction that reports as the underflow and a fine fraction reporting as the overflow. The feed stream is introduced under pressure with the solids subjected to centrifugal forces and drag forces in the hydrocyclone. Hydrocyclones are simulated using either of the two models developed by Plitt (1976) and Nageswararao (1978).

In Plitt's model structure there are dependent and non-dependent design variables (Irannajad, 2006). The dependent variables are cyclone throughput (Q), corrected cut size ($\mathrm{x_{50c}}$), volumetric flow split (S), and sharpness of classification (m). The non-dependent variables are the diameter of the cyclone ($\mathrm{D_c}$), the vortex finder ($\mathrm{D_o}$), the spigot ($\mathrm{D_u}$), the inlet ($\mathrm{D_i}$), and the free vortex height (h).

The mass balance around the hydrocyclone considers the mass flow rates of the feed stream, the underflow stream and the overflow stream. The selectivity

number for a size is defined by the ratio of the underflow stream (often to be recycled) to the feed stream. The fraction therefore sent to the finer stream becomes $1 - s_i$. The assumption here is that the classification is first-order. plotting the selectivity numbers against size produces a tromp curve, which is a partition curve.

2.5 Attainable region applied to ball milling

The attainable region (AR) is a method that was initially developed for the analysis, the design and the blending of chemical reactor networks (Khumalo, 2007). It was intended to assist in identifying the optimum milling circuit and all possible outcomes. This tool describes the set of all possible outcomes that can be achieved by the processes working within a particular system and subject to the constraints of that system.

It is now finding increasing application in comminution operations and in ball milling in particular. Metzger (2011) for example used the technique successfully to study ball milling for pharmaceutical applications. He also noted that one of the benefits or strengths of the AR tool is its capability to compare the results obtained from varying a parameter with the aim of identifying its optimal limits for production (Metzger, 2012). The AR technique is a tool that permits one to determine the set of all realisable or possible outcomes from a process of operation (Glasser and Hildebrandt, 1997). From this set, the optimal operating conditions meeting the stipulated standards under the specific constraints of the system can be identified (Khumalo *et al*., 2008).

A limitation of the attainable region technique is that it has not effectively been able to show the influence of the slurry density on the production of the required product. This is mainly a result of it being based on the population balance model which currently does not incorporate slurry concentration. Alternative methods investigated by other researchers to optimize ball milling operation include the

classification system efficiency method which is used to measure and increase the efficiency of ball milling (Mclvor, 2014).

As far as ball milling is concerned, the AR methodology has been used to generate the comminution path required to efficiently achieve a given product size distribution from a laboratory batch mill (Metzger, 2011). Furthermore, Mulenga and Bwalya (2015) demonstrated the potential of the AR technique in the optimisation of industrial milling operations under downstream size constraints. The AR method can be extended to classical circuit configurations.

It is important to note how the attainable region profile changed from circuit configuration to circuit configuration. That is what was undertaken in this research project.

2.6 Summary

This Chapter discussed the theoretical knowledge around ball milling. The population balance model which describes the process of grinding was presented. It utilizes the selection function and the breakage distribution function which are the functions of milling. The breakage mechanisms taking place during milling were discussed. The milling parameters under consideration in this study were also discussed. The different ball milling circuits were presented, their advantages and limitations discussed. The classifying hydrocyclone was also discussed. The attainable region was briefly discussed and will be fully presented practically in the Chapters to follow.

CHAPTER 3 DATA COLLECTION AND SIMULATION PROGRAMME

3.1 Introduction

This chapter details the procedure adopted in this study to generate the data for later analysis. All the work carried out was by computer simulation using MODSIM®, a simulator for mineral processing plants.

The software package is centred on the population balance modelling framework that makes it possible to perform the mass balance for any ore dressing plant amongst others (Mazzinghy *et al*., 2014). Also included in the simulation outputs are the water and solids flow-rates, the particle size distributions, the mineral grade compositions and the average mineral assays of all streams making up the flowsheet diagram of the plant. Metal content, element content and mineralogical makeup can all be included in the assay. A detailed report is generated and produced for the performance of each unit operation. The report can be used for detailed equipment design, equipment selection, costing as well as equipment and process evaluation. MODSIM® can accommodate a range of particulate properties such as mineralogical texture, particle shape and surface characteristics. These properties are known to have an impact on the behaviour of unit operations in mineral processing.

MODSIM® is organised around a library containing a number of modules. Within these modules are different unit operations, each with different models to choose from depending on the amount of data available. It has the capacity to allow the inclusion of additional models for unit operations. MODSIM® has the flexibility of permitting the addition of new models and/or the modification of existing models. This allows the incorporation of new developments in mathematical modelling of the unit operations.

One of the major advantages of MODSIM® over other simulation packages is that it can simulate the liberation of mineral species during comminution processes of crushing and milling. This means that the whole comminution process behaviour can be monitored, modified to suit the product requirements and controlled from feed through the product instantaneously. JKSimMet is another simulator which could have been used. The disadvantage with JKSimMet is that detailed feed characteristics are required for the mill and cyclone models to be applicable (Runge *et al*., 2014). The academic version 3.6 of MODSIM® was used for this work.

3.2 How MODSIM® is used

MODSIM® is a user-friendly simulator. The flowsheet is graphically constructed under the graphic editor. This graphic editor is run from the main menu, under the FILE drop-down menu, by starting a new job. This main menu is shown in Figure 3.1.

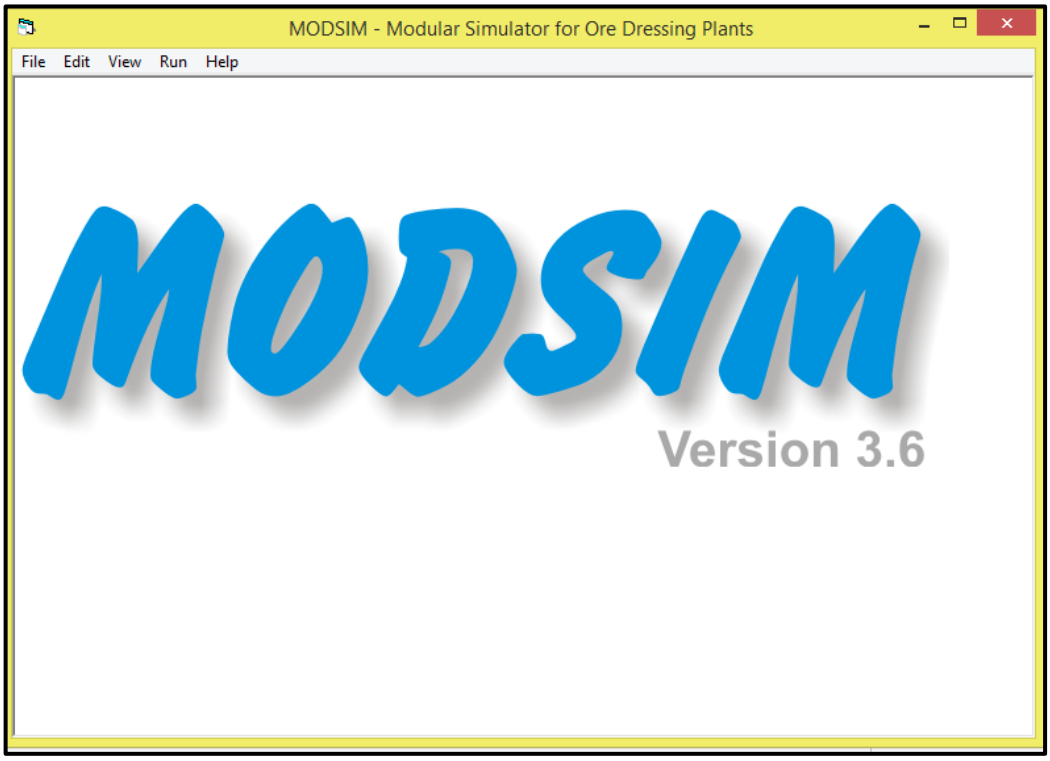

Figure 3.1 Main menu where operation is initiated in MODSIM®

From FILE a new job can be started, a previously saved existing job opened, the current job closed, and the current job saved. Jobs can also be packed into a single file for easy transfer.

From EDIT the following can be edited: the flowsheet, the system data, the unit model parameters, the output file format, and the name of the current job.

From the VIEW drop-down menu, instruction to view the following can be made: the flowsheet, the simulation results, the data output file, the report file, the stream properties, the particle size distribution (PSD), and the liberation distribution plots for each stream in the flowsheet, as shown in Figure 3.2.

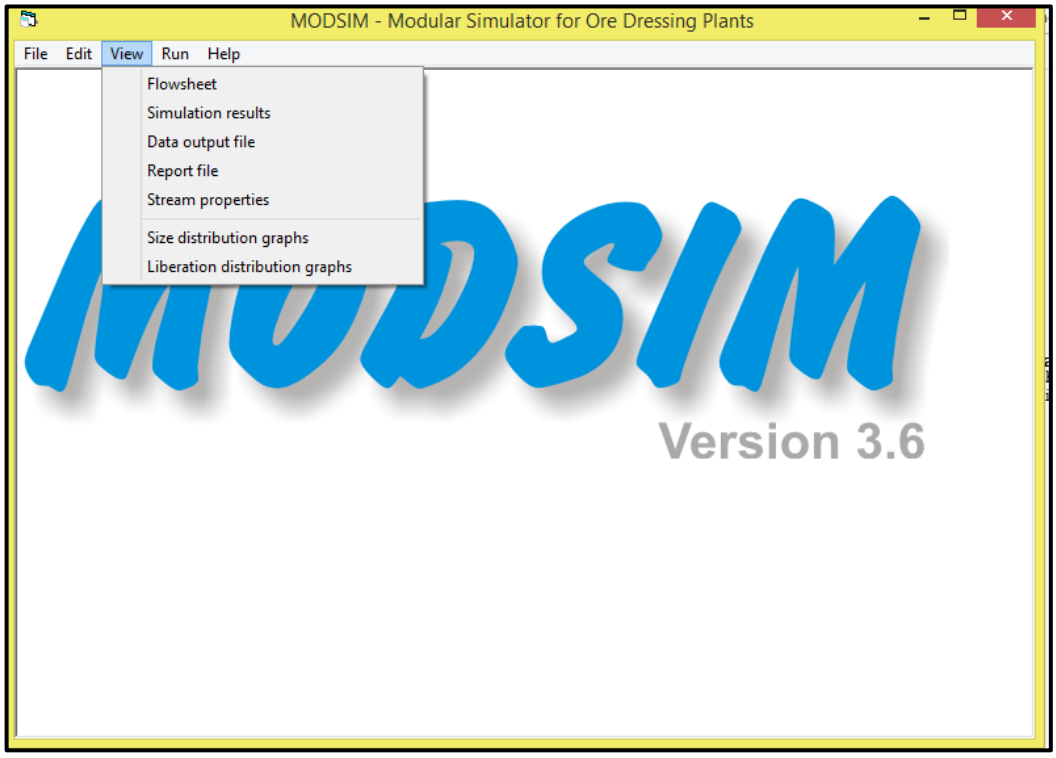

Figure 3.2 VIEW drop-down menu within the main window of MODSIM®

The RUN menu enables one to request execution of the final simulation model built in MODSIM®. The professional version has the flexibility of running repetitive simulations to find optimal combinations of model parameters. Five different files that assist in diagnosing any problems are found under RUN in the academic version while a sixth one is available in the professional version of MODSIM®.

3.3 Graphical Editor under MODSIM®

A flowsheet is one or more unit operations connected through the streams between them. The graphical editor is activated from the FILE menu by selecting the 'Start a new job' item. From the menu of the graphical editor, the unit operation of choice is selected from SELECT as shown from Figure 3.3. The streams are added from EDIT, where a choice of two different types of streams for slurry is available.

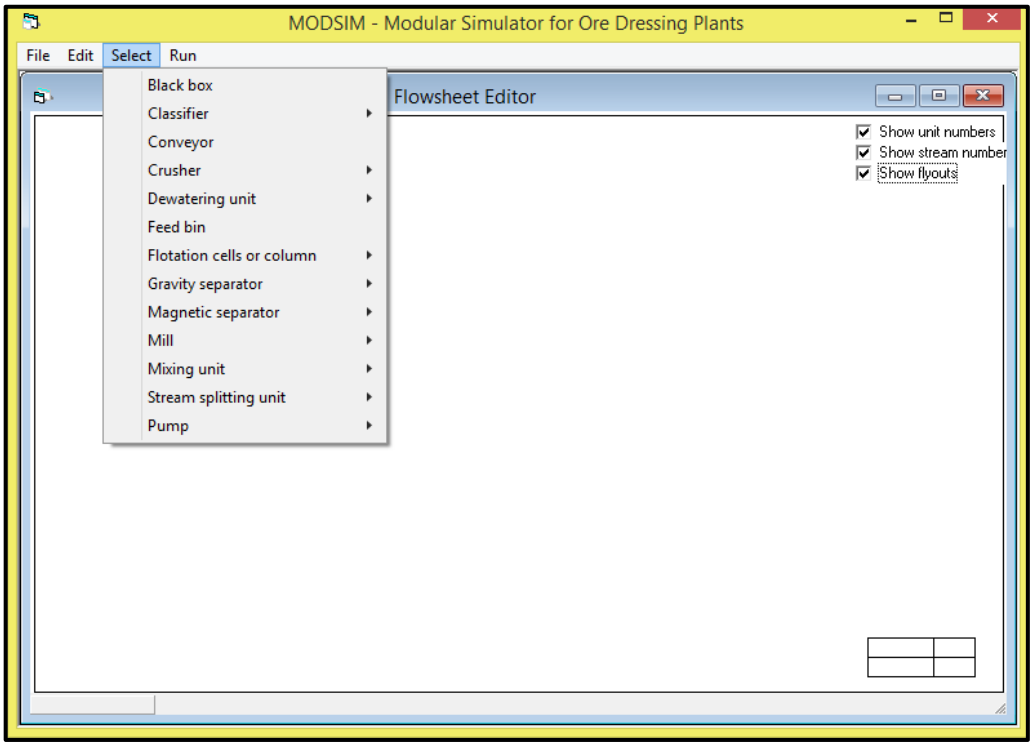

Figure 3.3 SELECT drop-down menu within the graphical editor of MODSIM®

The diagonal, 'Rubber-band cursor', is chosen if the input stream has to be diagonal. The horizontal and vertical, 'Rectangular cursor', is chosen if the input stream is to be horizontal or diagonal. The 'Add water stream' option permits the user to add a water stream to the unit operation in processes where dilution or density control is required. A stream is started from a unit operation to a unit operation except for the flowsheet feed streams and product streams. Feed streams are the beginning of the flowsheet and they end at a unit operation.

Product streams start from a unit operation and become the end of the flowsheet. Units only have a single feed stream except for a mixer, a sump and stockpile. These three apparatuses are the mixing units of MODSIM®. Thus, if a unit has to be fed by multiple streams, a mixer is placed before it. The exception to the single feed stream principle is the addition of a water stream. Water can be added to any unit where the need arises. To execute a simulation, the flowsheet is first drawn in the graphical editor.

The units and streams can be deleted from the flowsheet. This is done by clicking 'Delete' from the EDIT drop-down menu. Figure 3.4 shows this menu.

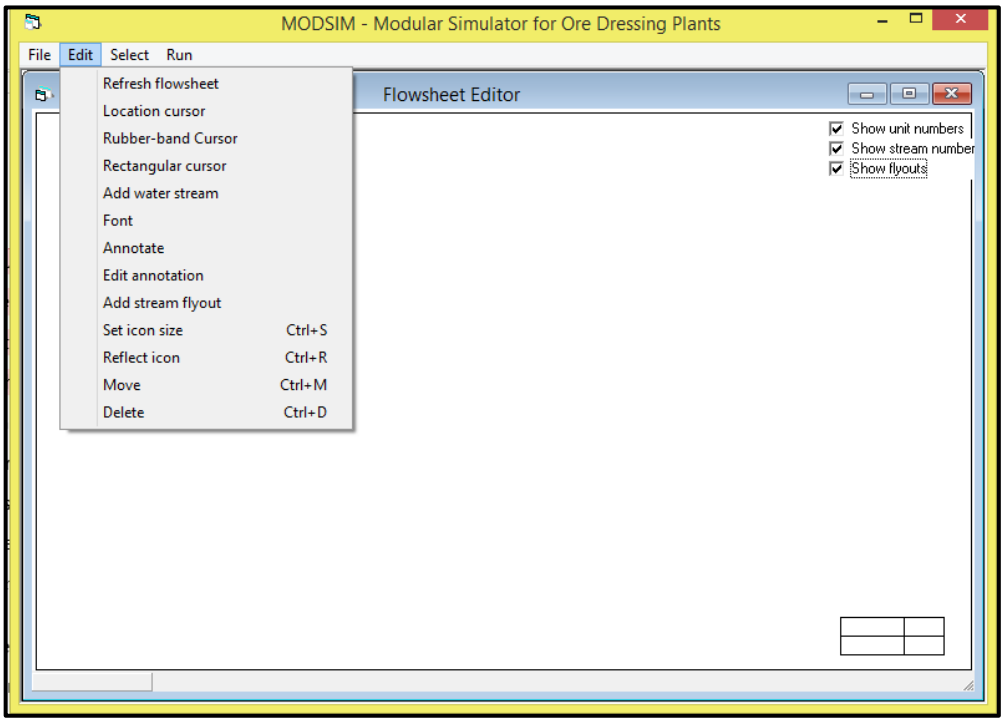

Figure 3.4 EDIT drop-down menu within the graphical editor of MODSIM®

Deleting a unit operation automatically deletes all streams connected to it. The units can also be moved within the graphical editor by selecting 'Move' from EDIT. Moving a unit deletes all output streams connected to it. Unit sizes are varied by selecting 'Set icon size' from EDIT before placing the unit. MODSIM® permits annotations to be added on the flowsheet. Annotations can be moved and deleted

at any point the same way these actions are performed on the unit operations. Annotations are added by selecting 'Annotate' from EDIT.

Once the flowsheet has been set-up, it is then accepted. Accepting the flowsheet is done by selecting 'Accept flowsheet' from the FILE menu. This takes the user back to the main window menu in Figure 3.1. From this window the system data is edited from EDIT by selecting 'Edit system data'. This is where all the streams can be named and where the feed characteristics and flows are specified. The feed streams are specified by stating their flow-rates, composition and particle size distribution. The details of each feed stream are entered into an input form. Figure 3.5 shows an example of the input form used for stream details. Stream names are supposed to start with an alphabetic letter.

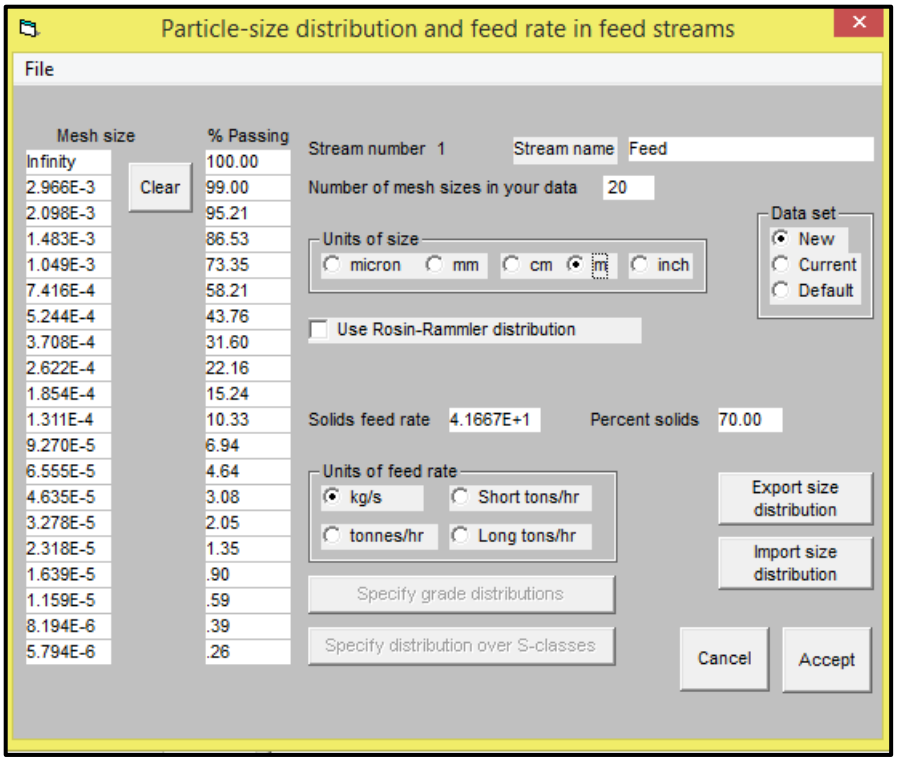

Figure 3.5 Feed stream input parameters

Once all the feed streams have been fully specified, the unit models must be selected. In order to simulate the process, each unit operation must be modelled. A choice of models is available for each unit operation. The selection of a specific model for each unit is based on what the behaviour of the unit is expected to be.

Models are found within the EDIT menu by selecting 'Edit unit model parameters' as shown in Figure 3.6.

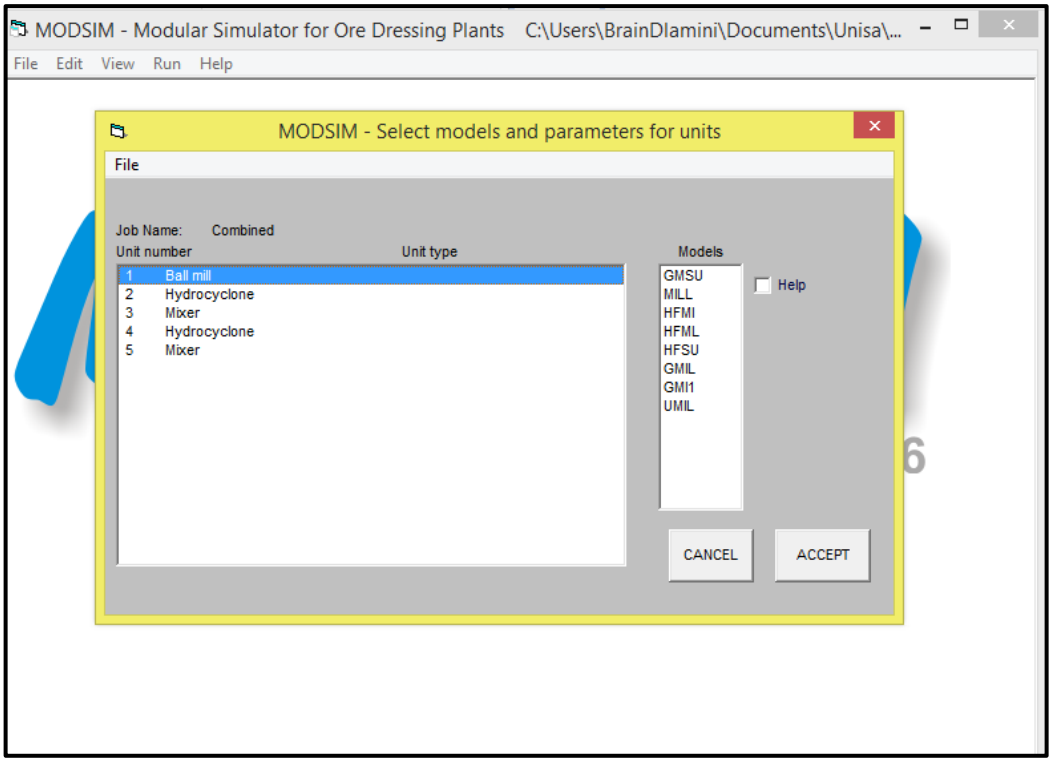

Figure 3.6 Illustration of the ball mill models available in MODSIM®

The flowsheet for this work contained a set of two unit operations, the ball mill and the hydrocyclone. These two unit operations are explained in the next sections.

3.4 Ball Mill

A ball mill is a unit operation used in comminution to grind and break down particles from their original size to smaller sizes. Size reduction is done by either abrasion, impact or compression or a combination of any of these. For the ball mill, the GMSU model was chosen. Table 3.1 shows the ball mill models of MODSIM® and their input parameters. The ball mill has a choice of 8 different models on MODSIM®. The GMSU model used in this study is discussed.

GMSU – this model is the ball mill model with Austin's scale-up procedure. Mixing is modelled using three perfectly mixed regions in series. For this model to be used, the selection and breakage functions parameters should have been determined from laboratory batch tests and the full-scale mill dimensions known. This is the model that was chosen for this study due to its detailed nature and its ability to be used for scale-up scenarios as the mill dimensions are specified. This model assumes that post-classification is present. As developed in King (1990), the liberation of the mineral phases is computed using the Andrews-Mika model. The selection and breakage function parameters used were those determined by Evangelos and Konstantinos (2017).

Table 3.1: MODSIM® Ball Mill parameters

Model	Input Parameters
GMSU	$a; \alpha; \mu; \lambda; \beta; \gamma; \delta; \emptyset$
MILL	$a; \alpha; \mu; \lambda; \beta; \gamma; \delta; \emptyset$
HFMI	$P; a; \zeta_1; \zeta_2; \beta; \gamma; \delta; \emptyset$
HFML	$P; a; \zeta_1; \zeta_2; \beta; \gamma; \delta; \emptyset$
HFSU	$P; a; \zeta_1; \zeta_2; \beta; \gamma; \delta; \emptyset; D; L; J; U\ N; x$
GMIL	$\tau; a; \alpha; \mu; \lambda; \beta; \gamma; \delta; \emptyset$
GMI1	Mill hold up; $a; \alpha; \mu; \lambda; \beta; \gamma; \delta; \emptyset$
UMIL	Residence time

Figure 3.7 shows the input page on MODSIM® for the GMSU model parameters. The ball mill model parameters are shown in Table 3.2

Table 3.2: Milling Parameters

Selection function parameters	$\boldsymbol{a}$	0.46
	α	1.13
	μ	2.11
	Λ	3.15
Breakage function parameters	β	6.2
	γ	0.8
	δ	0
	$\emptyset$	0.6

Simulations were run for each individual circuit configuration. Five parameters were varied for each circuit: feed flow rate F; mill speed ϕ_c; ball filling J; ball diameter $d_{\max}$; and slurry concentration by mass C_w. Eight simulations were run in each circuit while varying the feed flow rate from 10 tph to 150 tph. Seven simulations were run for each circuit whilst varying the mill speed from 30 % to 90 % of critical. The choice of this range was governed by Equation 2.4. To simulate the effects of ball filling, four simulations were run by varying ball filling from 20 % to 60 %. The choice of this range for ball filling was governed by Equation 2.2. Eight simulations were run for each circuit to simulate the effect of ball diameter on the product size by varying the ball diameter from 10 mm to 100 mm. A total number of 108 simulations were undertaken for this work to determine the optimal design parameters for the production of the desired product.

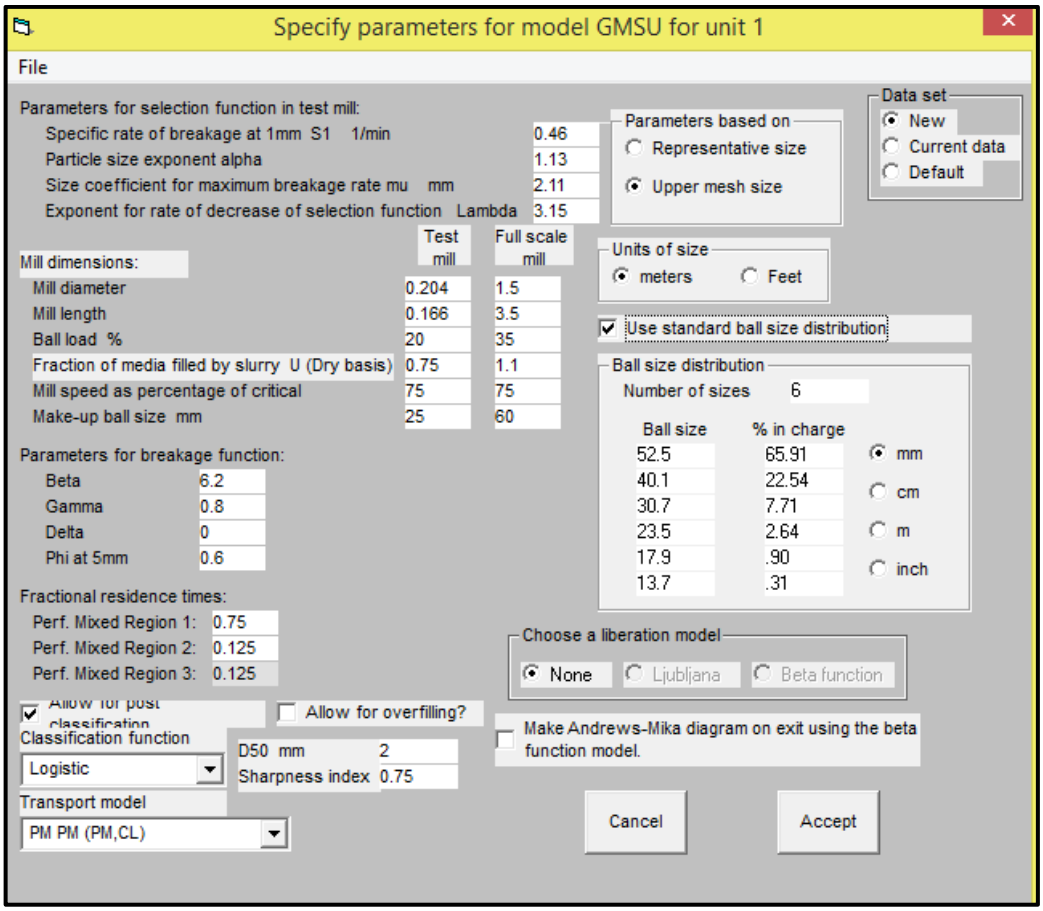

Figure 3.7 GMSU model parameters in MODSIM®

3.5 Hydrocyclone

The hydrocyclone has a choice of 3 models and of the three, the CYCA model was chosen. Roping, which is the abnormal underflow discharge sprouting out in the same diameter as the apex size resulting from an increase in the feed pressure, is tested using the Mular-Jull and the Concha criteria in this model (Mular and Jull, 1980). Roping is characterized by a low rotational speed and an increased underflow density resulting from the increased percentage solids (Concha *et al.*, 1996). The actual classification curve is calculated using the subroutine allowing for bypass fraction. The effect of slurry viscosity was modelled by scaling the d_{50} cut size by a factor as recommended by Kawatra *et al.* (1996). The other 2 models had limitations in that the bypass consideration is not fully modelled. The

assumption made regarding the hydrocyclone was that it does not change in behaviour. Figure 3.8 is the MODSIM® input page for the CYCA model.

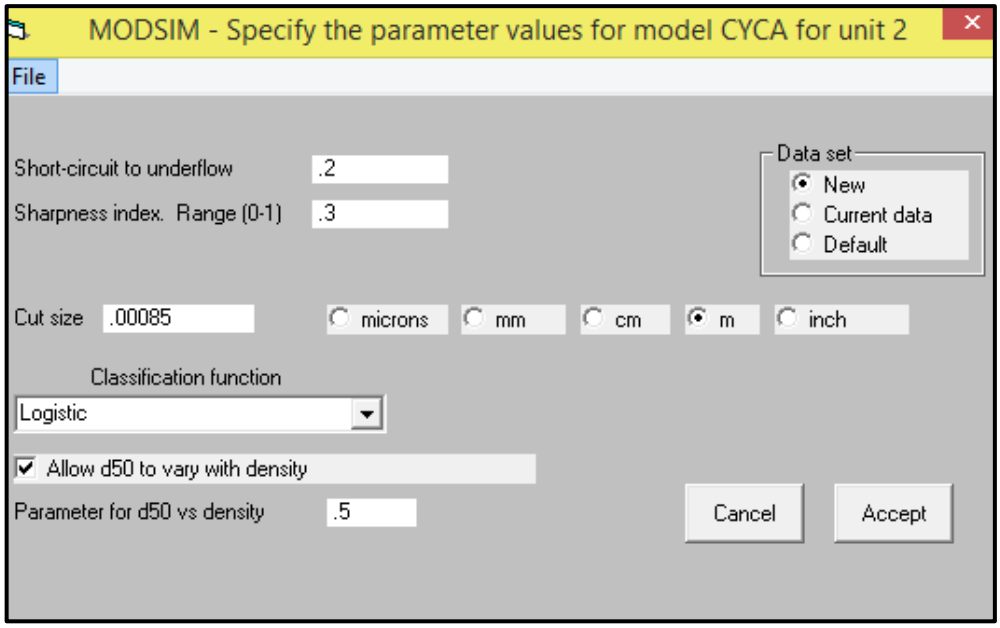

Figure 3.8 CYCA model input page on MODSIM®

The short-circuit to underflow and sharp index (SI) were left to default values. The cut size was 850 µm, with finer material being the product and coarser material sent to the mill as feed. The simulation is then ready to be run after completion of the model parameters' specification. The simulation is run by either selecting the RUN menu and 'run simulation' from the main window or by selecting run from the flowsheet editor or by right-clicking anywhere on the flowsheet editor. Once a simulation has been run, the output streams are specified, with results being obtained. The stream properties of each output stream can be obtained by right-clicking on the respective output stream and selecting 'display stream properties'. This gives the solids flow-rate, water flow-rate, slurry flow-rate, slurry volumetric flow-rate, percent solids by mass, percent solids by volume and the simulated size distribution. The size distribution plot can also be displayed by selecting 'plot size distribution' after right-clicking on the respective product stream.

The production of the product class m_2 was evaluated as a function of mill speed, flow-rate, density, ball filling and ball diameter. Figure 3.9 is the feed size

distribution as generated by MODSIM®. If the feed material contained more of course material, the graph would shift to the right signifying that more of the feed material is course. If it contained more of the fine material, the graph would shift to the left. Particles passing the 50 % mass fraction would be finer than observed in Figure 3.9.

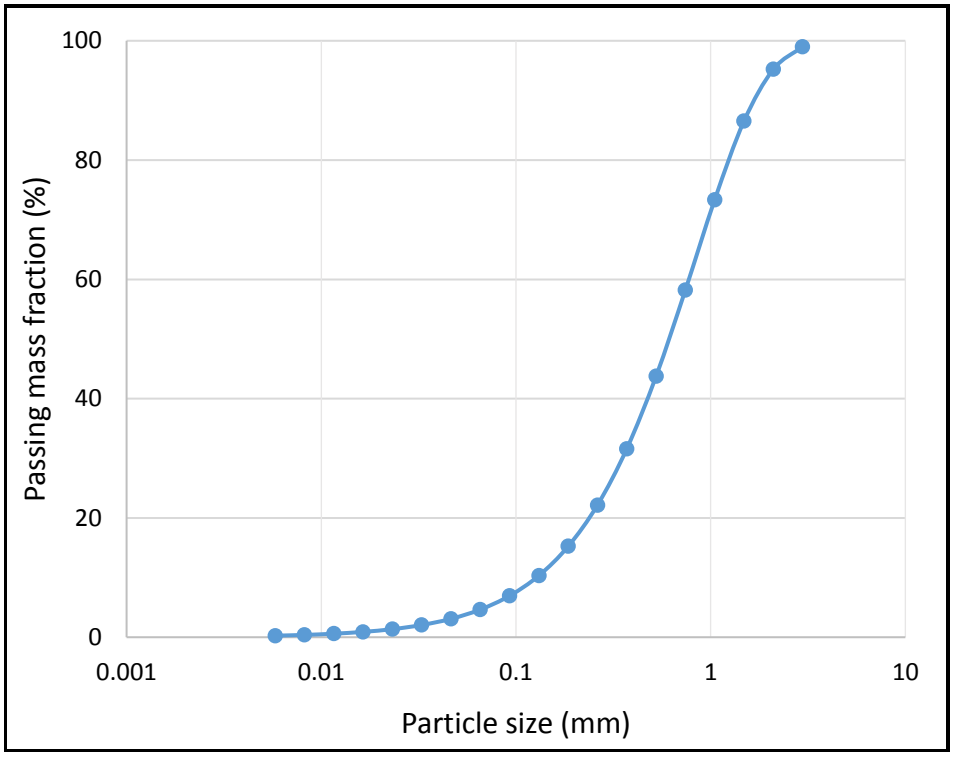

Figure 3.9 Feed size distribution used for all the simulations and milling circuit configurations considered

The use of MODSIM® enabled the simulations of the open milling circuit, the normal closed circuit, the reverse closed circuit and the general combined closed circuit. The challenge faced in conducting this work was in the elimination of the effects of energy from this analysis and the ignorance of the population balance model to take into consideration the slurry concentration. The data presented will be analysed in Chapter 4 from an attainable region point of view.

3.6 Simulation programme

To optimise the designs and operations of process plants, simulation programmes are beneficial. There are different simulators currently available in the market including BMCS, JKSimMet, COMSIM and MODSIM® (Irannajad et al, 2006). MODSIM® was chosen for the work covered in this research. In the next chapter it is explained why MODSIM® was the choice for this work based on the feed information that was available. The model parameters chosen for all unit operations are described; then, justified why they were chosen relative to other models. Secondly, the applicable equations to carry out the work are also described. The simulation flowsheets were set up as per Figures 2.2 to 2.5.

CHAPTER 4 ATTAINABLE REGION ANALYSIS OF THE PERFORMANCE OF THE SIMULATED MILLING CIRCUITS

The attainable region (AR) methodology was applied to the simulation output data collected in Chapter 3. The objective was to investigate the influence of different sets of milling conditions on the four circuit configurations. The construction of the AR profile for each circuit and their comparison thereof were central to the research. This chapter presents a summary of the simulation results from the AR point of view.

With the use of the AR technique, it is possible to find the optimal operating conditions of a circuit meeting a set of objective functions for the overall operation. This is done by identifying all the possible outcomes that can be achieved from the system by the processes working on the system subject to the constraints of that system. For the purpose of this work, the intention was to maximize the production of particles within the middlings class. This size class is termed m_2 and corresponds to particles of size between 850 µm and 300 µm. The feed class m_1 is defined as particles of size between 4700 µm and 850 µm and the fines class m_3 is made up of particles of size less than 300 µm. The definition of m_1, m_2 and m_3 was arbitrarily done for the purpose of this study; however, this is generally informed by separation operations subsequent to milling.

Milling circuits were set up in MODSIM® as described in Figures 2.2 to 2.5. The simulation results from MODSIM® were focused on the product fraction in size class m_2.

4.1 Open milling circuit

The open circuit is the simplest of all the configurations. The feed material directly enters the mill to be broken down and the product sent to downstream processes

as required. The circuit has no classifier and is suitable for feeds that can easily and immediately be broken down to the required product size specification. However, its reliability and efficiency lowers the more complex the feed is. Complexity of the feed material may be increased due to the size of the particles, hardness of the ore and/or shape of the particles among other factors. The reliability of the open circuit may be lowered as well due to the product specification range being smaller, that is, the size class m_2 being smaller. It may be challenging to achieve this product in one pass through the mill.

4.1.1 Effects of feed flow rate on mill product for the open milling circuit

The feed flow rate was varied between 10 tph and 150 tph to monitor its influence on the AR profile. The influence on the conversion of feed particles from size class m_1 to size class m_2 and m_3 can be seen in Figure 4.1.

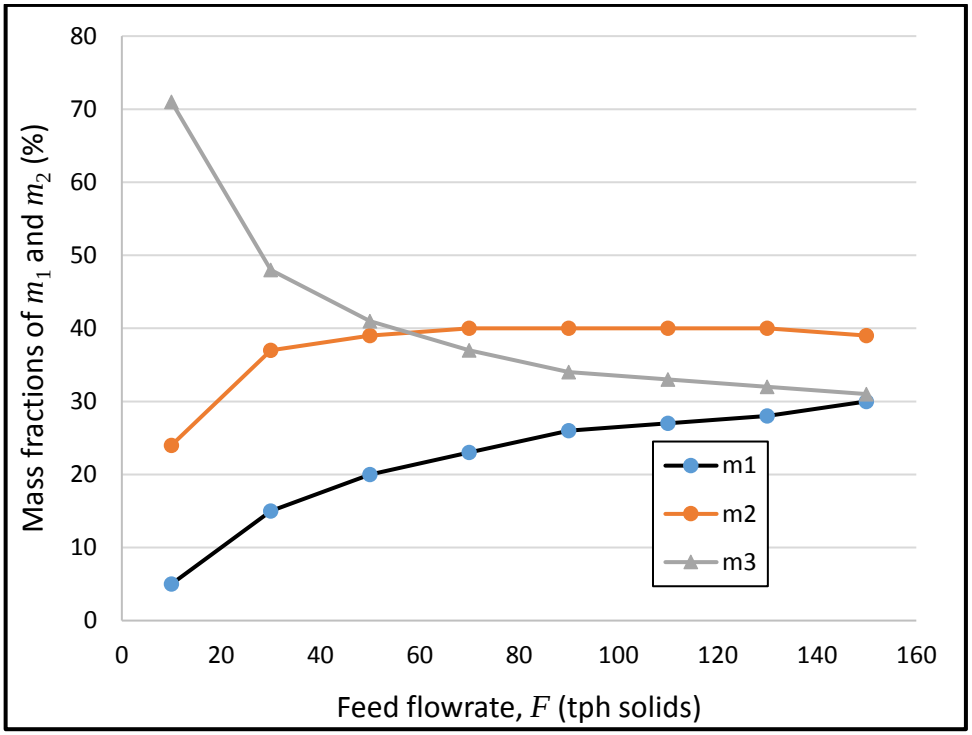

Figure 4.1 Milling kinetics of the open mill circuit as a function of feed flow-rate F. The following conditions applied: J = 35 %; ϕ_c = 70 % of critical speed; C_w = 70 %; and standard ball size distribution

As flow-rate is increased, reducing the residence time, more particles falling into size class m_2 are produced. At the same time more of the coarser particles are not milled effectively to the required product size with the increase in flow-rate. At lower flow-rates, more of the particles in size class m_3 are observed because the milling duration is longer thus producing more fine particles.

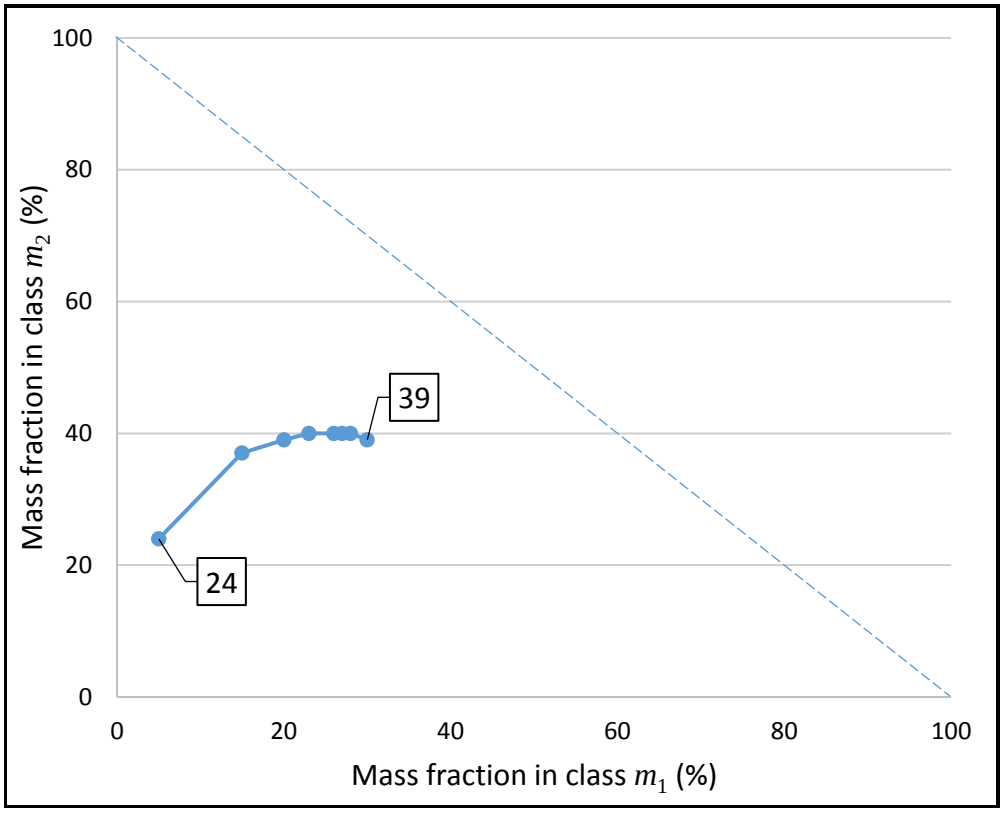

Figure 4.2 Effects of flow rate F on the mill product for the open milling circuit simulated under the following conditions: J = 35 %; C_w = 70 %; ϕ_c = 70 % of critical speed; and standard ball size distribution

From Figure 4.1 it can be observed that the flow rate corresponding to the optimum production of m_2 lies between 70 tph and 130 tph solids. At flow rates higher than 130 tph, the product tends to be coarser and at flow rates lower than 70 tph the production of particles within the size class of m_2 becomes lower. Figure 4.2 is the AR profile with respect to the effects of flow rate on the product size class m_2. The blue straight line is the ideal AR profile. What this means is that as the production of m_1 decreases, the production of m_2 must increase linearly, and

there must be zero production of m_3. The idea is convert all of m_1 into m_2. As observed in Figure 4.1, it can be seen in Figure 4.2 that when the flow-rate is low, the product is furthest from the ideal AR profile. This is the evidence of higher production of m_3, fine material. As the flow-rate is increased, less fine material is produced and the milling process moves closer to the ideal AR profile.

4.1.2 Effects of ball filling on mill product for the open milling circuit

The effects of ball filling on the product requirements of producing m_2 were assessed. Feed flow rate was kept constant at 100 tph, mill speed at 70 % of critical speed, slurry concentration at 70 % solids and ball size at standard ball size distribution with a maximum make-up diameter of 60 mm. Four ball filling sets were simulated on MODSIM®: J = 20, 30, 40 and 60 %. It can be seen from Figure 4.3 that at ball filling conditions of between 30 % and 40 %, the mill tends to produce more of the required product m_2. Conversely, the product size distribution becomes coarser when ball filling is decreased. It appears that the optimum production of m_2 is at a ball filling of between 30 % and 40 %.

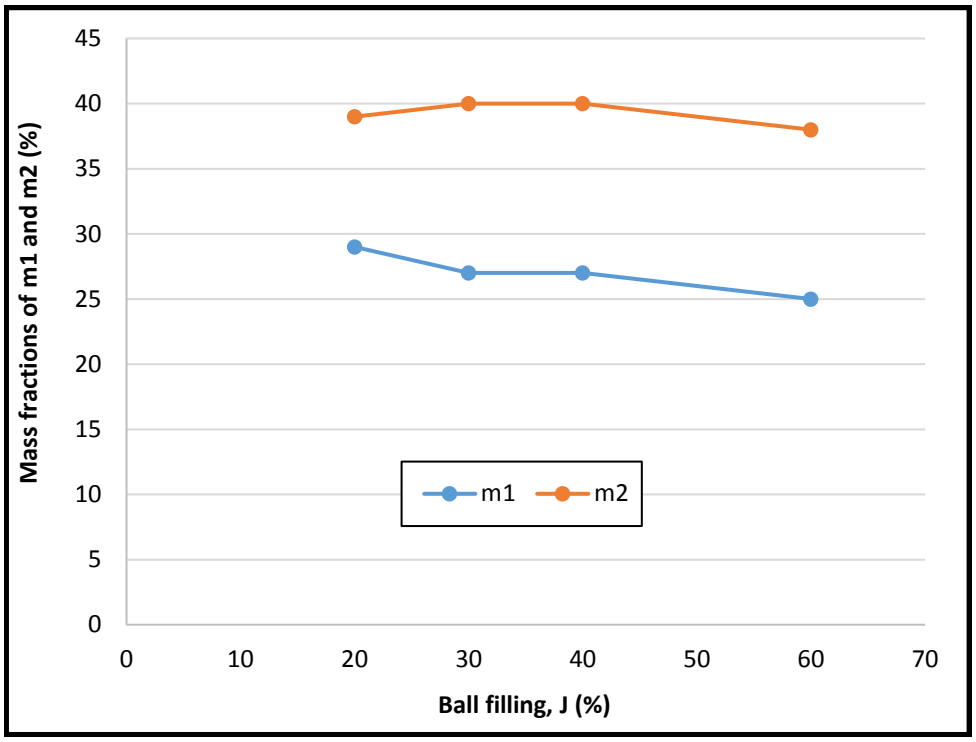

Figure 4.3 Milling kinetics of the open mill circuit as a function of ball filling J under the following simulation conditions: F = 100 tph; C_w = 70 %; ϕ_c = 70 % of critical; and standard ball size distribution

This is so because when ball filling is decreased, there are fewer grinding balls available for milling purposes, therefore more of the feed material is not milled to the required size class m_2. Likewise, at increased ball filling of 60 % there are more grinding balls available for milling thus resulting to more production of finer m_3 class. Figure 4.4 depicts the effects of ball filling on the mill product in the AR space. The ideal AR profile is depicted by the dotted blue line. At the highest ball filling of 60 %, the lowest production of m_2 is observed, at 38 %, and m_1 is also at the lowest. This shows that there is instead more production of m_3, hence that point being the furthest from the ideal AR profile. At the lowest ball filling there is more production of m_1.

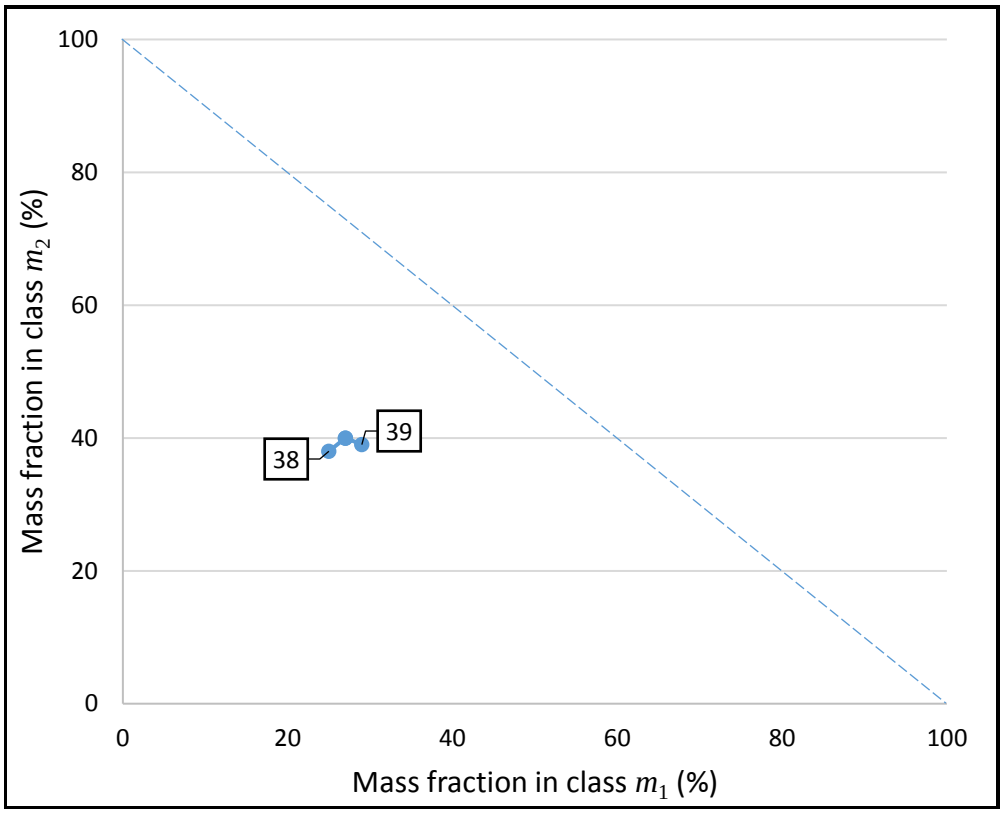

Figure 4.4 Effects of ball filling J on the mill product for the open milling circuit and under the following simulation conditions: F = 100 tph; C_w = 70 %; ϕ_c = 70 % of critical; and standard ball size distribution

4.1.3 Effects of fractional speed on mill product for the open milling circuit

Simulations were conducted to examine the effects of mill speed on the production of the required product by varying the mill speed from 30 % to 90 % of the critical speed. Upon closer inspection it can be seen from Figure 4.5 that the optimum production of m_2 is at 70 % of the critical speed. From the graph it can be seen that at a lower speed of 30 %, the production of m_2 is at its lowest and that of coarse material m_1 at its peak. As the rotational speed is increased, m_2 increases and remains fairly constant after speed 40 %, only peaking at a speed of 70 % then a slight drop is observed at a speed of 80 % and 90 % of the critical speed. Abrasion breakage is observed at lower speeds, with fewer particles exposed to breakage compared to when the rotational speed is increased, hence

the production of m_1 is higher. As speed increases, impact breakage is observed increasing the rate of breakage, until to a much higher level resulting to a centrifugal action and thus the observed drop at higher speeds.

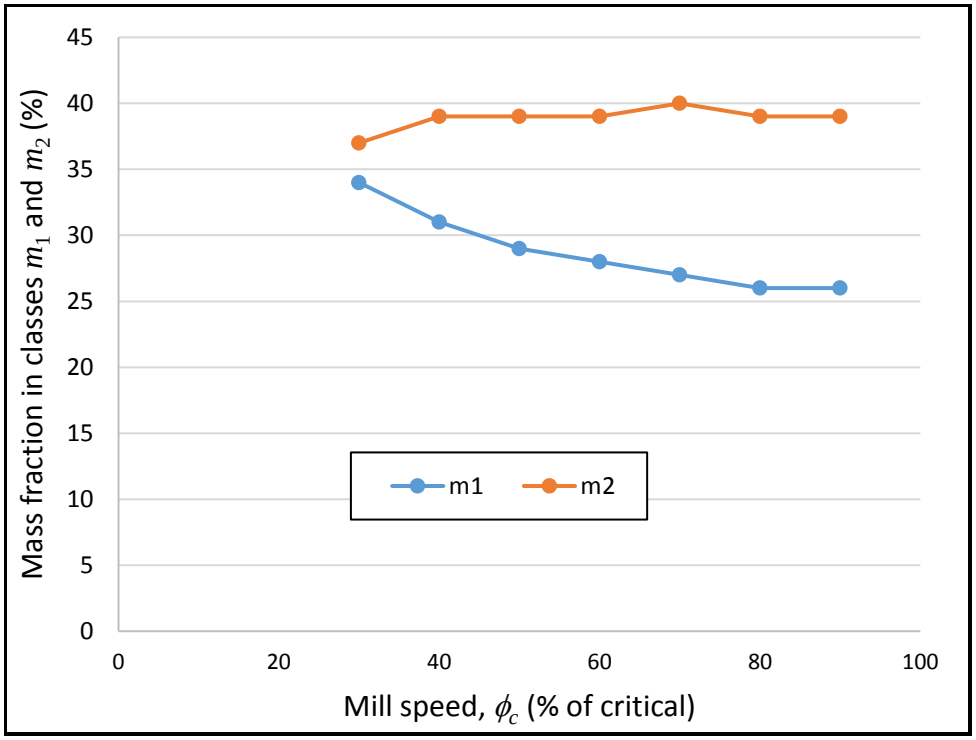

Figure 4.5 Milling kinetics of the open mill circuit as a function of mill speed ϕ_c simulated under the following conditions: F = 100 tph; J = 35 %; C_w = 70 %; and standard ball size distribution

The effect of mill speed on the product in the AR space is shown in Figure 4.6 with the ideal AR profile depicted by the dotted blue line. From Figure 4.6, it can be observed that at a low speed, there is more production of m_1. At low speeds there is minimal milling occurring in the mill and therefore resulting in the production of more coarse particles than at higher mill speeds. As the mill speed is increased, an increase in the production of m_2 is observed, with the corresponding decrease in the production of m_1.

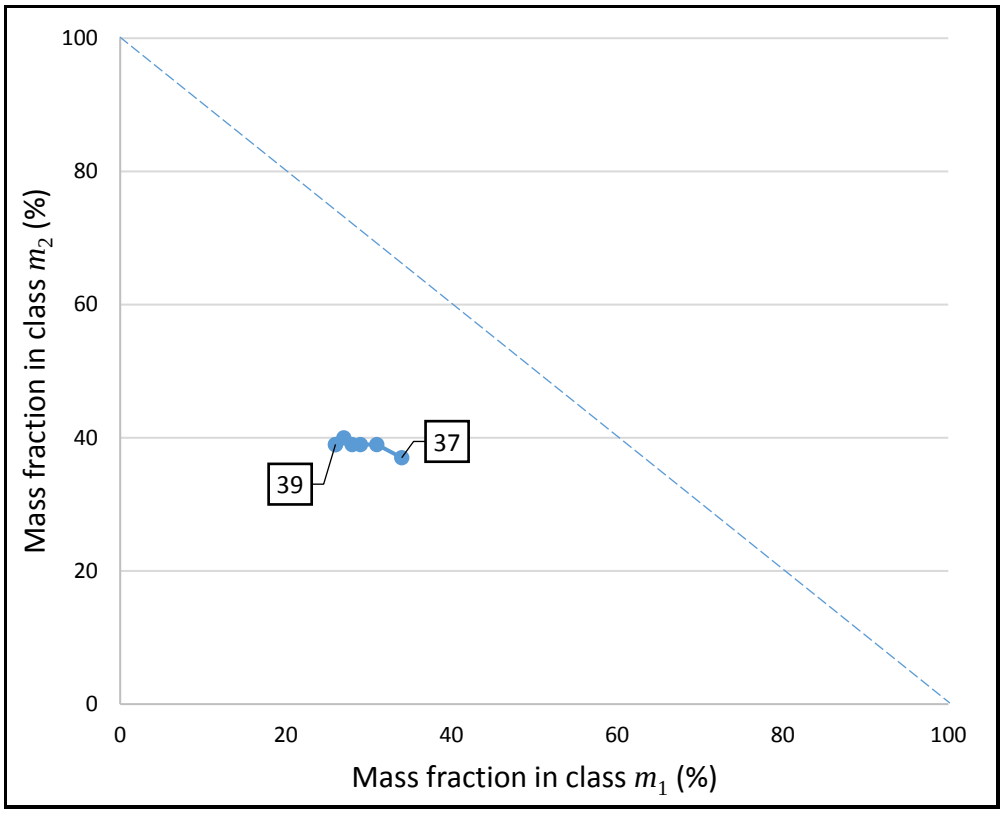

Figure 4.6 Effects of mill speed ϕ_c on the mill product for the open milling circuit simulated under the following conditions: F = 100 tph; J = 35 %; C_w = 70 %; and standard ball size distribution

4.1.4 Effects of slurry concentration on mill product for the open milling circuit

Simulations on varying the mill environment by varying the percentage solids in the feed stream show an insignificant influence to the mill product. Figure 4.7 shows a constant production of both m_1 and m_2 for all sets. From Figure 4.8, it can be seen that slurry concentration has very little, if any, influence on the production of m_2 in the study considered on this work. Figure 4.8 shows very little insights on the performance of the milling circuit.

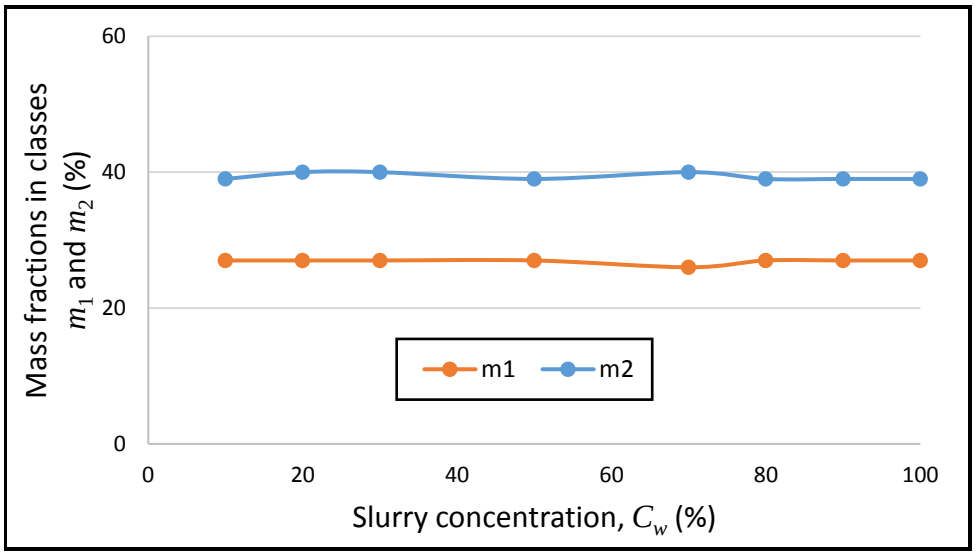

Figure 4.7 Milling kinetics of the open mill circuit as a function of slurry density C_w. The following conditions applied: F = 100 tph; J = 35 %; ϕ_c = 70 % of critical; and standard ball size distribution

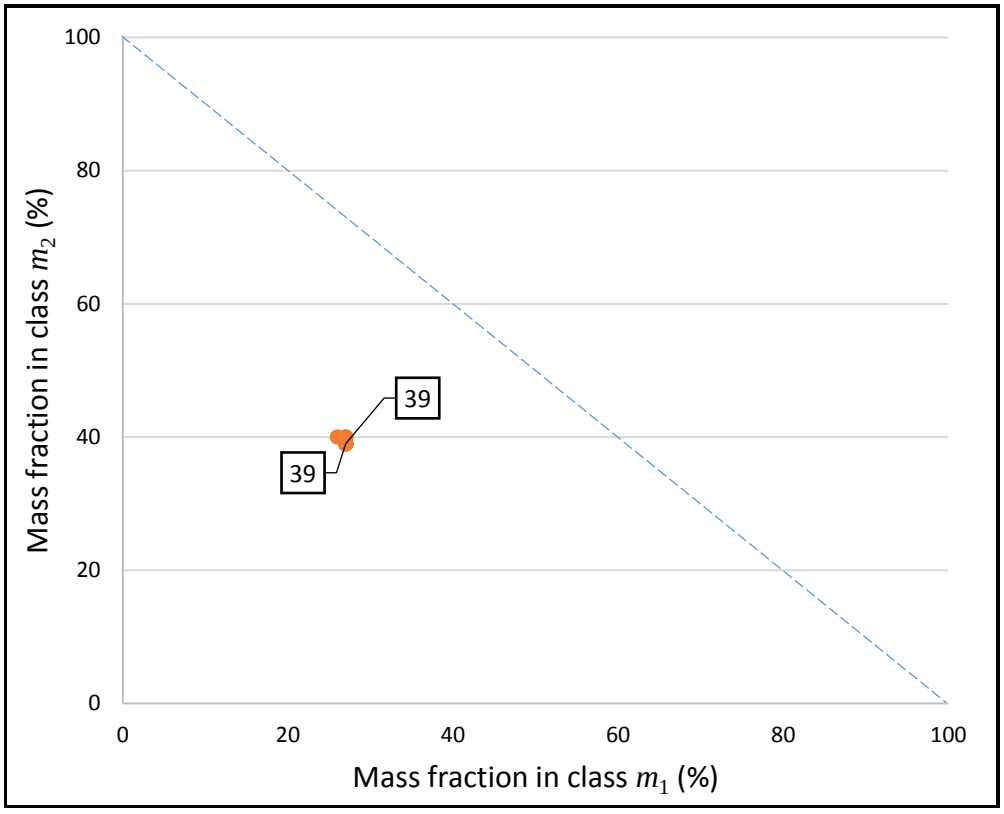

Figure 4.8 Effects of slurry concentration C_w on the mill product for the open milling circuit simulated under the following conditions: F = 100 tph; J = 35 %; ϕ_c = 70 % of critical; and standard ball size distribution

It can be concluded that density has little or no influence in the production of the product. This is because of the current population balance model MODSIM® is based on. This model does not take into account the effects of density.

4.1.5 Effects of ball size on mill product for the open milling circuit

The last set of simulation for the open circuit configuration was to assess the influence of ball size on the mill product. Ball size was varied from 10 mm to 100 mm. Figure 4.9 shows that the optimum production of m_2 occurred between 60 mm and 80 mm. Small ball sizes resulted in a finer product and larger ball sizes were not effective in grinding to the required specification.

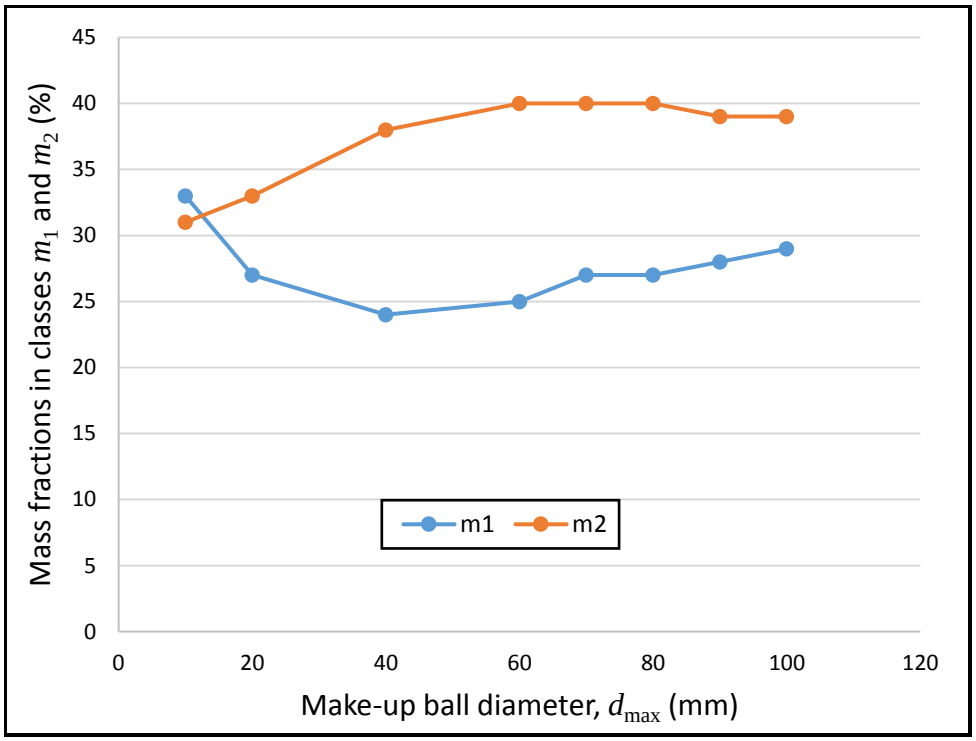

Figure 4.9 Milling kinetics of the open mill circuit as function make-up ball diameter d_{max} under the following simulation conditions: F = 100 tph; J = 35 %; C_w = 70 %; and ϕ_c = 70 % of critical

Figure 4.10 depicts the effects of make-up ball diameter d_{max} on the mill product in the AR space. The ideal AR profile is shown by the dotted blue line. What is

observed from Figure 4.10 is that with the smallest ball size of 10 mm, more production of m_1 and less production of m_2 is observed. Also, for the same production of m_1 at two different ball sizes, there are two different amounts of m_2 produced. This is evident at a ball diameter of 20 mm and at a ball diameter of 70 mm where the production of m_1 is 27 % whilst a production of 33 % and 40 % of m_2 respectively is observed. This is because at a ball diameter 20 mm there is more production of m_3 instead than at ball diameter of 70 mm.

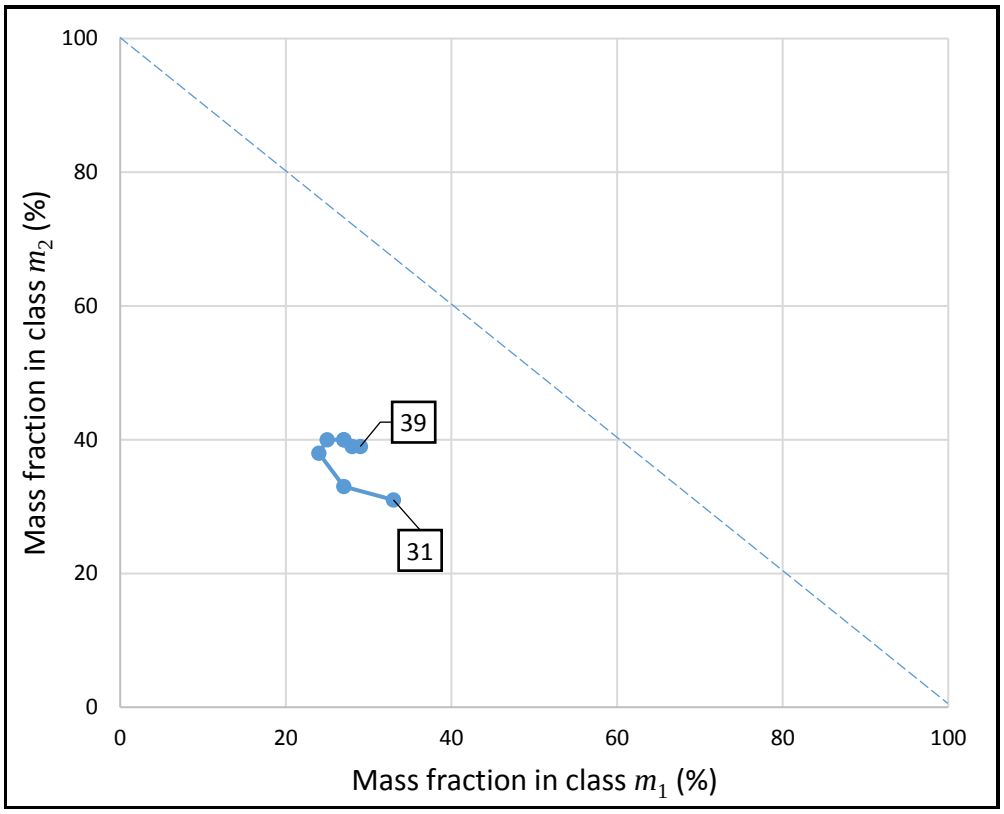

Figure 4.10 Effects of make-up ball diameter $d_{\max}$ on the mill product for the open milling circuit and under the following simulation conditions: F = 100 tph; J = 35 %; C_w = 70 %; and ϕ_c = 70 % of critical

4.2 Normal closed circuit

The normal closed circuit has a post-classifier, returning the underflow back into the mill feed for regrinding as shown in Figure 2.3. The product material not

meeting the specification is recycled back to the feed as hydrocyclone underflow to ensure that the final product meets the required specification.

Eight simulations were run corresponding to feed flow rates between 10 tph and 150 tph. Seven simulations were run whilst varying the mill speed from 30 % to 90 % of the critical speed. To simulate the effects of ball filling, four simulations were executed changing the ball filling between 20 % and 60 %. The effects of ball diameter on the product size were observed by changing the ball diameter between 10 mm and 100 mm, running eight simulations.

4.2.1 Effects of feed flow rate on mill product for the normal closed circuit

Figure 4.11 is the result of varying the feed-flow rate from 10 tph to 150 tph to observe the influence of the AR methodology. It can be observed that the optimum production of m_2 is at a flow rate of 110 tph solids where 43 % of the mill product is within m_2. At flow rates lower than 110 tph the product becomes finer than the required product specification.

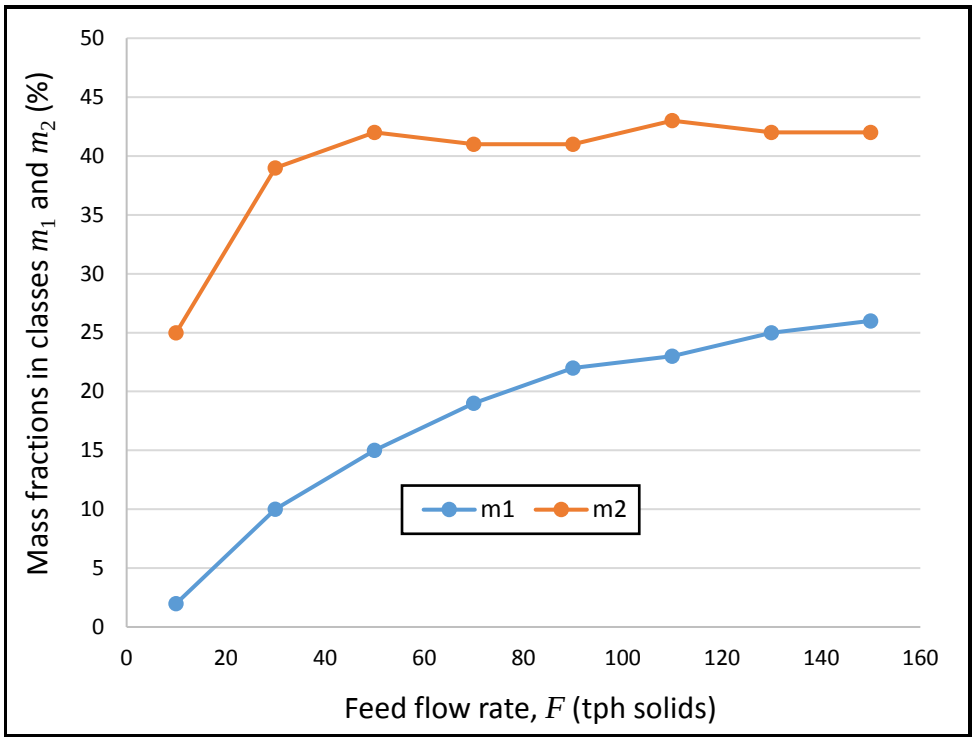

Figure 4.11 Milling kinetics of the normal closed circuit as a function of feed flow rate F simulated under the following conditions: J = 35%; C_w = 70 %; ϕ_c = 70 % of critical; and standard ball size distribution

Figure 4.12 shows the effect of feed flow rate on the normal closed circuit in the AR space. It can be observed from Figure 4.12 that at lower flow-rates, there is less production of m_2 and even lesser production of m_3. This is evidence that most of the produced particles fall in the class of m_3, which is the fine material. This is a result of the longer timeframe the particles spend in the mill. As the flow rate is increased, increased production of particles in the class of m_2 is observed and more particles in m_1 are also the result of that milling process. This results in the milling process shifting closer to the ideal AR profile.

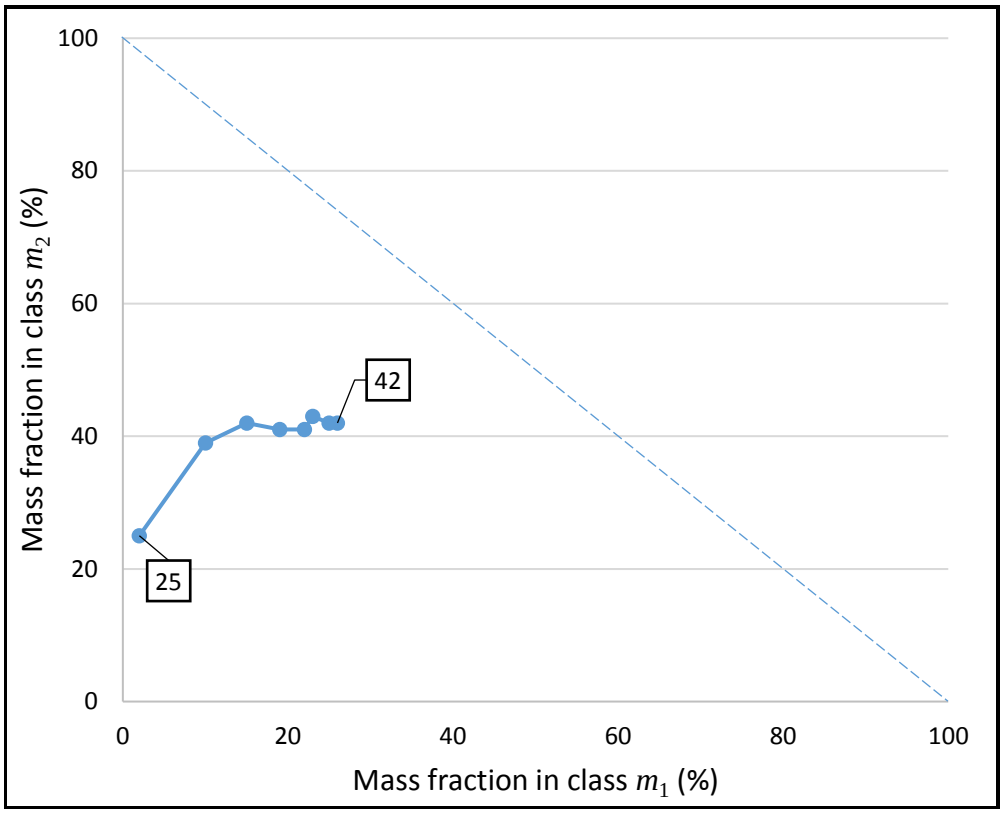

Figure 4.12 Effects of flow rate F on the mill product for the normal closed circuit simulated under the following conditions: J = 35 %; C_w = 70 %; ϕ_c = 70 % of critical; standard ball size distribution

4.2.2 Effects of ball filling on mill product for the normal closed circuit

The effect of ball filling on the product requirements was assessed. Feed flow rate was kept constant at 100 tph, mill speed at 70 % of critical, slurry concentration at 70 % solids by mass and ball size at standard size distribution. Four different ball filling sets were simulated in MODSIM®, J = 20 %, 30 %, 40 % and 60 %. Figure 4.13 depicts the effect of ball filling on the product. It can be seen that at ball filling conditions of between 30 % and 40 %, the behaviour tends to be producing more of the required product and when ball filling is decreased the product size distribution becomes coarser. It appears that the optimum production of m_2 is around 30 % < J < 40 %, although the change seems to be minimal. The

corresponding response of m_1 is that less production is observed between 30 % and 40 % of ball filling.

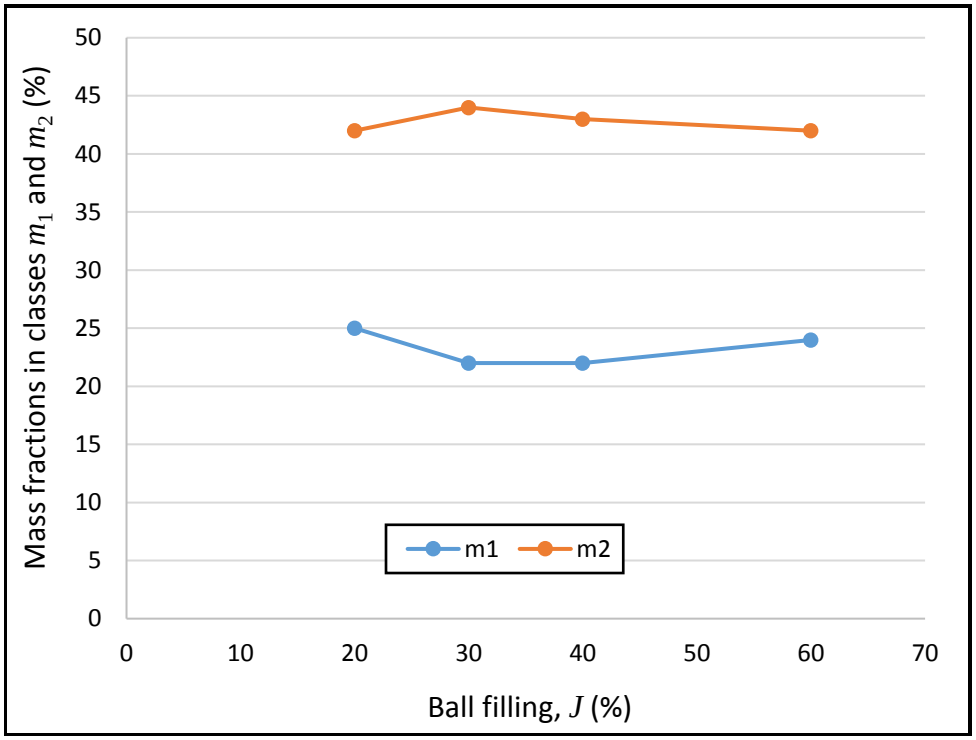

Figure 4.13 Milling kinetics of the normal closed circuit as a function of ball filling J under the following simulation conditions: F = 100 tph; C_w = 70 %; ϕ_c = 70 % of critical; and standard ball size distribution

The demonstration in the AR space of the effect of ball filling is observed in Figure 4.14. The ideal AR profile is depicted by the dotted blue line. As observed in Figure 4.13, the effect of ball filling in this case seems to be small. Figure 4.14 shows that with higher production of m_2, m_1 is lower.

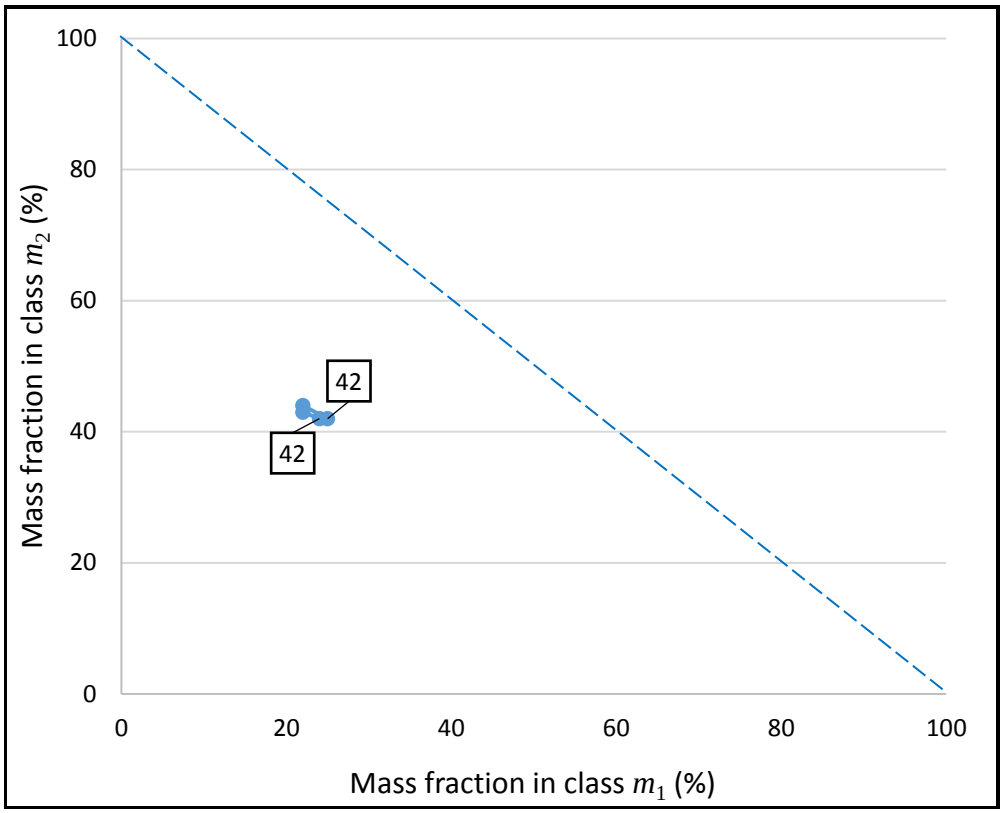

Figure 4.14 Effects of ball filling J on the mill product for the normal closed circuit simulated the following conditions: F = 100 tph; C_w = 70 %; ϕ_c = 70 % of critical; and standard ball size distribution

4.2.3 Effects of mill speed on mill product for the normal closed circuit

Simulations were conducted to examine the effect of mill speed on the production of the required product by varying the mill speed from 30 % to 90 % of critical. Upon closer inspection it can be seen from Figure 4.15 that the optimum production of m_2 is between 60 % and 90 % of critical. The production of m_3 is also plotted here to further show the dynamics happening. From the figure it can be seen that at a lower speed of 30 % the production of m_2 is at its lowest. As speed is increased, m_2 gradually increases and stabilises (plateaus) from 60 % speed onwards. However, a slight drop in m_2 is observed at 50 % speed with a corresponding increase in m_3. It seems m_1 is quickly exhausted as speed increases but drops no further from 80 % speed. The opposite is observed for m_3 during the

drop of m_1, with m_3 increasing as speed is increased then stabilising at 80 % to 90 % as well.

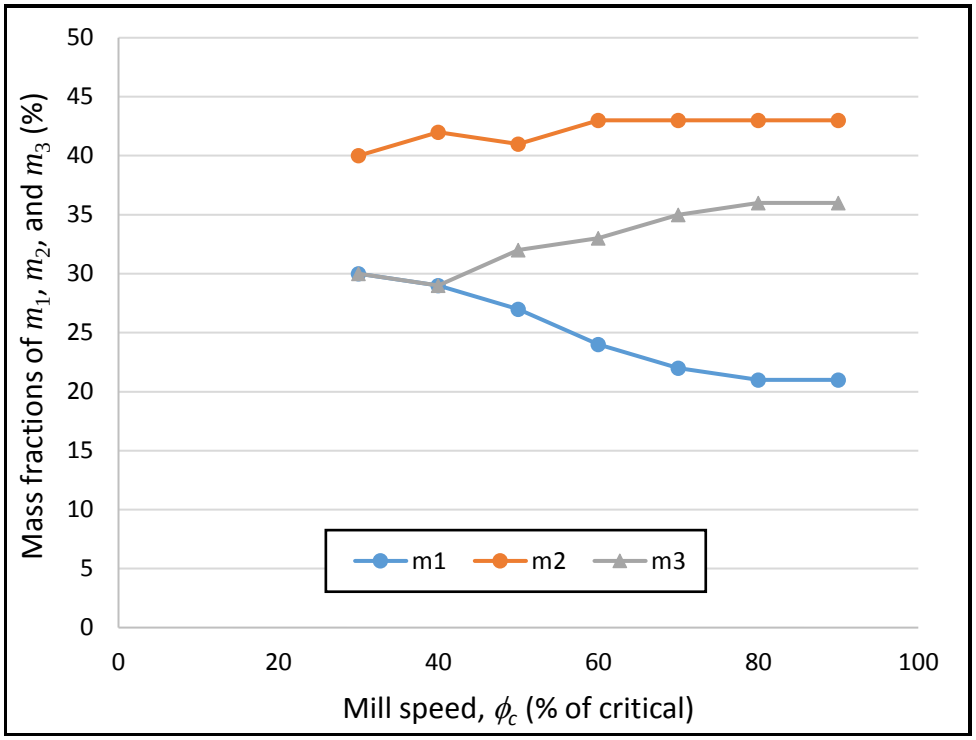

Figure 4.15 Milling kinetics of the normal closed circuit as a function of mill speed ϕ_c under the following simulation conditions: F = 100 tph; J = 35 %; C_w = 70 % of critical; and standard ball size distribution

Figure 4.16 depicts the effects of mill speed on the product in the AR space. It can be noted that as m_2 increases, m_1 decreases. The milling process seems to be moving away from the ideal AR profile, but that is because the rate of decrease in the production of m_1 is higher than the rate of increase in the production of m_2.

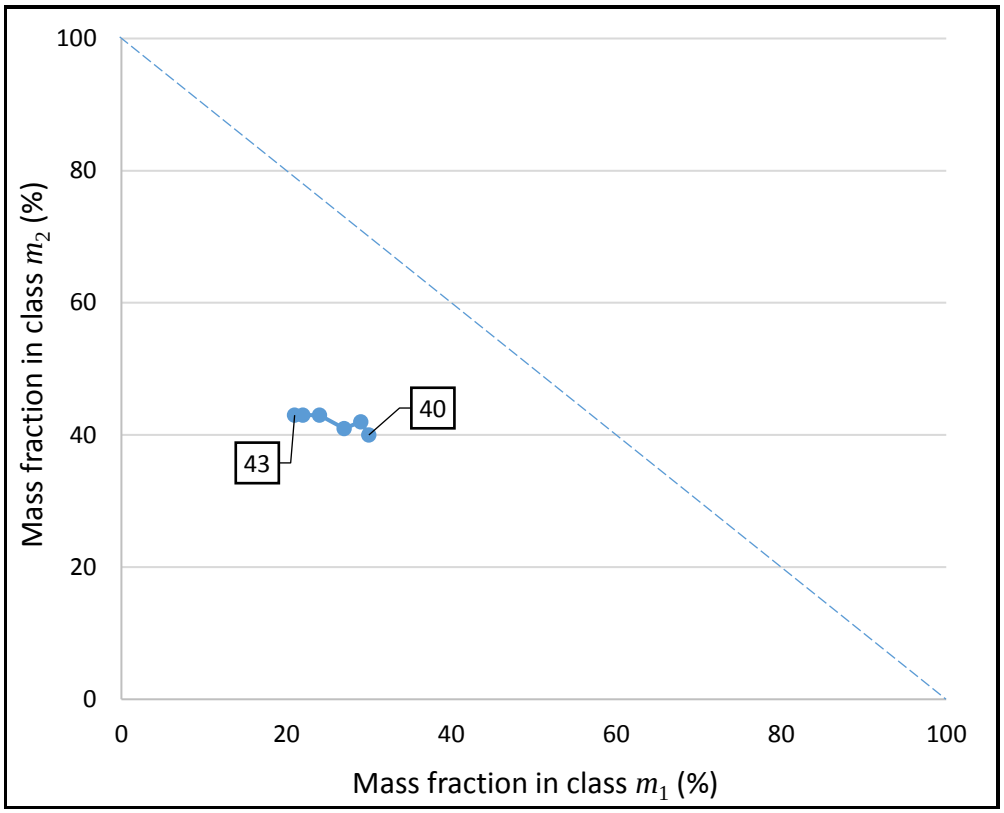

Figure 4.16 Effects of mill speed ϕ_c on the mill product for the normal closed circuit simulated under the following conditions: F = 100 tph; J = 35 %; C_w = 70 %; and standard ball size distribution

4.2.4 Effects of slurry density on mill product for the normal closed circuit

The variations on mill environment showed minimal influence on the mill product. From Figure 4.17, a stabilized feedback is observed. There is no change in both the production of m_1 and that that of m_2. Figure 4.18 shows that the density has very little influence just like with the open milling circuit, if any, on the production of m_2 in the study considered on this work.

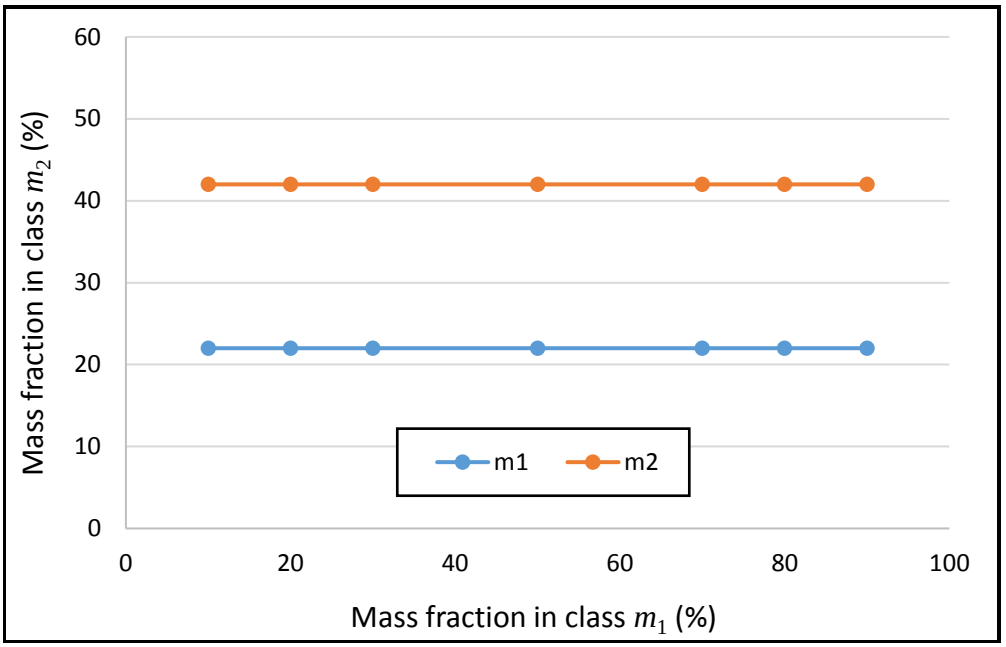

Figure 4.17 Milling kinetics of the normal closed circuit as a function of slurry concentration C_w. The following conditions applied: F = 100 tph; J = 35 %; ϕ_c = 70 % of critical; and standard ball size distribution

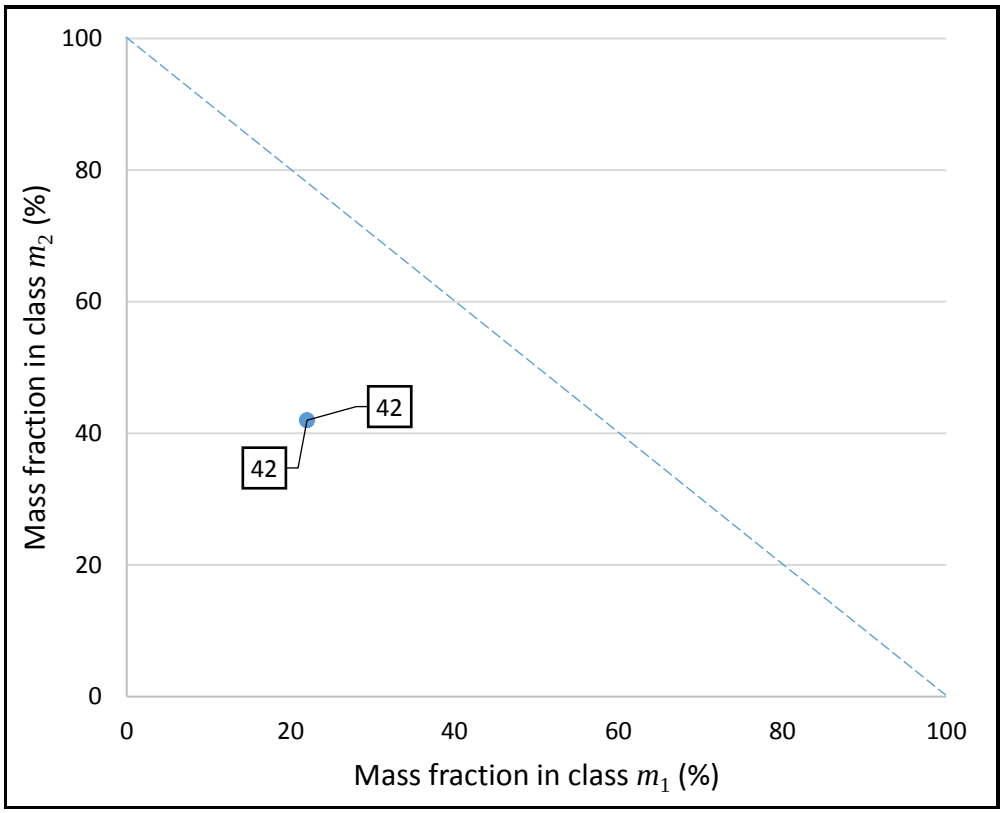

Figure 4.18 Effects of slurry concentration C_w on the mill product for the normal closed circuit and under the following simulation conditions: F = 100 tph; J = 35 %; ϕ_c = 70 % of critical; and standard ball size distribution

As observed with the open circuit, the influence of the variation of density is minimal. The change in circuit configuration did not have an influence on the observation.

4.2.5 Effects of ball size on mill product for the normal closed circuit

The influence of ball size on the mill product was assessed. The ball size was varied from 10 mm to 100 mm. Figure 4.19 shows that the optimum production of m_2 occurred at 80 mm where 43 % of production was observed. The larger ball sizes were not as efficient in grinding to the required specification and the smaller ball sizes resulted in more fines being produced. The plot of m_3 shows a spike for balls of size 10 mm to 20 mm, then a decrease in the production of m_3 is observed as the ball size is increased.

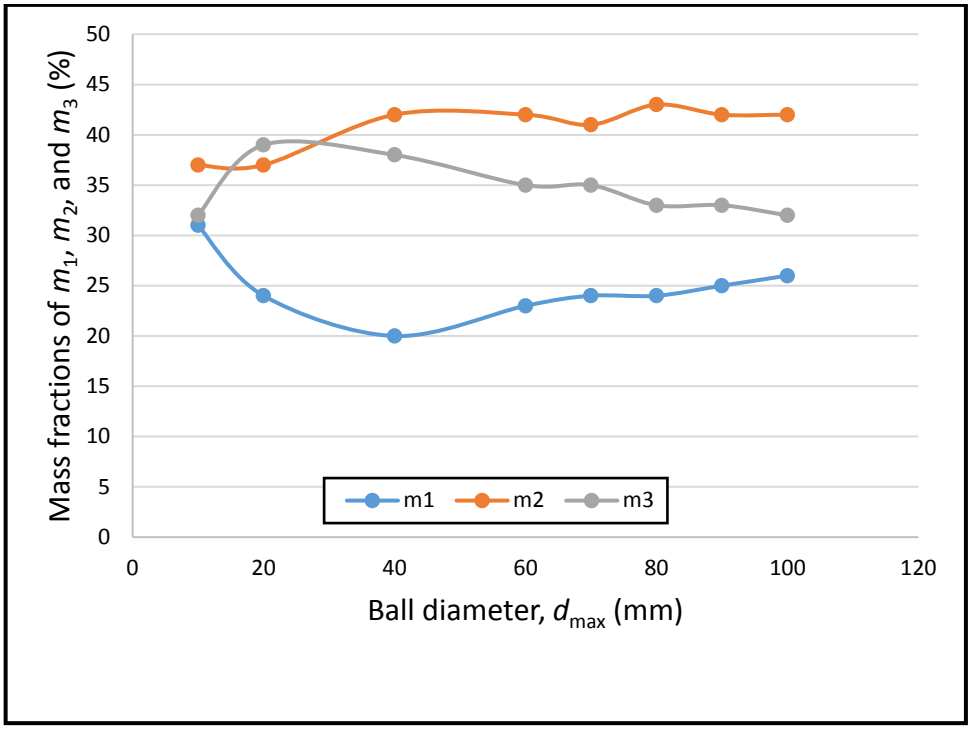

Figure 4.19 Milling kinetics of the normal closed circuit as function of ball diameter $d_{\max}$. The following simulation conditions were used here: F = 100 tph; J = 35 %; C_w = 70 %; and ϕ_c = 70 % of critical

The effects of ball diameter on mill product in the AR space are shown in Figure 4.20 with the ideal AR profile depicted by the dotted blue line. It can be observed that as the production of m_1 decreases, the production of m_2 increases. However, further increases in the size of the balls result to an increase in the production of m_1, and hence the C-shaped pattern is observed in Figure 4.20.

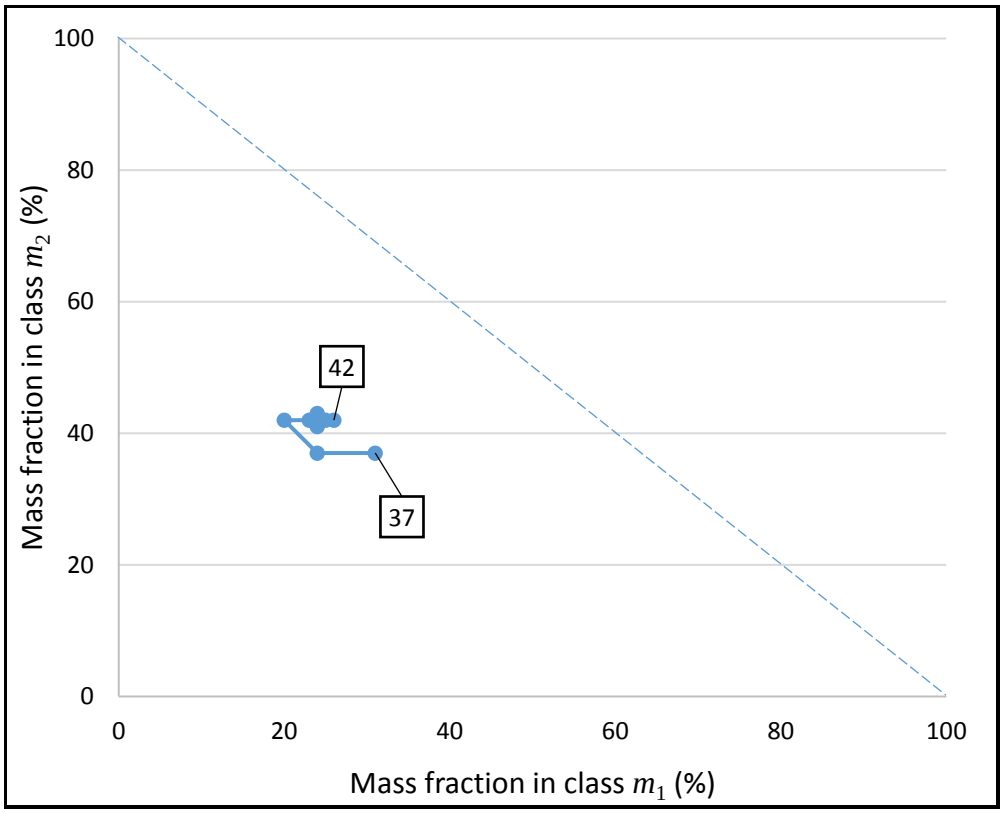

Figure 4.20 Effects of make-up ball diameter $d_{\max}$ on the mill product for the normal closed circuit and under the following simulation conditions: F = 100 tph; J = 35 %; C_w = 70 %; and ϕ_c = 70 % of critical

4.3 Reverse closed circuit

The reverse closed circuit reduces the load on the mill by separating out fine particles meeting the product specification before feeding into the mill as shown in Figure 2.3. This saves the energy usage. This circuit also acts as a post-classifier with the cyclone classifying the mill product and returning the underflow for regrinding.

4.3.1 Effects of feed flow rate on mill product for the reverse closed circuit

The feed flow rate was varied to observe the influence of the AR methodology on feed flow rate. Figure 4.21 shows that the optimum production of m_2 is at a solids

flow rate of 150 tph where 44 % of the product is observed. The flow rate was varied from 10 tph to 150 tph. At flow rates below 70 tph the product becomes finer, hence the production of particles in the class of m_2 is lowest at these flow-rates and highest for particles in the class of m_3, with m_3 decreasing as flow-rate increases. The production of m_1 steadily increases with flow-rate whilst m_2 increases faster, peaks around 70 tph, then slightly drops reaching a valley around 110 tph before increasing again.

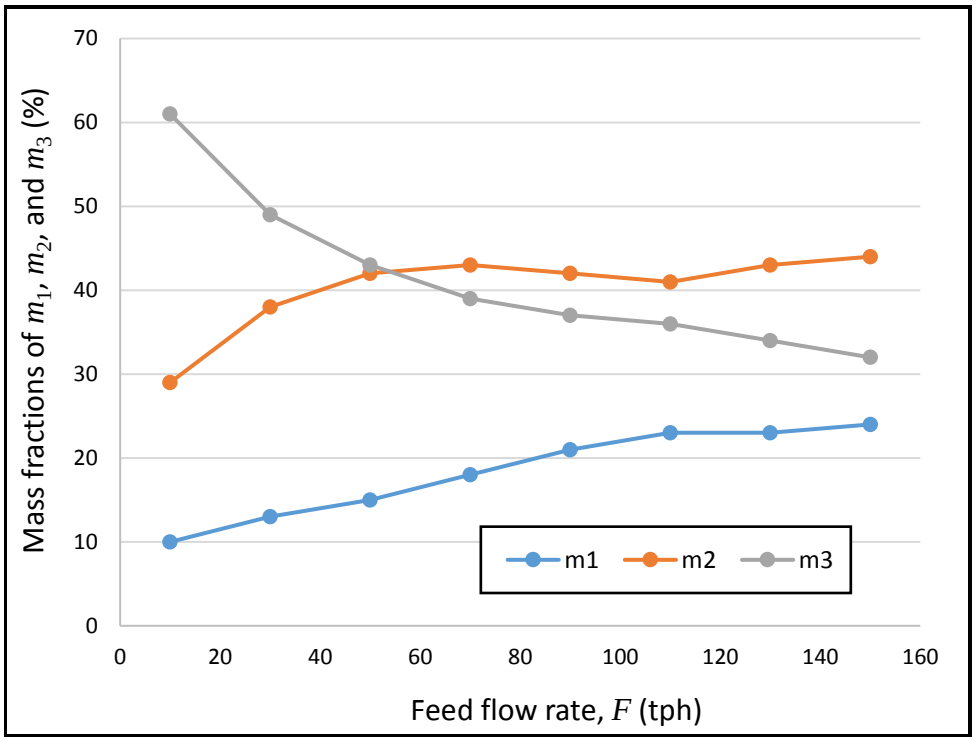

Figure 4.21 Milling kinetics of the reverse closed circuit as a function of feed flow rate F. The following simulation conditions were used in this case: J = 35 %; C_w = 70 %; ϕ_c = 70 % of critical; and standard ball size distribution

Figure 4.22 shows the effects of feed flow rate on the reverse closed circuit in the AR space. At low flow-rates, both the production of both m_1 and m_2 is low. As flow rate is increased, m_1 increases gradually and m_2 increases at a faster rate, moving the milling process towards the AR profile. A slight dip is observed where m_1 is 21 % and m_2 is 42 %, after which when m_1 is 23 % a sharp increase in m_2 to the maximum is observed.

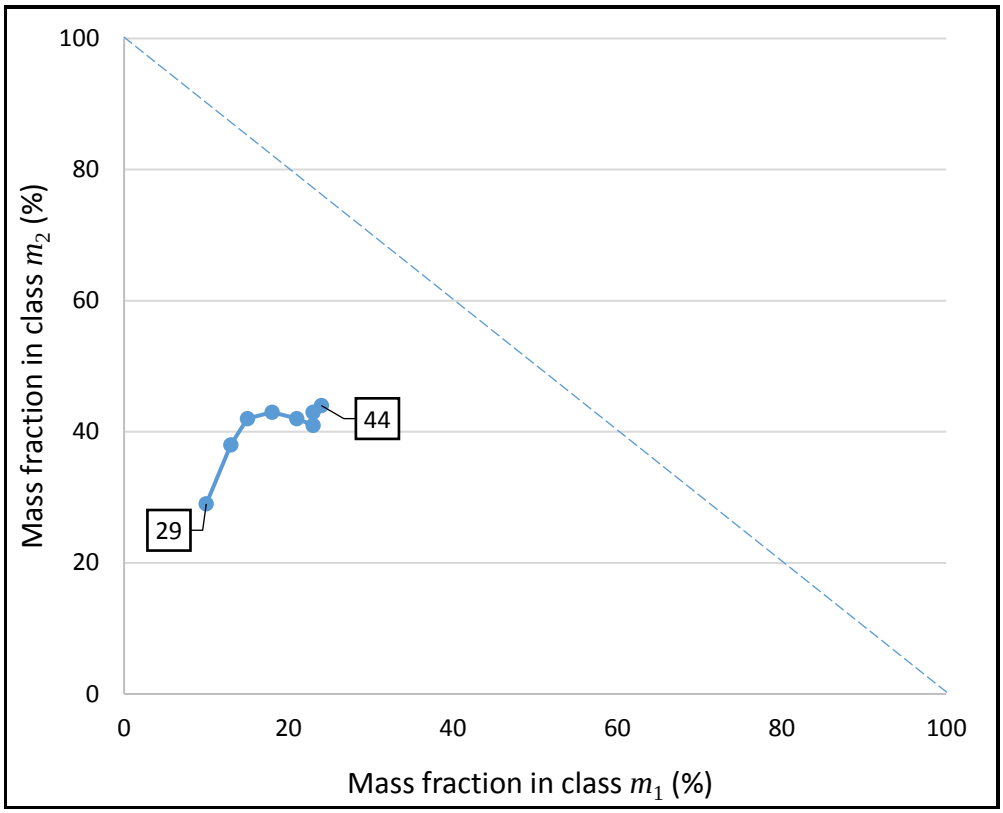

Figure 4.22 Effects of flow rate F on the mill product for the reverse closed circuit. Simulation conditions: J = 35 %; C_w = 70 %; ϕ_c = 70 % of critical; and standard ball size distribution

4.3.2 Effects of ball filling on mill product for the reverse closed circuit

The effect of ball filling on the product requirements was assessed. Feed flow rate, mill speed, density and ball size were kept constant. Four ball fillings were simulated in MODSIM®, J = 20 %, 30 %, 40 % and 60 %. The effect of ball filling on the product is depicted by Figure 4.23. It can be seen that the production of m_2 is equal at all sets simulated unlike with the open and normal closed circuits. It is observed that m_1 slightly decreases with increase in ball filling until a point when J = 40 %, then a slight increase is observed. The opposite is observed for m_3. A slight increase is observed to a peak at J = 40 %; then, a slight decreased is seen.

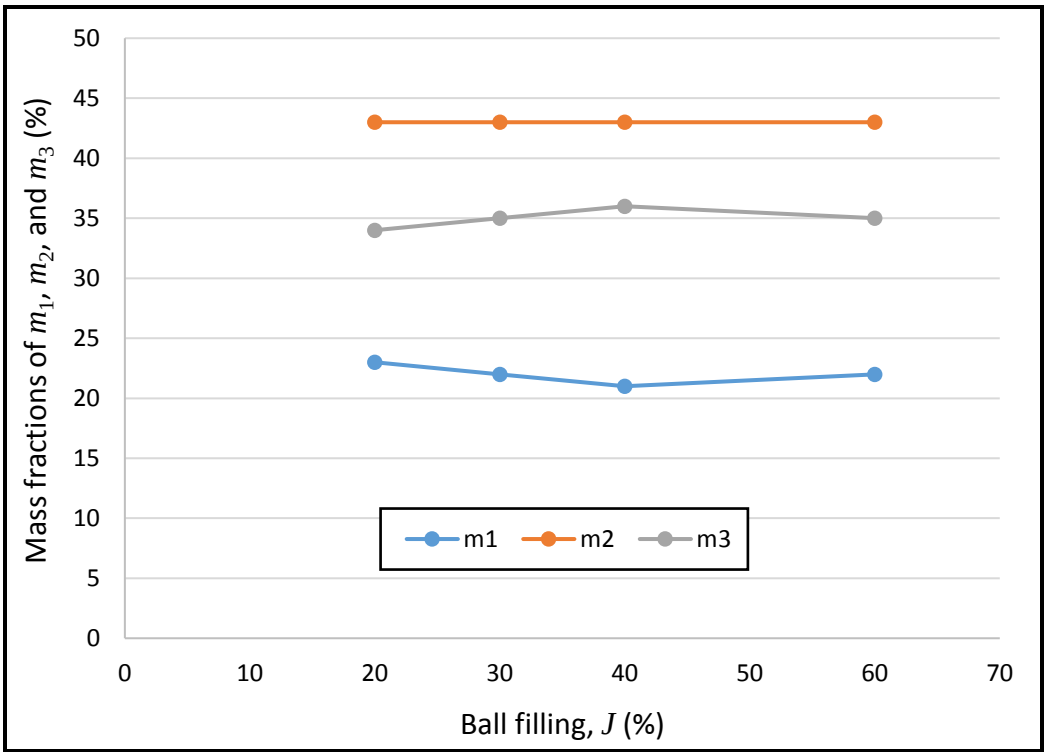

Figure 4.23 Milling kinetics of the reverse closed circuit as a function of ball filling J. The following simulation conditions were used: F = 100 tph; C_w = 70 %; ϕ_c = 70 % of critical; and standard ball size distribution

Figure 4.24 depicts the effect of ball filling on the product in the AR space. The ideal AR profile is depicted by the dotted blue line. As can be seen, there is not much variation or change in m_2. The change in m_1 is also minimal.

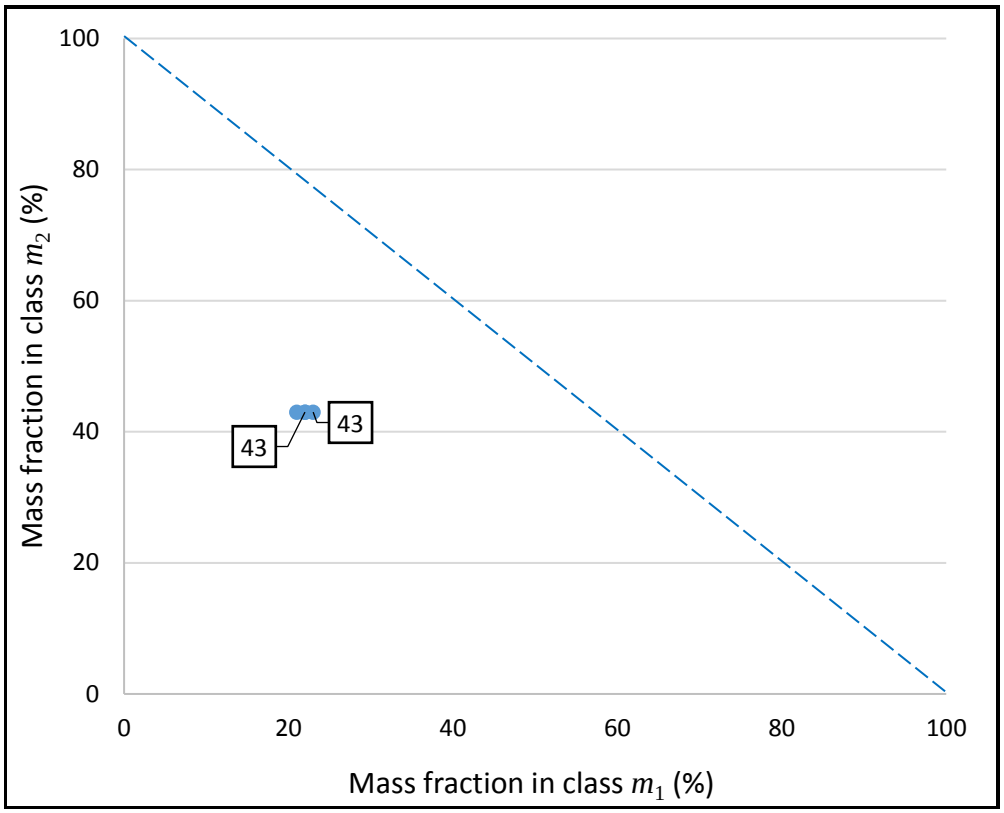

Figure 4.24 Effects of ball filling J on the mill product for the reverse closed circuit. Simulation conditions: F = 100 tph; C_w = 70 %; ϕ_c = 70 % of critical; and standard ball size distribution

This means that at lower ball filling conditions up until a ball filling of 40 %, more fine material production is observed. As the ball filling is increased beyond 40 %, less fines are produced and more of the coarser material is produced.

4.3.3 Effects of mill speed on mill product for the reverse closed circuit

The effect of mill speed ϕ_c on the production of the required product by varying mill speed ϕ_c from 30 % to 80 % of critical speed was examined. It can be seen from Figure 4.25 that the optimum production of m_2 is at 60 % of critical speed. Figure 4.25 shows that the production of m_2 increases to peak at 60 %, drops, then stabilizes at 70 % and slightly drops again after 80 %. The production of m_1 decreases with increase in speed.

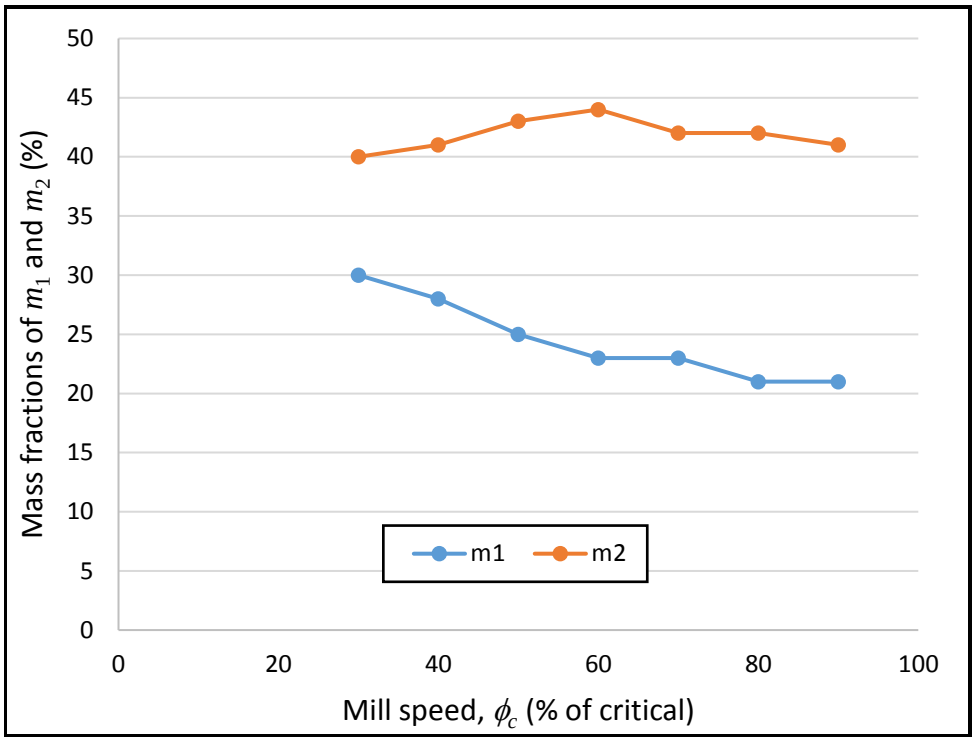

Figure 4.25 Milling kinetics of the reverse closed circuit as a function of mill speed ϕ_c. The following simulation conditions applied here: F = 100 tph; J = 35 %; C_w = 70 %; and standard ball size distribution

The effect of mill speed on the product in the AR space is shown in Figure 4.26 with the ideal AR profile depicted by the dotted blue line. As m_1 decreases, m_2 is seen to be increasing to a point where m_1 is equal to 23 %. At this point there is an observed decrease in m_2.

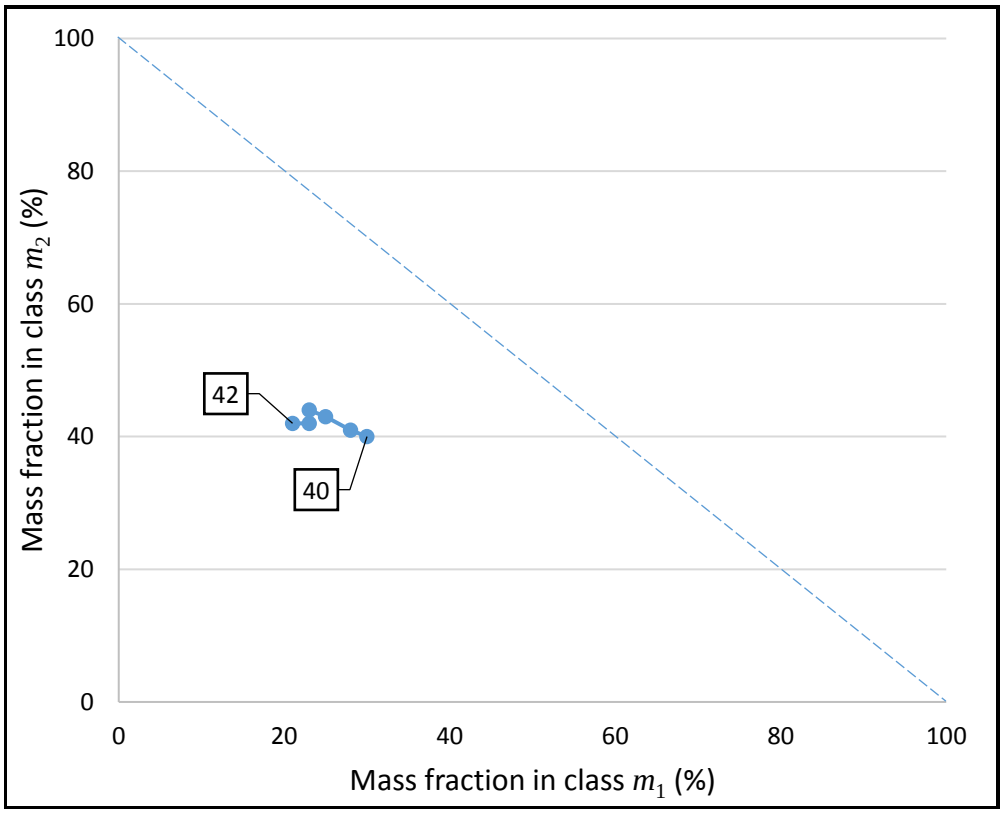

Figure 4.26 Effects of mill speed ϕ_c on the mill product for the reverse closed circuit under the following simulation conditions: F = 100 tph; J = 35 %; C_w = 70 %; and standard ball size distribution

An increase in mill speed increased the chances of breakage within the mill, hence the observed increase in the production of m_2. A further increase beyond the speed of 80 % of critical speed then results to a spinning effect of the material within the mill, reducing the chances of impact for breakage.

4.3.4 Effects of slurry density on mill product for the reverse closed circuit

As previously noted in Figure 4.7, Figure 4.8, Figure 4.17 and Figure 4.18, simulations on varying the mass concentration C_w of the feed slurry show no influence to the mill product. From Figure 4.27, it appears that slurry concentration has very little influence on the production of m_2 in the study considered on this work.

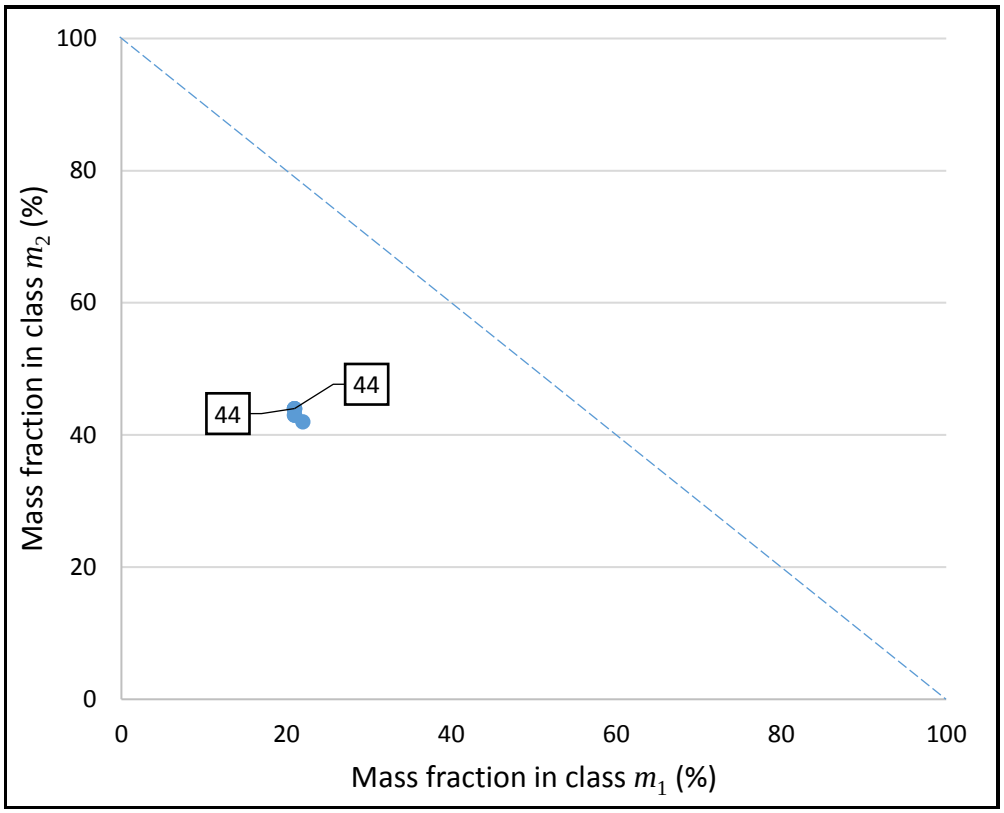

Figure 4.27 Effects of slurry concentration C_w on the mill product for the reverse closed circuit simulated under the following conditions: F = 100 tph; J = 35 %; ϕ_c = 70 % of critical; and standard ball size distribution

4.3.5 Effects of ball size on mill product for the reverse closed circuit

The ball size was varied from 10 mm to 100 mm. Figure 4.28 shows that m_2 increases with increasing ball diameter whilst m_1 first decreases then increases from a ball diameter of 40 mm. The optimum production of m_2 occurred at 70 mm where 45 % of production was observed. Smaller ball sizes resulted in more fines being produced.

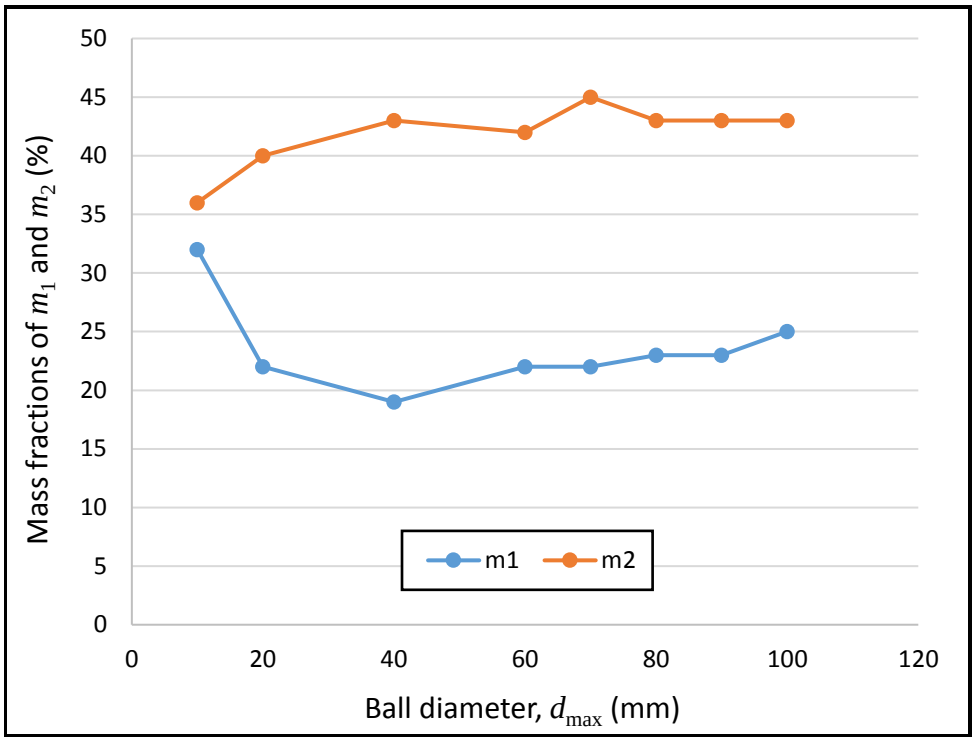

Figure 4.28 Milling kinetics of the reverse closed circuit as a function of ball diameter $d_{\max}$. The following simulation conditions applied in this case: F = 100 tph; J = 35 %; C_w = 70 %; and ϕ_c = 70 % of critical

From Figure 4.29, an increase in m_2 as m_1 decreases is observed. This figure depicts the effects of make-up ball size on the mill product in the AR space. A change in the production behaviour of m_1 is observed when m_1 then begins to increase with increase in ball size.

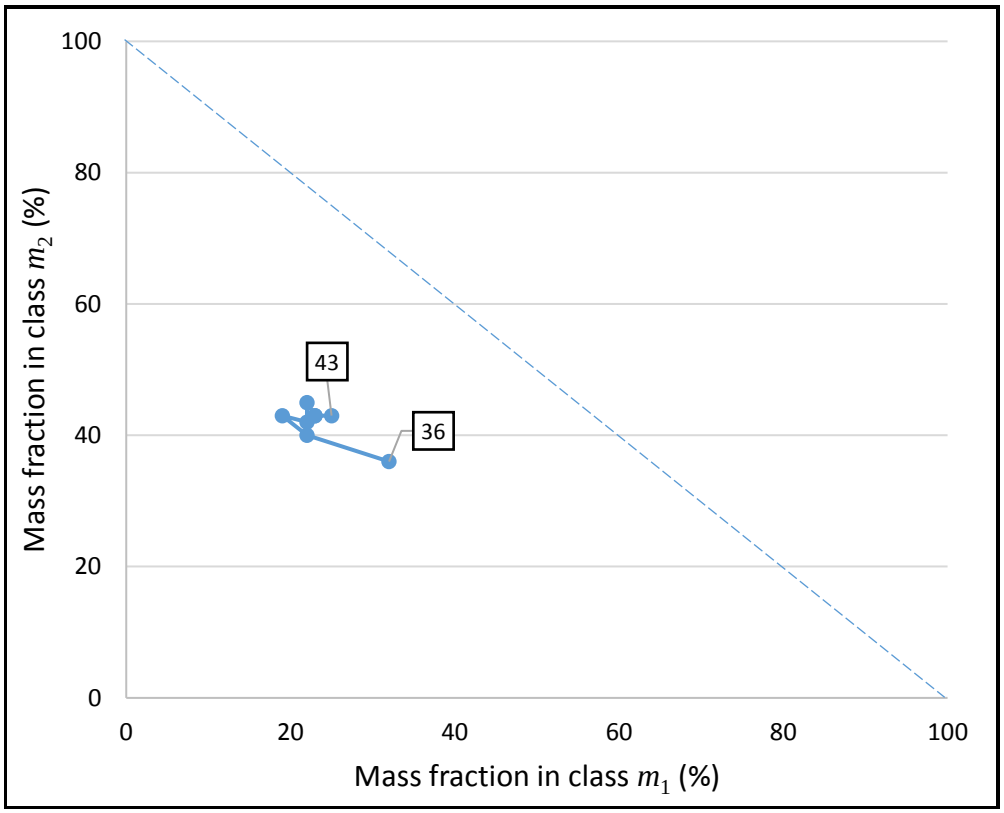

Figure 4.29 Effects of ball diameter $d_{\max}$ on the mill product for the reverse closed circuit under the following simulation conditions: F = 100 tph; J = 35 %; ϕ_c = 70 % of critical; and C_w = 70 %

4.4 Combined closed circuit

The combined milling circuit consists of both the pre-classifier and post-classifier. Both classifier overflows are mixed together as the final product, as shown in Figure 2.4. This is regarded as the most efficient configuration compared to the previous three since the material meeting the product specification in the feed stream is separated before feeding the mill to be mixed with the product and also the mill product not meeting the product specification is recycled back to the mill.

4.4.1 Effects of feed flow rate on mill product for the combined closed circuit

The feed flow rate was varied to observe the influence of the AR methodology on feed flow rate. From Figure 4.30, a sharp increase is seen in the production of m_2 with increase in flow-rate to begin stabilising at about 50 tph onwards. The optimum production of m_2 is at a solids flow rate of between 70 tph and 110 tph where 44 % of the product is observed. The flow rate was varied from 10 tph to 150 tph. It is observed that m_1 also increases with an increase in flow-rate, however, only steadily.

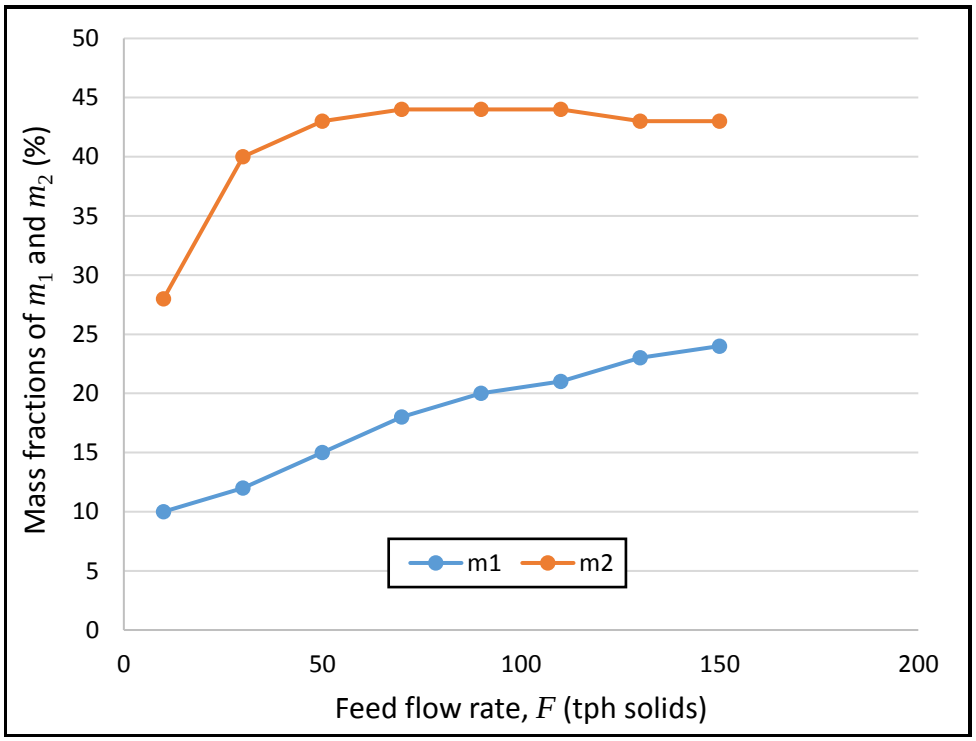

Figure 4.30 Milling kinetics of the combined closed circuit as a function of feed flow rate F. The following simulation conditions were used here: J = 35 %; C_w = 70 %; ϕ_c = 70 % of critical; and standard ball size distribution

Figure 4.31 shows what is observed from Figure 4.30 on the AR space. The sharp increase in the production of m_2 is observed, then stabilising, with a plateau observed from around 18 % of m_1.

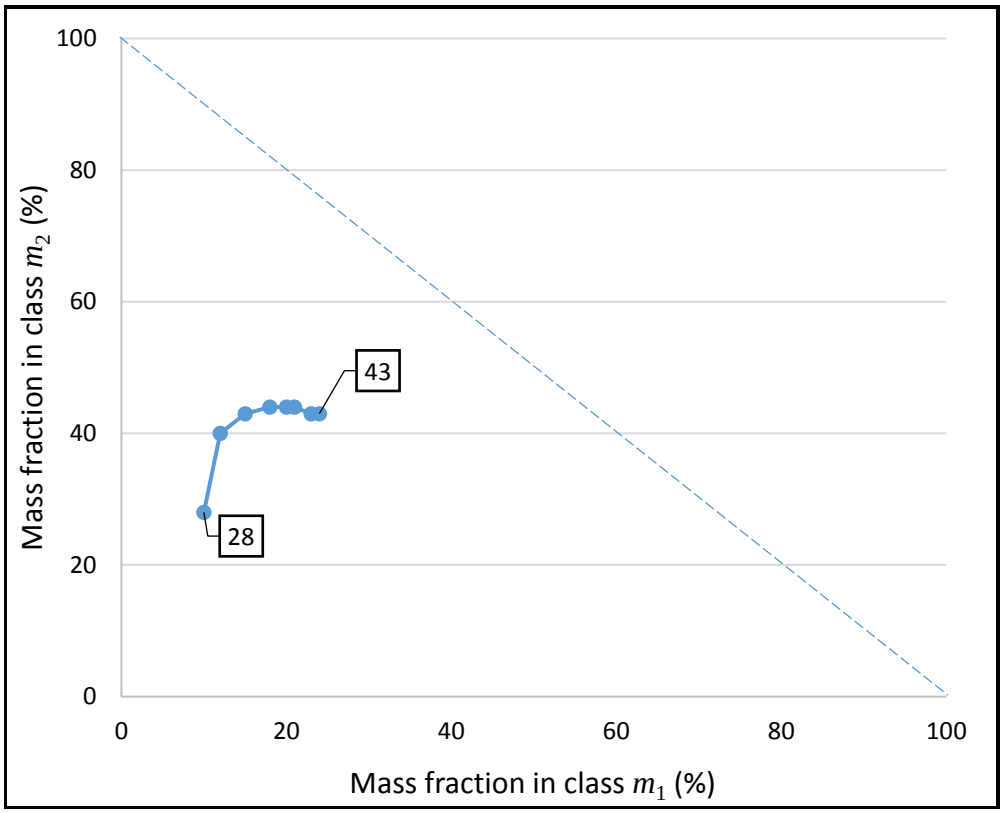

Figure 4.31 Effects of flow rate F on the mill product for the combined closed circuit simulated under the following conditions: J = 35 %; C_w = 70 %; ϕ_c = 70 % of critical; and standard ball size distribution

4.4.2 Effects of ball filling on mill product for the combined closed circuit

The effect of ball filling on the product requirements was assessed. Feed flow rate, mill speed, slurry concentration and ball size distribution were kept constant. From Figure 4.32, m_2 is seen to be decreasing until at a ball filling of 30 % where the production of m_2 starts increasing. The steady increase is observed until at a ball filling of 60 %. For the same conditions, m_1 also decreases until at a ball filling of 40 % where an increase is observed. Four different ball filling sets were simulated in MODSIM®, J = 20 %, 30 %, 40 % and 60 %.

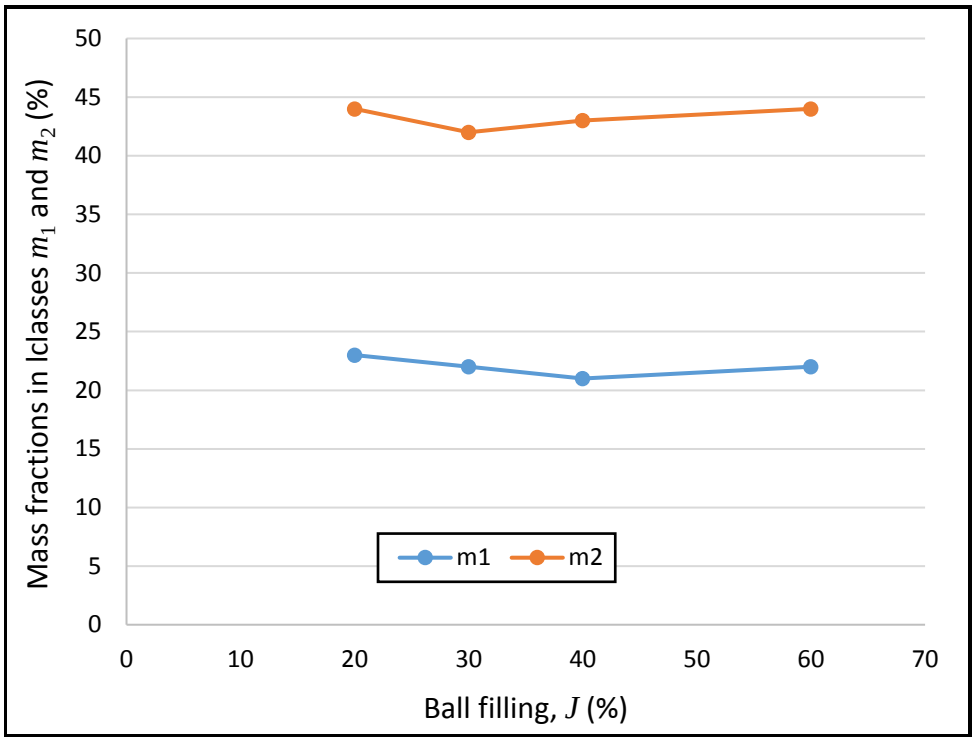

Figure 4.32 Milling kinetics of the combined closed circuit as a function of ball filling J. The following simulation conditions applied in this case: F = 100 tph; C_w = 70 %; ϕ_c = 70 % of critical; and standard ball size distribution

Figure 4.33 depicts the effects of ball filling J on the mill product in the AR space. Very little can be observed from this figure since the mass fractions of m_2 are close to each other for every data point of ball filling. The production of m_2 is similar to the production of m_1.

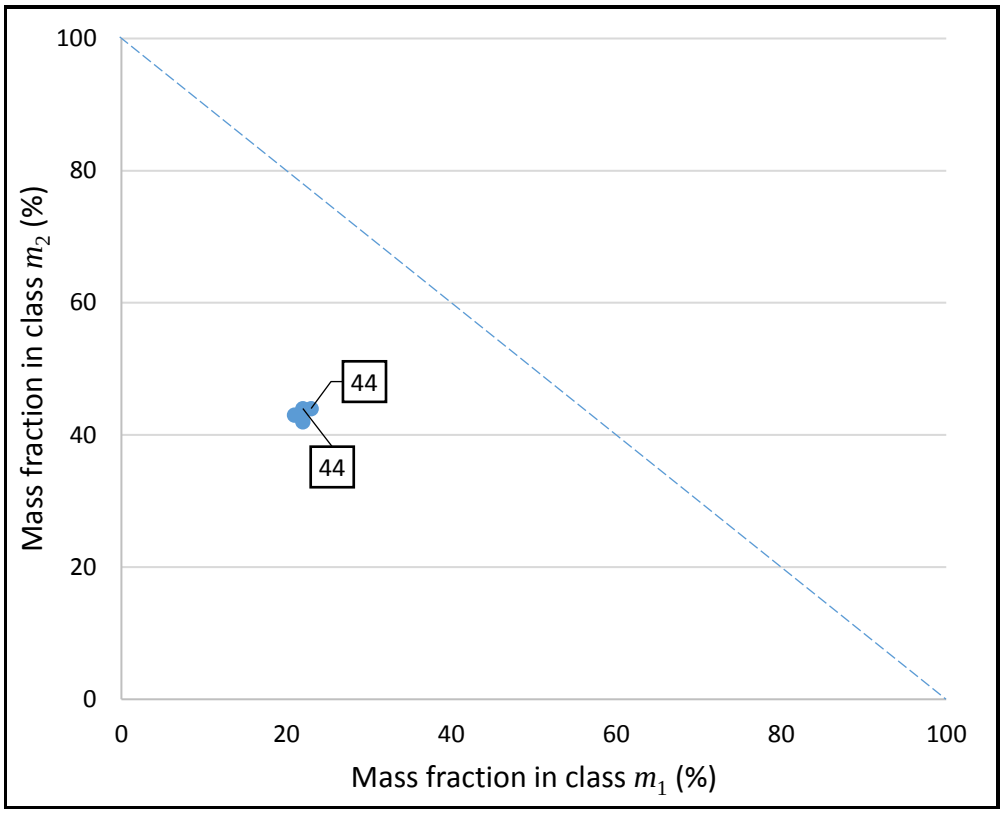

Figure 4.33 Effects of ball filling J on the mill product for the combined closed circuit simulated under the following conditions: F = 100 tph; C_w = 70 %; ϕ_c = 70 % of critical; and standard ball size distribution

4.4.3 Effects of mill speed on mill product for the combined closed circuit

Simulations were conducted to examine the effects of mill speed on the production of the required product by varying the mill speed from 30 % to 90 % of critical. Upon closer inspection it can be seen from Figure 4.34 that the production of m_2 is fairly similar to that of the reverse closed circuit. Optimum production is at 60 % of critical. From the graph it can be seen that at lower speeds the production of m_2 is stable. As mill speed ϕ_c is increased, m_2 increases to a peak at 60 % then slightly decreases after 70 % of critical.

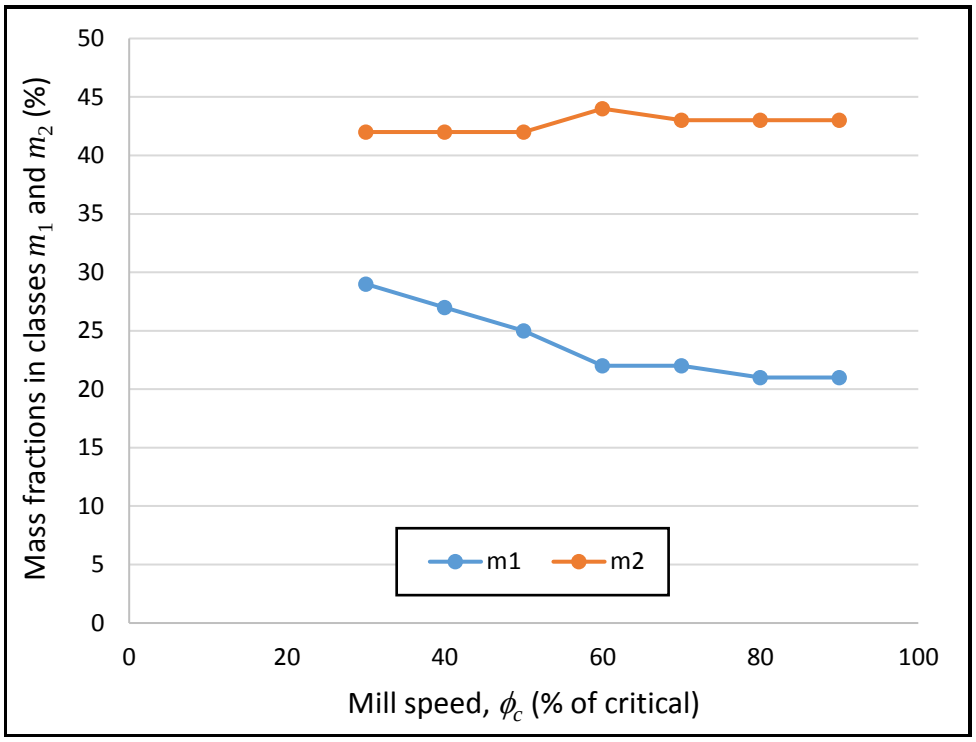

Figure 4.34 Milling kinetics of the combined closed circuit as a function of mill speed ϕ_c. The following simulation conditions applied: F = 100 tph; J = 35 %; C_w = 70 %; and standard ball size distribution

It is seen from Figure 4.35 that with a decrease in m_1 there is an increase in m_2. This figure depicts the effects of mill speed on the product in the AR space. The milling process seems to be moving away from the AR profile. This behaviour is observed because m_1 decreases at a much faster rate than that at which m_2 increases.

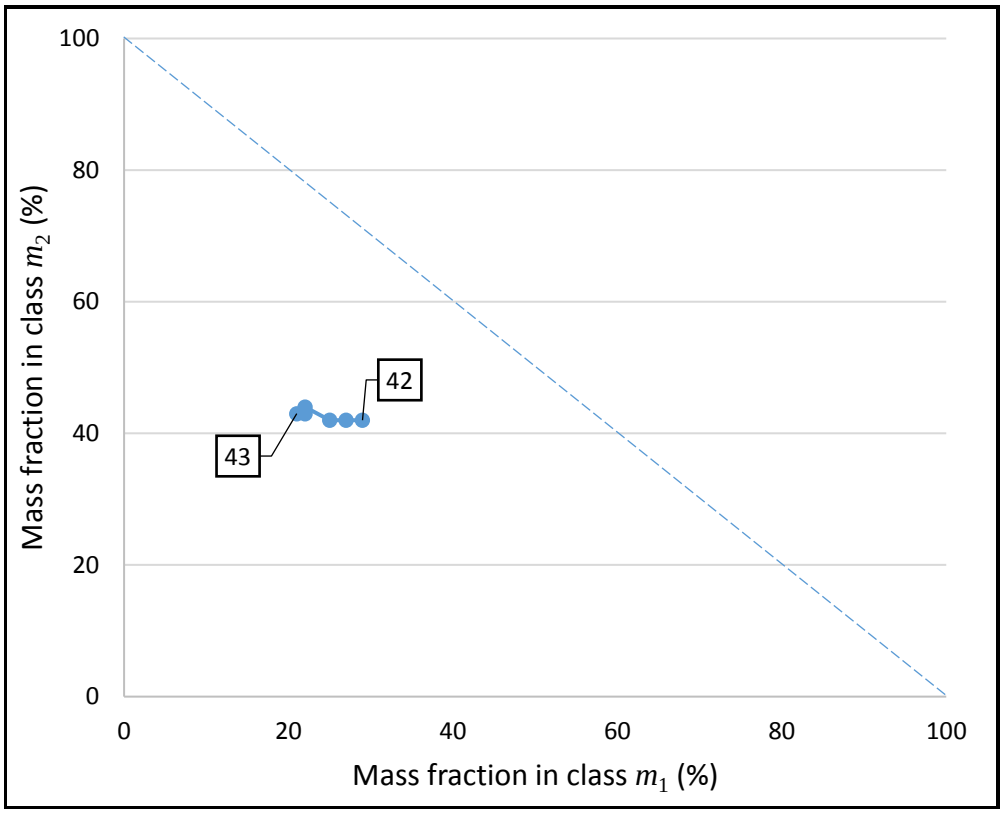

Figure 4.35 Effects of mill speed ϕ_c on the mill product for the combined closed circuit under the following simulation conditions: F = 100 tph; J = 35 %; C_w = 70 %; and standard ball size distribution

4.4.4 Effects of slurry density on mill product for the combined closed circuit

Varying the mill environment seems to have very little influence on the mill product. From Figure 4.36, it appears that slurry concentration has very influence on the production of m_2 in the study considered on this work.

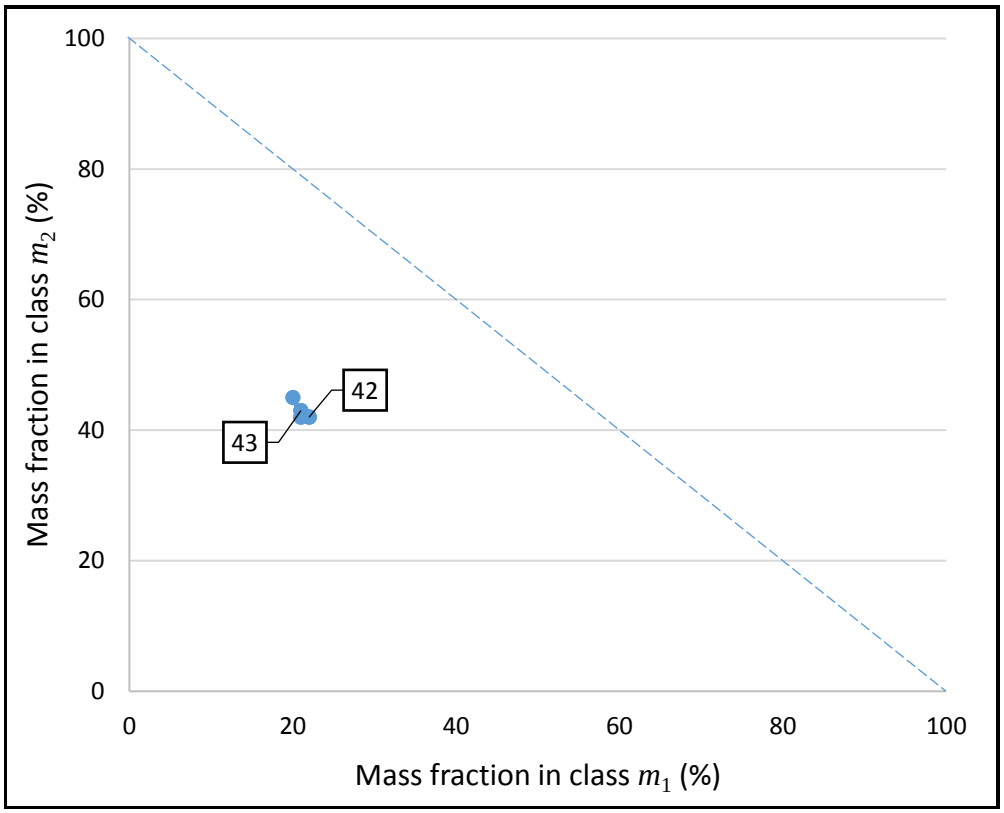

Figure 4.36 Effects of slurry concentration C_w on the mill product for the combined closed circuit. Simulation conditions: F = 100 tph; J = 35 %; ϕ_c = 70 % of critical; and standard ball size distribution

4.4.5 Effects of ball size on mill product for the combined closed circuit

Assessment on the influence of the ball size showed that the optimum production of m_2 occurred at between 60 mm and 90 mm where 44 % of production was observed, as seen from Figure 4.37. The make-up ball size was varied from 20 mm to 100 mm. it is seen that m_2 increases steadily with increase in ball diameter.

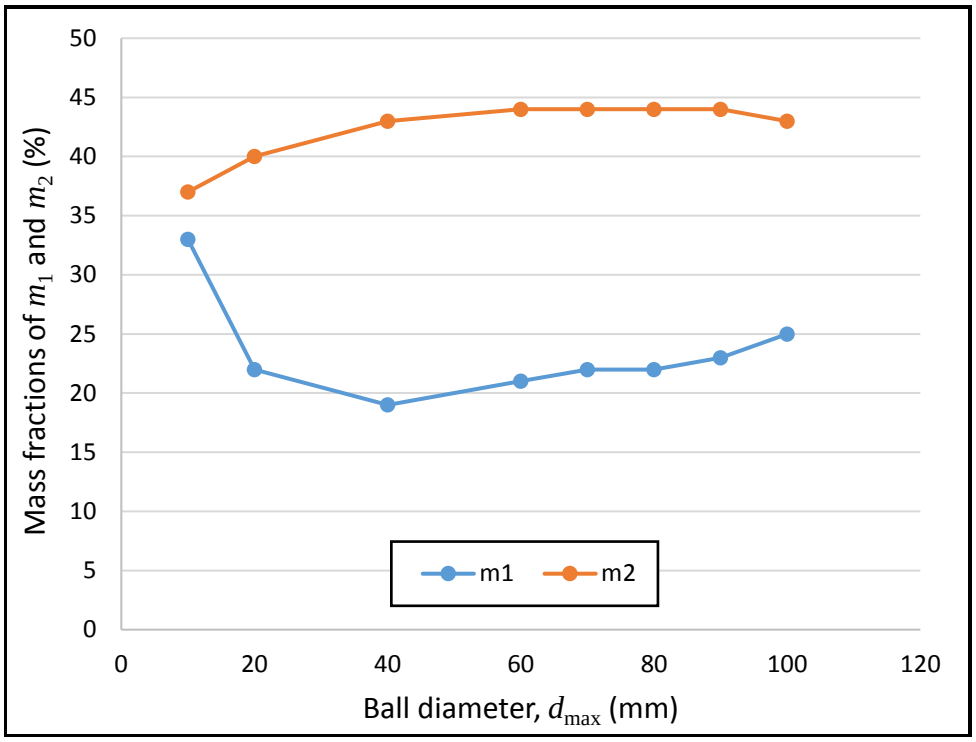

Figure 4.37 Milling kinetics of the combined closed circuit as a function of make-up ball diameter d_{max}. The following simulation conditions applied: F = 100 tph; J = 35 %; C_w = 70 %; and ϕ_c = 70 % of critical

Figure 4.38 depicts the effects of make-up ball diameter on the product in the AR space. There is an observed decrease in m_1 as m_2 increases. However, an increase in m_1 is then observed from 19 % of m_1 as m_2 continues to increase. The ideal AR profile is shown by the dotted blue line.

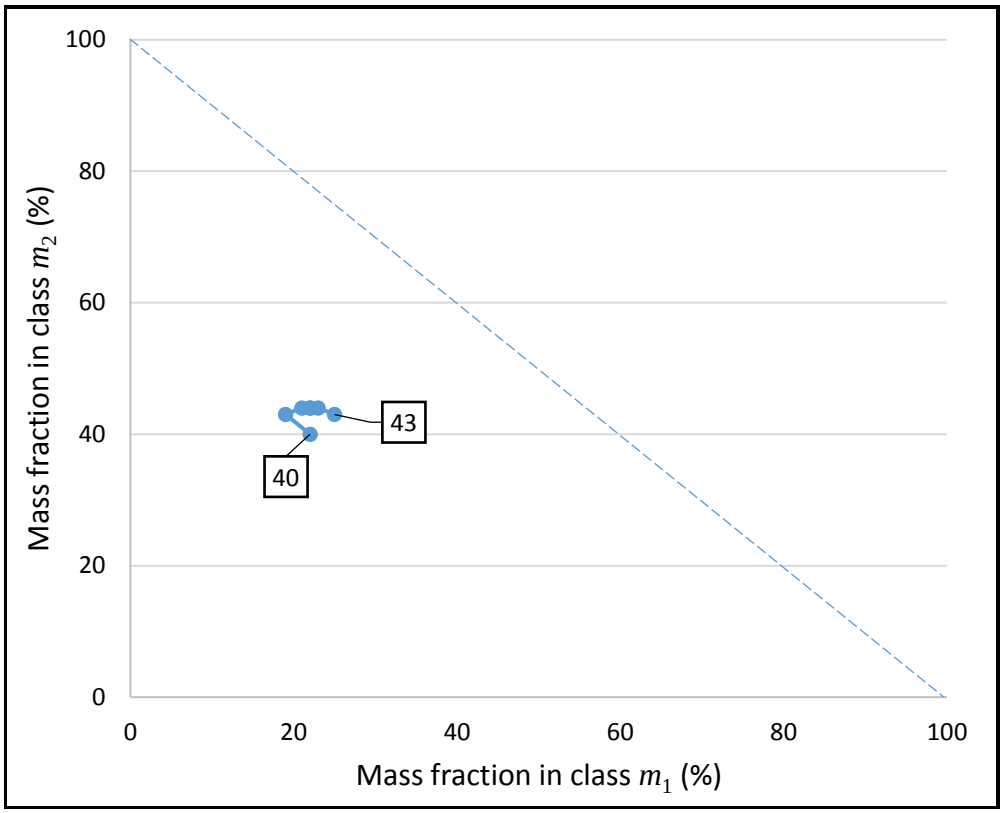

Figure 4.38 Effects of make-up ball diameter $d_{\max}$ on the mill product for the combined closed circuit simulated under the following conditions: F = 100 tph; J = 35 %; C_w = 70 %; and ϕ_c = 70 % of critical

4.5 Significance of the findings

The findings collected from this work provide some insight into the process of milling subject to the parameters which were varied of flow-rate, ball filling, mill speed, slurry density and ball diameter. Chapter 5 describes these findings in detail and elaborates on the reasons thereof.

The open circuit, being the simplest of all four circuits, attempts to achieve the required product in one pass through the mill. The production of m_2 was the lowest with this circuit compared to the others.

The normal closed circuit and the reverse closed circuit which utilise classifiers produce better results of m_2 than the open circuit. The combined closed circuit produces the highest production of m_2 overall.

What this means is that based on the study and limitations of this work, the combined closed circuit would be the better configuration for the required product. However, the minimum of the open circuit in milling still does produce a quantity not too far-fetched from that of the combined closed circuit.

CHAPTER 5 COMPARISON OF THE PERFORMANCE OF THE FOUR CLASSICAL MILLING CIRCUIT CONFIGURATIONS

The use of MODSIM® made it easier to observe the influences of the different parameters on ball milling. Mulenga and Bwalya (2015) validated the MODSIM® simulations against experimental data and concluded that the simulation model predicted the mill product satisfactorily. Their product objective was the production of particles between 75 µm and 10 µm for downstream flotation.

This chapter covers the evaluation of the efficiency of all four circuit configurations by comparing their behaviour against each other. The evaluated parameters of milling which are feed flow-rate, ball filling, mill speed, density and ball filling from all four circuits are compared against each other based on the results presented in Chapter 4.

5.1 Effects of feed flow rate

To discuss the effects of flow rate on mill product, the optimum production of m_2 was observed to be at a flow rate of between 70 tph and 130 tph for the open milling circuit. Let it be mentioned that the required product in this study is fairly coarse compared to previous studies of researchers such as Keshav *et al.* (2011). This choice was made to observe the influence of the attainable region methodology on this size material.

With that said, at flow rates higher than 130 tph the product became coarser. At higher flow rates, it was noted that the residence time in the mill becomes lower and as such the breakage time is shortened, yielding therefore a coarser product. At lower flow rates than 70 tph the material spends more time in the mill resulting to a finer product, falling into m_3.

If the downstream process required about 75 µm mill product, lower flow rates into the mill would have been required instead.

A flow-rate of 110 tph for the normal closed circuit proved to yield the optimum production of m_2. Likewise, higher flow-rates than that yielded a coarser product and lower flow-rates yielded a finer product constituting of lesser required product specification. The behaviour was slightly different with the reverse closed circuit. This was not expected, with increase in flow-rate. Over-grinding is reduced from the mill by firstly removing the portion of the feed that already meets the product specification, material finer than 850 µm. The mill product is then passed through the hydro-cyclone again with coarser material returned back to the mill feed. The results with this configuration show some improvement compared to the open and normal closed circuit configurations, as show in Figure 5.1. More production of m_2 and less production of m_1 is observed except at a flow-rate of 30 tph where m_2 is 40 % on the normal closed circuit and 38 % on the reverse closed circuit, and at the flow-rate of 110 tph where m_2 is 43 % on the normal closed circuit and 41 % on the reverse closed circuit as shown in Table 5.1, Figure 4.11 And Figure 4.21. For example, at 130 tph feed flow rate 40 % of m_2 and 28 % of m_1 is produced with the open circuit, 42 % of m_2 and 25 % of m_1 with the normal closed circuit, and 43 % of m_2 and 23 % of m_1 with the reverse closed circuit.

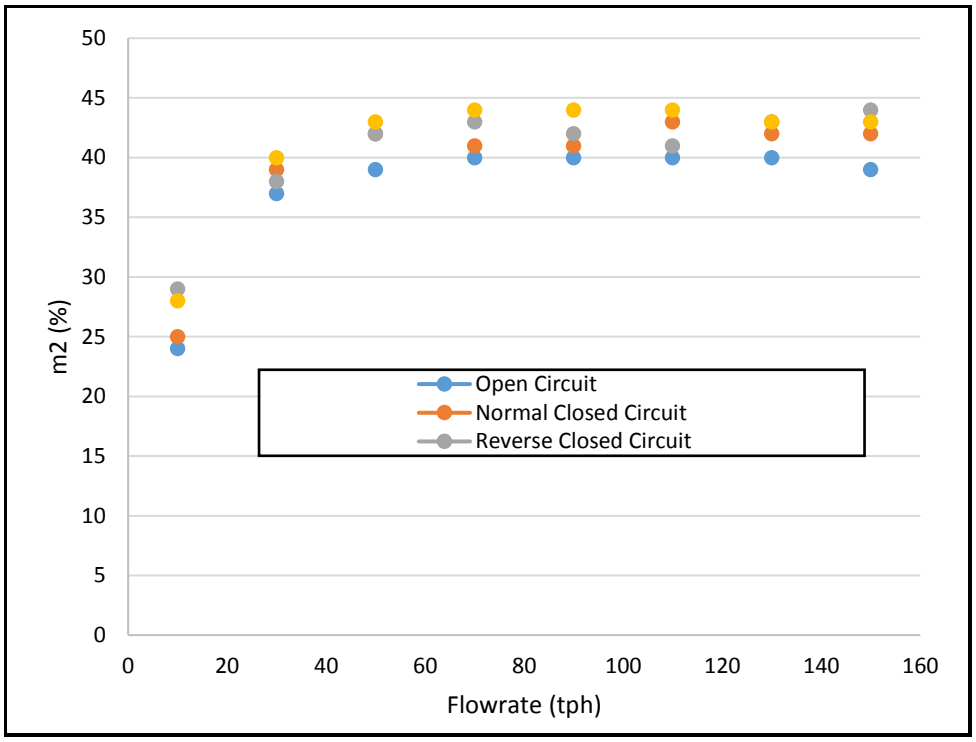

Figure 5.1 Milling kinetics on all four classical milling circuit configurations as a function of feed flow-rate F. The following simulation conditions were used here: J = 35 %; C_w = 70 %; ϕ_c = 70 % of critical speed; and standard ball size distribution

At low flow-rates less production of m_2 is observed as with the other milling circuits. However, the production of m_2 increases steadily as the feed to the hydro-cyclone is increased. This effectively removes the material which already meets the product specification first. At low flow-rates some of the material meeting the product specification would otherwise report back to the mill as hydro-cyclone underflow, due to lack of enough centrifugal action within the hydrocyclone to cut all the necessary finer material to report to overflow stream. The optimum production of the required product for this circuit is observed at the maximum flow rate which is 150 tph.

Lastly, the combined closed circuit consistently showed a marginally higher production of m_2 relative to the rest of the milling circuit configurations. This is because this circuit is optimised, with the particles in class m_2 within the feed removed prior to milling and the coarser particles recycled back to the mill for

regrind. From 30 tph upwards, this circuit produces a higher proportion of m_2. Figure 5.1 shows the production of m_2 with this configuration. However, this does not necessarily mean that it is the best choice for the scope of this work. The significance would have been considered if the production of m_2 was significantly higher than that of the other circuit configurations. The higher the flow rate the lesser the residence time will be within the mill.

5.2 Effects of ball filling

The effects of ball filling indicated that the optimum production of m_2 in the case of open circuit is reached at a ball filling of between 30 % and 40 %. It is understood that at that ball filling, the fraction filled by solids, also known as powder filling U, is 0.6 to 1.1 and that is the optimum powder filling for the maximum breakage rate of particles (Austin *et al*., 1984). At this point the mill is neither under-filled nor overfilled and the rate of breakage is at a maximum.

To effectively discuss the effect of ball filling it is necessary to consider powder filling at the same time. Under-filling is the result of having more collision spaces between balls inside the mill. This may be caused by having more balls than necessary or inefficiently less slurry. This increases the contact between ball to ball and a lot of energy is lost that way resulting in low values of breakage rates. This is the case observed with J > 60 %. At J < 30 % conditions of over-filling are observed. At this stage the collision spaces are already saturated and as a result powder cushioning becomes the consequence reducing drastically the ball to ball to powder nipping collisions.

The normal-closed circuit configuration exhibits the similar behaviour as that observed from the open circuit with the optimum production being between 30 % and 40 % of ball filling. However, production of m_2 in this case is higher with a minimum of 42 % and a maximum of 44 % compared to the open circuit whose minimum production of m_2 is at 38 % and the maximum production at 40 % as

observed in Figure 5.2. This is because the coarser mill product is recycled back to the mill in the normal closed circuit as opposed to the open circuit. That is why the production of m_1 is more in the open circuit than in the normal closed circuit.

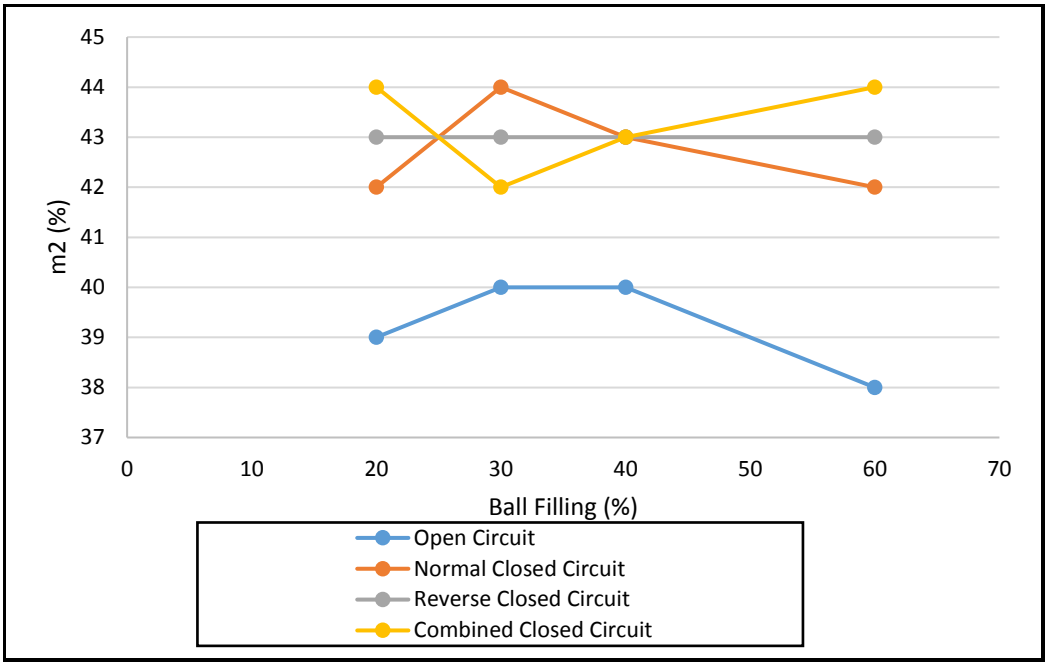

Figure 5.2 Comparison of the production of middlings m_2 as a function of ball filling J for the four circuit configurations under the following simulation conditions: F = 100 tph; C_w = 70 %; ϕ_c = 70 % of critical; and standard ball size distribution

The reverse closed circuit was constant in the production of m_2. The combined closed circuit m_2 production dropped from 44 % to 42 % then increased to 44 % again from a ball filling of 30 %. This was because more fines were rather produced at this point as compared to the reverse closed circuit. It is strange to observe such behaviour as the expectation would be to see an increased production of m_2 at the optimum powder-to-ball filling conditions. The observation with the reverse-closed circuit configuration is that there is less of the m_1 class in the product stream. This is because most of the coarser material captured pre-milling and post-milling by the pre- and post-hydrocyclones respectively is sent through to the mill for grinding down to the required product size specification in the combined closed circuit.

5.3 Effects of mill speed

Next, the effect of mill speed on mill product indicated that more of the required product, m_2 class, is produced at a speed of between 60 % and 80 % of critical. At lower speeds, the motion of grinding balls within the mill is cascading, often with the balls moving en masse. The chances of impact and interactions between ball, material and ball are minimal and hence breakage is minimal (Austin *et al*., 1984). If there is any interaction, the impact is not enough for a satisfactory breakage. At high rotational speeds, a cataracting effect of grinding balls is observed and at speeds higher than the critical speed, a centrifuging effect of the balls would be observed. Figure 5.3 shows the comparison of all the circuit in the production of m_2.

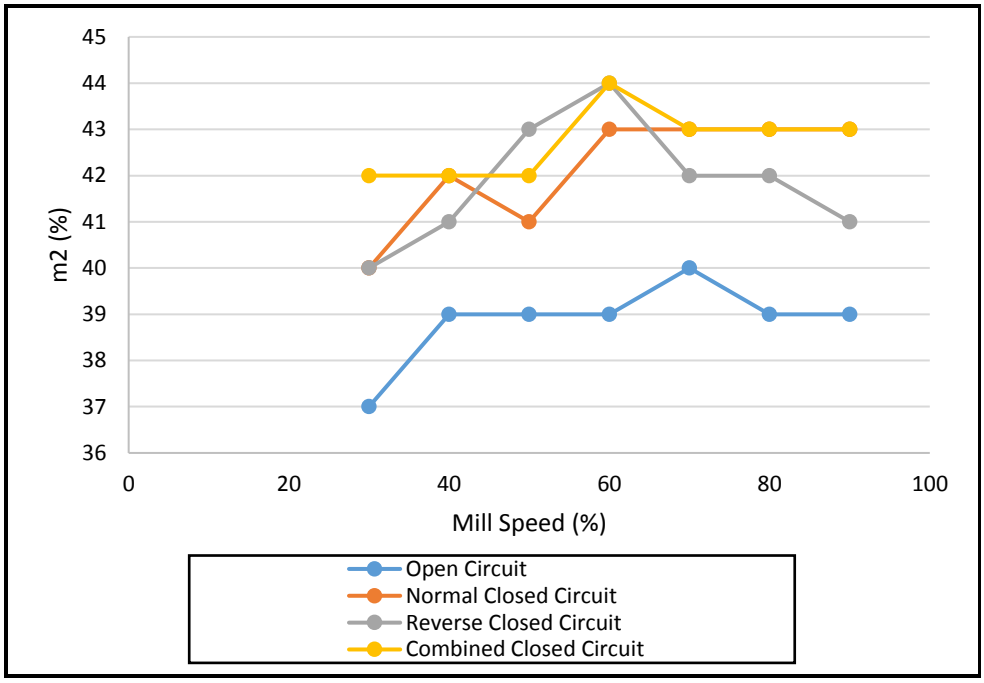

Figure 5.3 Effects of mill speed ϕ_c on the mill product for the four circuit configurations simulated under the following conditions: F = 100 tph; J = 35 %; C_w = 70 %; and standard ball size distribution

As the mill rotates, breakage occurs when the balls strike particles nipped on other balls. Three breakage mechanisms are likely to occur depending on the mill speed. Fracturing occurs as a result of massive impact; compression occurs as a result of extensive stresses applied on the particle beyond its compressive strength; and

abrasion is the result of rubbing of the surfaces. At higher mill speeds fracturing occurs and compression, that is why the production of m_2 increases with increase in mill speed. At lower mill speeds abrasion results. As observed by Austin *et al.* (1984), the maximum rate of breakage results at approximately the speed of maximum power draw, which is normally around 75 % of critical, depending on the ball load. This was observed from the simulations.

5.4 Effects of ball diameter

For ball diameter, larger ball diameters proved to result in the highest production of the required product specification m_2. This was expected due to the nature of the feed being coarse. Larger ball diameters break larger particles more efficiently but are very poor at breaking smaller particles (Katubilwa and Moys, 2009). Likewise, smaller ball diameters are ineffective at breaking larger particles because these particles cannot be easily nipped and fractured thus resulting to a slow breakage rate. Also, the accumulation of fine material in the mill cushions the breakage of the remaining larger particles (Austin *et al*., 1984). With the feed material considered for this study being coarser, a larger ball diameter was the most effective in the production of the required product, along with the added advantage of having hydrocyclones within the circuits with hydrocyclones.

5.5 Effect of slurry concentration

Lastly, the effects of slurry concentration on the mill product did not have a notable effect of consideration. There are limitations to the population balance model. The model does not yet incorporate the influence of slurry concentration in it and therefore changes as a result of the mill density were not much expected, especially from MODSIM® which utilises the population balance model. On all the four circuit configurations simulated, slurry concentration did not show any changes in the production of m_2. This indicates that the model which does not

represent reality by not incorporating the influence slurry concentration in it is limited.

5.6 Concluding remarks

It can be concluded that the combined closed circuit is the better performing circuit. Although this circuit has the most unit operations and thus possibly an increase in operating costs for the Plant, this may be worth it in the long run on the performance of the process and the economic benefit for the Operation. However, the other three circuits are still within an acceptable range of production of m_2 within the scope of the work covered in this study.

CHAPTER 6 CONCLUSIONS AND RECOMMENDATIONS

6.1 Introduction

This Chapter summarizes the findings from this work and presents recommendations based on the observed limitations and challenges. The attainable region technique is a useful technique in the optimisation of milling by identifying the optimum operating conditions within a milling circuit configuration subject to the parameters of that process of milling

6.2 Summarised findings

The attainable region technique was evaluated against a number of milling parameters which were flow-rate, ball filling, mill speed, density and ball size. It was also evaluated for the effect it has on different milling circuit configurations. The feed material was 4700 µm. The feed class m_1 was between 4700 µm and 850 µm, product class m_2 was between 850 µm and 300 µm, and the third class m_3 was the fines product less than 300 µm. First, flow-rate was varied from 10 tph to 150 tph solids while all the other parameters were kept constant. This was done for the open milling circuit, normal closed circuit, reverse closed circuit and the general combined circuit. More production of the product specification was observed from the higher flow-rates. The production of m_2 started to show an increase from a flow-rate of 70 tph upwards. This was expected as the required product is quite a fairly large material.

Secondly, ball filling was varied from 20 % to 60 %. The highest production of the product specification was observed between 30 % and 40 %. This is the region in which the mill is neither over-filled nor under-filled and therefore the best production of what is required is expected. The attainable region technique was successful in identifying this region.

Thirdly, the mill speed was varied. Optimum production of m_2 was observed between 70 % and 80 % of the critical speed. This was the best speed at which the centrifuging effect was not observed, and the mill was also not too slow for the balls to only roll over (cascading) without effective breakage.

Then the slurry density was also varied. Not much effect was observed with the variation of density. The attainable region technique applied in MODSIM® which is based on the population balance model that lacks the inclusion of density in its formulation did not seem to have an effect.

Lastly, ball diameter was varied from 20 mm to 100 mm. larger balls break large material effectively. Therefore, the optimum production of m_2 was observed at larger ball diameters.

Based on all these results, it can be concluded that the attainable region technique is successful in identifying the best operating conditions for a given feed material to achieve the required product.

6.3 Recommendations for future work

A few recommendations or future works are necessary for the improvement in determining the influence of the attainable region theory. The following future works are recommended:

- Modification of the population balance model to fully incorporate slurry concentration.
- The use of real plant data to determine the ability of the attainable region technique in optimising the operation as opposed to using assumed parameters.
- The use of a smaller feed size distribution

The expansion of the scope of this work to cover multiple ranges of m_1, m_2 and m_3, that is different feed size distributions, is required before a general conclusion can be made about the efficiency of the different circuit configurations covered. This will also shed some more light on the influence of the attainable region technique on the different size distributions of the feed material.

LIST OF REFERENCES

Austin, L.G., Klimpel, R.R., Luckie, P.T., 1984. Process engineering of size reduction: Ball milling. Society of Mining Engineers of the AIME, New York, USA

Baskar, N., Asokan, P., Saravanan, R., Prabhaharan, G., 2005. Optimization of machining parameters for milling operations using non-conventional methods. The International Journal of Advanced Manufacturing Technology, vol. 25, pp. 1078 – 1088

Bilgili, E., Scarlett, B., 2005. Population balance modeling of non-linear effects in milling processes. Powder Technology, vol. 153, pp. 59 – 71

Chimwani, N., 2014. An attainable region approach to optimizing product size distribution for flotation purposes. PhD thesis, University of the Witwatersrand, Johannesburg, South Africa

Coetzee, L.C., Craig, I.K., Kerrigan, E.C., 2010. Robust nonlinear model predictive control of a run-of-mine ore milling circuit. IEEE transactions on Control Systems Technology, vol. 18, pp. 222 – 229

Coghill, W.H., De Vaney, F.D., 1937. Ball mill grinding kinetics in a pilot scale. U.S. Bureau of Mines Tech Bulletin. Publication No. 581, USA

Concha, F., Barrientos, A., Montero, J., Sampaio, R., 1996. Air core and roping in hydrocyclones. International Journal of Mineral Processing, vol. 44 – 45, pp. 743 – 749

Curry, J.A., Ismay, M.J.L., Jameson, G.J., 2014. Mine operating costs and the potential impacts of energy and grinding. Minerals Engineering, vol. 56, pp. 70 – 80

Danha, G., Bhondayi, C., Hildebrandt, D., 2015. A laboratory scale application of the attainable region technique on a platinum ore. Powder Technology, vol. 274, pp. 14 – 19

Eipstein, B., 1947. The material description of certain breakage mechanisms leading to the logarithmic-normal distribution. Journal of the Franklin Institute, vol. 244, no. 12, pp. 471 – 477

Eipstein, B., 1948. Logaritmico-normal distributions in breakage of solids. Ind. Eng. Chem., vol. 40, pp. 2289 – 2291

Evangelos, P., Konstantinos, K., 2017. Improved modelling of the grinding process through the combined use of the matrix and population balance models. Minerals, vol. 7, no. 67, pp. 1 – 17

Gardner, R.P., Austin, L.G., 1962. A chemical engineering treatment of batch grinding. Symposium Zerkleinern, Rumpf, H. and Behrens, D., Eds., Verlag Chemie, Duseldorf, W. Germany, pp. 217 – 248

Glasser, D., Hildebrandt, D., 1997. Reactor and process synthesis. Computers and Chemical Engineering, vol. 21, Suppl. 1, S775 – S783

Gupta, A., Yan, D.S. 2006. Mineral processing design and operation: an introduction. Elsevier, Perth, Australia

Hlabangana, N., Danha, G., Hilderbrandt, D., Glasser, G., 2016. Use of the attainable region approach to determine major trends and optimize particle breakage in a laboratory mill. Powder Technology, vol. 291, pp. 414 – 419

Irannajad, M., Farzanegan, A., Razavian, S.M., 2006. Spreadsheet-based simulation of closed ball milling circuits. Minerals Engineering, vol. 19, pp. 1495 – 1504

Jankovic, A., Sinclair, S., 2006. The shape of product size distributions in stirred mills. Minerals Engineering, vol. 19, pp. 1528 – 1536

Katubilwa, F.M., 2009. Effect of ball size distribution on milling parameters. Master's dissertation, University of the Witwatersrand, Johannesburg, South Africa

Katubilwa, F.M., Moys, M.H., 2009. Effects of ball size distribution on milling rate. Minerals Engineering, vol. 22, no. 15, pp 1283 – 1288

Kawatra, S.K., Bakshi, A.K., Rusesky, M.T., 1996. The effect of slurry viscosity on hydrocyclone classification. International Journal of Mineral Processing, vol. 48, pp. 39 – 50

Khumalo, N., 2007. The application of the attainable region analysis in comminution. PhD thesis, University of the Witwatersrand, Johannesburg, South Africa

Khumalo, N., Glasser, D., Hilderbandt, D., Hausberger, B., 2008. Improving comminution efficiency using classification: An attainable region approach. Powder Technology, vol. 187, pp 252 – 259

King, R.P., 1990. Calculation of the liberation spectrum in products produced in continuous milling circuits. Proc. 7th European Symposium on Comminution, Ljubljana, South Africa, vol. 2, pp. 429 – 444

King, R.P., 2001. Modelling and simulation of mineral processing systems, Butterworth-Heinemann, Oxford, United Kingdom

King, R.P., Schneider, C.L., 1990. Mineral liberation and the batch comminution equation. Comminution Centre, University of Utah, Salt Lake City UT, USA, 84112

Kobayashi, A., Nagasaka, H., Lizuka, K., Yoshida, H., 2004. Characteristics of open- and closed-circuit grinding systems. Separation and Purification Technology, vol. 36, pp. 157 – 165

Kumar, S., Ramkrishna, D., 1997. On the solution of population balance equations by discretization – 111. Nucleation, growth and aggregation of particles. Chemical Engineering Science, vol. 2, no. 24, pp. 4659 – 4679

Kwon, J., Jeong, J., Cho, H., 2016. Simulation and optimisation of a two-stage ball mill grinding circuit of molybdenum ore. Advanced Powder Technology, vol. 27, pp. 1073 – 1085

Liu, Y., Spencer, S., 2004. Dynamic simulation of grinding circuits. Minerals Engineering, vol. 17, pp. 1189 – 1198

Mazzinghy, B.D., Galery, R., Schneider, C.L., Alves, K.V., 2014. Scale-up and simulation of Vertimill pilot test operated with copper ore. Journal of Materials Research and Technology, vol. 3, no. 1, pp. 86 – 89

Mclvor, R.E., 2014. Plant performance improvements using grinding circuit "classification system efficiency". Mining Engineering, vol. 66, no. 9, pp. 67 – 71, September

Mclvor, R.E., 2006. Industrial validation of the functional performance equation for ball milling and pebble milling circuits. Mining Engineering, pp. 47 – 51, November

Metzger, M.J., 2011. Numerical and experimental analysis of breakage in a mill using the attainable region approach. PhD thesis, The State University of New Jersey, New Brunswick, USA

Metzger, M.J., Desai, S.P., Glasser, D., Hildebrandt, D., Glasser, B.J., 2012. Using the attainable region analysis to determine the effect of process parameters on breakage in a ball mill. American Institute of Chemical Engineers Journal, vol. 58, pp. 2665 – 2673

Monov, V., Sokolov, B., Stoenchev, S., 2012. Grinding in ball mills: modelling and process control. Cybernetics and Information Technologies, vol. 12, pp. 52 – 68

Morrell, S., 2008. A method for predicting the specific energy requirement of comminution circuits and assessing their energy utilization efficiency. Minerals Engineering, vol. 5, pp. 1 – 24

Mular, A.L., Jull, N.A., 1980. The selection of cyclone classifiers, pumps and pump boxes for grinding circuits. In Mular, A.L., Bhappu, R.B. (Ed.) Mineral Processing Plant Design, 2nd Ed., pp. 376 – 403

Mulenga, F.K., Bwalya, M.M., 2015. Application of the attainable region technique to the analysis of a full-scale mill in open circuit. Journal of the Southern African Institute of Mining and Metallurgy, vol. 115, no. 8, pp. 729 – 740

Mulenga, F.K., Mwashi, A.M.M., 2018. Use of the attainable region approach for the determination of the run-of-mine size distribution for optimal downstream processing. Society of Mining Professors 6th Regional Conference 2018, Birchwood Hotel and Conference Centre, Johannesburg, 12 – 13 March 2018, The Southern African Institute of Mining and Metallurgy, pp. 141 – 154

Norgate, T., Jahanshahi, S., 2010. Improving the sustainability of primary metal production – the need for a life cycle approach. In: Proceedings of the XXV International Mineral Processing Conference (IMPC), Brisbane, Australia, pp. 3575 – 3584,

Olejnik, T.P., 2012. Analysis of the breakage rate function for selected process parameters in quartzite milling. Chemical and Process Engineering, vol. 33, no. 1, pp. 117 – 129

Otwinowski, H., 2006. Energy and population balances in comminution process modelling based on the information entropy. Powder Technology, vol. 167, pp. 33 – 44

Prasher, C., 1987. Crushing and grinding handbook. Wiley, New York, USA

Ramkrishna, D., 2000. Population balances: Theory and applications to particulate systems in engineering. Purdue University, School of Chemical Engineering, West Lafayette, Indiana. Academic Press, San Diego, USA

Rowland, C.A., Kjos, D.M., 1980. Mineral processing plant design. SME/AIME, pp. 239 – 278

Rosenblat, Y., Grant, E., Levy, A., Kalman, H., Tomas, J., 2012. Selection and breakage functions of particles under impact loads. Chemical Engineering Science, vol. 71, pp. 56 – 66

Runge, K.C., Tabosa, E., Holtham, P., Valle, R., 2014. Grinding and flotation circuits integration and optimization. 3rd International Meeting of Metallugy, At Lima, Peru, pp. 1 – 7

Samarak, D., Tumidajski, T., Brozek, M., Gawenda, T., Naziemiec, Z., 2010. Aspects of comminution flowsheets design in processing of mineral raw materials. Mineral and Energy Economic Research, vol. 26, pp. 60 – 69

Sedlatschek, K., Bass, L., 1953. Contribution to the theory of milling processes. Powder Metallurgy Bulletin, vol. 6, pp. 148 – 153

Seodigeng, T.G., 2005. Numerical formulations for attainable region analysis. PhD thesis, University of the Witwatersrand, Johannesburg, South Africa

Silva, A.C., Silva, E.M.S., De Rezende, R.A., 2013. Circulating load calculation in mineral processing closed circuit operations. 16th IFAC Symposium on Automation in Mining, Mineral and Metal Processing, August 25 – 28, 2013, San Diego, California, USA, pp. 45 – 50

Steyn, C.W., Brooks, K.S., de Villiers, P.G.R., Muller, D., Humphries, G., 2010. A holistic approach to control and optimization of an industrial ball milling circuit. 13th Symposium on Automation in Mining, Mineral and Metal Processing, Cape Town, South Africa

Teng, S., Wang, P., Zhu, L., Young, M.W., Gogos, C.G., 2010. Mathematical modelling of fluid energy milling based on a stochastic approach. Chemical Engineering Science, vol. 65, no. 15, pp. 4323 – 4331

Toneva, P., Peukert, W., 2007. Modelling of mills and milling circuits. In Handbook of Powder Technology, Eds. A.D. Salman, M. J. Hounslow, and J.P.K. Seville, vol. 12, pp 874 – 911

Unland, G., Szczelina, P., 2002. Course crushing of brittle rocks by compression. 10th European Symposium on Comminution, Heidelburg, Germany

Vanni, M., 2000. Approximate population balance equations for aggregate-breakage processes. Journal of Colloid and Interface Science, vol. 221, no. 2, pp 143 – 160

Verkoeijen, D., Pouw, G.A., Meesters, G.M.H., Scarlett, B., 2002. Population balances for particulate processes – a volume approach. Chemical Engineering Sciences, vol. 57, pp. 2287 – 2303

Wang, X., Gui, W., Yang, C., Wang, Y., 2011. Wet grindability of an industrial ore and its breakage parameters estimation using population balances. International Journal of Mineral Processing, vol. 98, pp. 113 – 117

Wei, D., Craig, I.K., 2008. Grinding mill circuits – a survey of control and economic concerns. Proceedings of the 17th World Congress, The international Federation of Automatic Control, Seoul, South Korea

Wills, B.A., Napier-Munn, T.J., 2006. Minerals processing technology: an introduction to the practical aspects of ore treatment and mineral recovery. Elsevier Science and technology Books, 7th Ed., New York, USA

APPENDICES

Appendix A

Open Circuit Product Size Distribution

Mesh Size (m)	% Passing
0.395E-02	99.999
0.279E-02	99.888
0.198E-02	97.851
0.140E-02	91.463
0.988E-03	80.562
0.699E-03	66.520
0.494E-03	51.859
0.349E-03	38.721
0.247E-03	28.075
0.175E-03	19.998
0.124E-03	14.094
0.874E-04	9.888
0.617E-04	6.928
0.437E-04	4.853
0.309E-04	3.413

0.218E-04	2.401
0.154E-04	1.704
0.109E-04	1.207
0.772E-05	0.862
0.546E-05	0.620
0.386E-05	0.448
0.273E-05	0.325
0.193E-05	0.236
0.136E-05	0.173
0.00	0.000

Normal Closed Circuit Product Size Distribution

Mesh Size (m)	**% Passing**
0.395E-02	100.000
0.279E-02	99.960
0.198E-02	98.811
0.140E-02	93.545
0.988E-03	82.197
0.699E-03	66.625
0.494E-03	50.771

0.349E-03	37.181
0.247E-03	26.556
0.175E-03	18.688
0.124E-03	13.030
0.874E-04	9.050
0.617E-04	6.278
0.437E-04	4.353
0.309E-04	3.030
0.218E-04	2.110
0.154E-04	1.481
0.109E-04	1.038
0.772E-05	0.734
0.546E-05	0.523
0.386E-05	0.374
0.273E-05	0.269
0.193E-05	0.194
0.136E-05	0.140
0.00	0.000

Reverse Closed Circuit Product Size Distribution

Mesh Size (m)	% Passing
0.395E-02	99.995
0.279E-02	99.912
0.198E-02	99.094
0.140E-02	95.332
0.988E-03	86.138
0.699E-03	71.595
0.494E-03	55.288
0.349E-03	40.751
0.247E-03	29.278
0.175E-03	20.760
0.124E-03	14.611
0.874E-04	10.256
0.617E-04	7.198
0.437E-04	5.054
0.309E-04	3.564
0.218E-04	2.515
0.154E-04	1.790
0.109E-04	1.272

0.772E-05	0.911
0.546E-05	0.658
0.386E-05	0.476
0.273E-05	0.346
0.193E-05	0.253
0.136E-05	0.185
0.00	0.000

Combined Closed Circuit Product Size Distribution

Mesh Size (m)	**% Passing**
0.395E-02	99.995
0.279E-02	99.912
0.198E-02	99.093
0.140E-02	95.329
0.988E-03	86.133
0.699E-03	71.590
0.494E-03	55.286
0.349E-03	40.752
0.247E-03	29.279
0.175E-03	20.761

0.124E-03	14.612
0.874E-04	10.257
0.617E-04	7.198
0.437E-04	5.055
0.309E-04	3.564
0.218E-04	2.515
0.154E-04	1.790
0.109E-04	1.272
0.772E-05	0.912
0.546E-05	0.658
0.386E-05	0.476
0.273E-05	0.346
0.193E-05	0.253
0.136E-05	0.185
0.00	0.000

Appendix B

Table 5.1: The production of m_2 on all four milling circuits as a function of flow-rate

Flow-rate (tph)	m_2 Production in Open Circuit (%)	m_2 Production in Normal Closed Circuit (%)	m_2 Production in Reverse Closed Circuit (%)	m_2 Production in Combined Closed Circuit (%)
10	24	25	29	28
20	37	39	38	40
50	39	42	42	43
70	40	41	43	44
90	40	41	42	44
110	40	43	41	44
130	40	42	43	43
150	39	42	44	43